2009

Standing Waves Of Spatially Discrete Fitzhugh-nagumo Equations

Joseph Segal
University of Central Florida

STANDING WAVES OF SPATIALLY DISCRETE FITZHUGH-NAGUMO EQUATIONS

by

JOSEPH M. SEGAL
B.S. Davidson College, 2006

A thesis submitted in partial fulfillment of the requirements
for the degree of Master of Science
in the Department of Mathematics
in the College of Sciences
at the University of Central Florida
Orlando, Florida

Fall Term
2009

Advisor: Brian E. Moore

ABSTRACT

We study a system of spatially discrete FitzHugh-Nagumo equations, which are nonlinear differential-difference equations on an infinite one-dimensional lattice. These equations are used as a model of impulse propagation in nerve cells. We employ McKean's caricature of the cubic as our nonlinearity, which allows us to reduce the nonlinear problem into a linear inhomogeneous problem. We find exact solutions for standing waves, which are steady states of the system. We derive formulas for all 1-pulse solutions. We determine the range of parameter values that allow for the existence of standing waves. We use numerical methods to demonstrate the stability of our solutions and to investigate the relationship between the existence of standing waves and propagation failure of traveling waves.

ACKNOWLEDGMENTS

I would like to thank Dr. Brian Moore for all of his help on this work. He has spent countless hours meeting with me over the past year, discussing problems and offering his constructive input. He also spent much of his work time on his own reviewing many drafts of this paper. It is much of his research and ideas that I am following and advancing in this work and it was he who gave me the inspiration to take on this project.

I would also like to thank the other members of my thesis committee, Dr. Ram Mohapatra and Dr. David Rollins, for their willingness to participate in this important process with me.

TABLE OF CONTENTS

LIST OF FIGURES

1 INTRODUCTION

1.1 Problem History and Motivation

In 1952 A. L. Hodgkin and A. F. Huxley performed experiments and created their model of wave propagation in a squid axon [1]. This model describes the process of excitation and propagation of waves of electric current through nerve cell membrane. This process is governed by the flow of ions, mainly of sodium and potassium, into and out of nerve cells. In 1963 Hodgkin and Huxley were awarded the Nobel Prize in Science and Medicine for their work on this field.

In 1961 Richard FitzHugh introduced his model [2], which is a simplification of the Hodgkin Huxley (H-H) model. The H-H model has four variables and the FitzHugh-Nagumo (FH-N) model is a reduction down to two variables. The purpose of the creation of the FH-N model was to form a more general qualitative model of an excitable system by isolating the mathematical properties of excitation and wave propagation and ignoring the electrochemical dynamics of sodium and potassium ion flow. The two variables that are left in the model are a voltage variable and a recovery variable. An advantage of this reduction is that we are able to view the solutions of this two-dimensional system using phase portraits, which is not possible with a four-dimensional system.

The name Nagumo is included in the name of the FH-N model because of work done by J. Nagumo [3] in showing that the FH-N equations can model the dynamics of a physical electrical circuit system which he constructed.

Here is the general form of a continuous FH-N model, with subscripts denoting differentiation:

$$u_t = Du_{xx} - v - f(u) \tag{1.1}$$

$$v_t = bu - rv \tag{1.2}$$

For our applications u is the voltage variable and v is the recovery variable. The parameter D is called the diffusion coefficient. The terms b and r are recovery parameters. The function $f(u)$ is referred to as the nonlinearity of the system.

While both FitzHugh and Nagumo originally studied the system using a smooth cubic nonlinearity, McKean [4] introduced the study of this system using a piecewise linear nonlinearity, which we use in this paper. Many others have followed suit and opted to use McKean's nonlinearity in their study of the FH-N and related models, such as in [7, 8, 11, 14, 15, 18, 19, 21].

Besides using different nonlinearities, there are other major differences between some FH-N type models that can be chosen to suit different applications. The model can be formulated to be spatially multi-dimensional, as in [15], or spatially one-dimensional, as in this paper and many others. Spatially multi-dimensional models can be used to study applications where waves can travel in many directions, such as in cardiac tissue.

Our formulation of the system is intended to model waves in a single nerve axon, which is a long thin nerve fiber inside insulating Myelin sheath. The Myelin sheath covers most of the axon, but there are breaks in the insulation at places called nodes of Ranvier. At these nodes ions flow in and out of the axon, allowing for conduction of the action potential. Some FH-N type models are spatially discrete and some are spatially continuous. We choose to model the system as spatially discrete, with the space between each node of Ranvier represented by a node on a 1-D lattice. The ionic potential or voltage at each of the cells is given by a value at each node on the lattice. It is important to note that we are using a model that is spatially discrete not to approximate something we believe is truly continuous in nature, but because we believe that studying a nerve axon as a string of discrete release sites, rather than as a continuous wire, can reveal important results.

As is pointed out by Keener [11], there can be very different qualitative behavior between spatially discrete and spatially continuous models. In a spatially continuous FH-N model, if a traveling wave solution exists for a specific value of the diffusion coefficient, then traveling wave solutions exist for all values of $D > 0$. In a spatially discrete FH-N model though, we can have traveling waves for some values of the diffusion coefficient, while for other values of the diffusion coefficient we cannot, all other parameters held constant.

Much research has been done on the related system that only has one equation with one variable, the voltage variable. This is called the Nagumo equation as is generally written:

$$u_t = Du_{xx} - f(u) \tag{1.3}$$

This research studies "fronts", waves that are monotonic. Work on the discrete Nagumo equation as a model of propagation in a nerve axon was pioneered by Bell [9, 10].

FH-N models such as the one we use also include a recovery variable, which generalizes the effects of the three gating variables from the H-H model. Inclusion of the recovery variable in the model is meant to temporarily decrease the excitability of nodes that have already been stimulated, allowing the nodes to return back to their resting state after a wave passes. Studying these "pulse" waves is much more realistic to the physical system, although it is also considerably more complicated. In Figure 1.1 we show pictures of a front wave from a discrete Nagumo model and a pulse wave from a discrete FH-N model.

According to Keener [16], for the Nagumo equation, "propagation failure occurs if and only if there are standing waves." In studying front waves of the discrete Nagumo equation, [6, 14] have demonstrated a phenomena called the *Interval of Propagation Failure*. By finding standing waves and the parameters that allow for their existence, they have also found the conditions for propagation failure, or the inability of traveling waves to propagate through the media. This is a main motivation for our approach to this problem. Although we do not already have the same connection between the existence of standing waves and propagation failure for pulse waves as we do for fronts, we similarly intend to study propagation failure

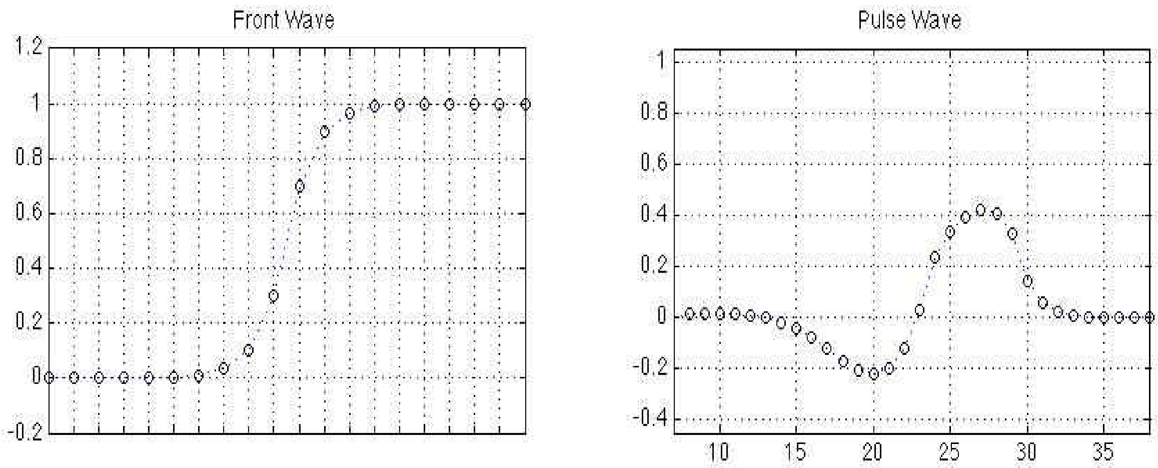

Figure 1.1: On the left a front wave. On the right a pulse wave.

of pulse waves by finding standing waves and the conditions for their existence.

Stability of traveling front waves of the discrete Nagumo equation has been studied in [12]. Stability of standing front waves of the discrete Nagumo equation has been studied in [9, 23]. Stability of traveling pulse waves of the continuous FH-N equations has been studied in [8]. Global attractors of traveling waves for the discrete FH-N model has been studied in [20].

Of particular relevance to our work is the work in [6] and [7]. In [6] Humphries, Moore, and Van Vleck find standing front wave solutions to the discrete Nagumo equation with the McKean nonlinearity and investigate conditions for their existence. We follow their approach in using the theory of Jacobi operators from [5] in finding these steady states. In [7] Elmer and Van Vleck find candidate traveling wave solutions to the discrete FH-N model with the McKean nonlinearity. In our paper we investigate their results and make connections to our results.

Our contribution to the subject is to find explicit formulas for all possible standing single hump pulse waves for a discrete FH-N model. We find all possible parameter values that allow for the existence of these standing waves. We investigate the connection between the existence of standing pulse waves and propagation failure of traveling pulse waves. We also advance this work by following [6] in using the theory of Jacobi operators to find these steady states. This technique can be used in the future to find steady states of discrete FH-N models with inhomogeneous media and with other nonlinearities.

In the next section we set up the problem to be investigated. In Chapter 2 we derive standing wave solutions to our system. In Chapter 3 we simplify these solutions into a compact form. In Chapter 4 we look at conditions of the parameters required for the existence of standing waves. In Chapter 5 we discuss various numerical experiments we have performed to illustrate properties of the standing waves. In Chapter 6 we discuss our conclusions and possible future work on this problem.

1.2 Our Problem

We consider steady state solutions to the spatially discrete FitzHugh-Nagumo equations

$$\dot{u}_k(t) = Lu_k(t) - v_k(t) - f(u_k(t); a), \tag{1.4}$$

$$\dot{v}_k(t) = bu_k(t) - rv_k(t), \tag{1.5}$$

where $u_k(t)$ and $v_k(t)$ map $\mathbb{R}^+ \cup \{0\} \to \mathbb{R}$, $k \in \mathbb{Z}$ indicates a particular element of the one-dimensional lattice, $\dot{u} = \frac{du}{dt}$ and $\dot{v} = \frac{dv}{dt}$. Also, the recovery parameters satisfy $b \geq 0$ and $r > 0$. The FitzHugh-Nagumo equations above can be called lattice differential equations, spatially discrete partial differential equations, or differential-difference equations. In general the operator L, a difference Laplacian operator, is of the form

$$Lu_k(t) = \alpha_k(u_{k+1}(t) - u_k(t)) + \alpha_{k-1}(u_{k-1}(t) - u_k(t)), \tag{1.6}$$

with $\alpha_k \in \mathbb{R}^+, \forall k \in \mathbb{Z}$. The α_k are called the diffusion coefficients and represent the amount of interaction between adjacent points on the lattice. We study the case of homogeneous media, so all the diffusion coefficients are the same along the entire lattice, $\alpha_k = \alpha, \forall k \in \mathbb{Z}$, and the operator L takes the form

$$Lu_k(t) = \alpha(u_{k+1}(t) - 2u_k(t) + u_{k-1}(t)), \tag{1.7}$$

with $\alpha \in \mathbb{R}^+$. This single value, α, is *the* diffusion coefficient. Although we do not solve it here, we are looking forward to the case of inhomogeneous diffusion, where the diffusion coefficients do vary along the lattice.

We take this time to look at the equation (1.4) of the voltage variable and identify the different "forces" that are at work within the equation. Equation (1.4) can be written as:

$$\dot{u}_k(t) = \alpha(u_{k+1}(t) - u_k(t)) + \alpha(u_{k-1}(t) - u_k(t)) - v_k(t) - f(u_k(t)). \tag{1.8}$$

Conceptually, this says that for a point with index k, the movement of that point, $\dot{u}_k(t)$, is governed by four different "forces" given on the right side of the equation. The first term, $\alpha(u_{k+1}(t) - u_k(t))$, is the effect of the point just to the right with index $k+1$. The second term, $\alpha(u_{k-1}(t) - u_k(t))$, is the effect of the point just to the left with index $k-1$. Each point is affected by the two points on either side of it, which pull the point closer to them, with "force" proportional to the difference in voltage between the points and proportional to the diffusion parameter α. The third term, $-v_k(t)$, is the effect of the recovery wave on the voltage wave. The higher the recovery variable is at a point, the more it pulls the voltage variable down at that point. The last term is the nonlinearity, $f(u_k(t))$, also known as the "forcing term" , which is important in causing a wave to travel along the lattice or not. We look at the nonlinearity in the next section. In a steady state solution, all of these four "forces" are in perfect balance at each point along the lattice.

1.2.1 The Nonlinearity

The nonlinearity $f : \mathbb{R} \to \mathbb{R}$ is typically taken to be the derivative of a double-well potential, such as the cubic

$$f(u; a) = u(u - a)(u - 1), \tag{1.9}$$

or the McKean caricature of the cubic [4], which is the piecewise linear function

$$f(u; a) = u - h(u - a) \tag{1.10}$$

where h is the Heaviside function

$$h(u) = \begin{cases} 0, & u < 0 \\ [0, 1]\,, & u = 0 \\ 1, & u > 0. \end{cases} \tag{1.11}$$

and $a \in (0, 1)$ is known as the detuning parameter. It is known that the parameter a largely determines the wave speed of a traveling wave. Hence it also is important to the existence of standing waves, or waves with zero speed. Figure 1.2 shows the function (1.10), the McKean caricature of the cubic, for different values of a. The cubic function (1.9) is plotted as well to show the comparison. The nonlinearity (1.10) is special in that it is much easier to deal with for this problem than (1.9), yet it shares some important features of that function, such as having the same zeros. They are also similar in that $f > 0$ for $0 < u < a$, and $f < 0$ for $a < u < 1$. Both (1.9) and (1.10) are zeroth order approximations of the functional in the H-H model that we are approximating, so it is certainly acceptable that we choose to use (1.10) over (1.9). In other words, just because we a making a choice of nonlinearity that is easier to work with, there is no mathematical reason to think that we will end up with a model whose behavior less resembles that of the H-H model.

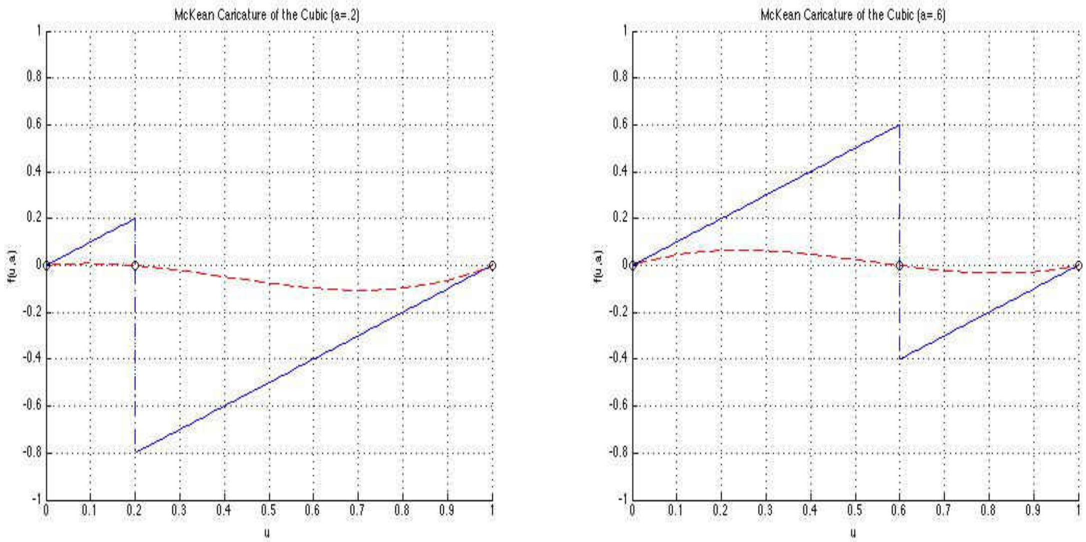

Figure 1.2: McKean caricature of the cubic for a=.2 and a=.6 with the corresponding cubic functions. Circles at the zeros.

Both nonlinearities (1.10) and (1.9) are functions that are the derivative of a double-well potential function. In Figure 1.3 we show the double-well potential functions that correspond with each nonlinearity. We also plot the derivatives of those double-well potential functions, the nonlinearities themselves. The zeros of each nonlinearity are the equilibrium points of that nonlinearity. As with any potential function, objects are drawn to the areas of lowest potential. For a double-well potential, points are drawn to the bottoms of the wells, which are located at $u = 0$ and $u = 1$. These are the *stable* equilibrium points. The value $u = a$ is also an equilibrium point, but looking at the potential functions, we see that for everywhere around this equilibrium point, points are drawn away from a into one of the two wells. This situation can be visualized as a ball sitting on top of a smooth mountain with valleys on either side. If the ball is sitting on the very top it can stay still, but if it is knocked off the top even slightly it will roll all the way down into one of the valleys below. This in an

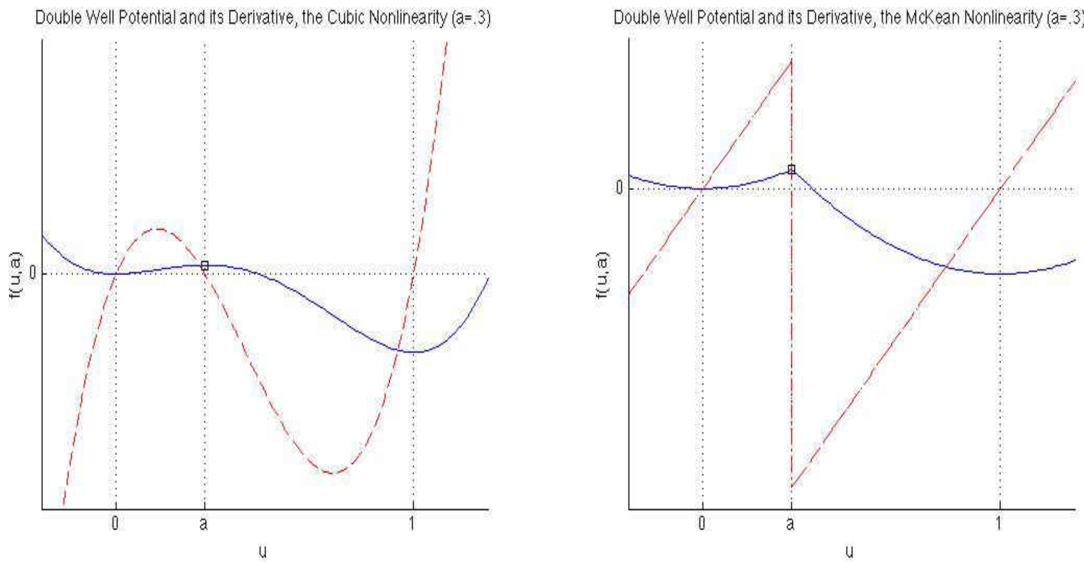

Figure 1.3: Double-well potential functions corresponding to each nonlinearity with their derivatives plotted as dashed lines. On the left the cubic nonlinearity. On the right the McKean nonlinearity. For each nonlinearity shown $a = .3$

example of an *unstable* equilibrium point. The point $u = a$ is an unstable equilibrium point. Therefore the *effect of the nonlinearity* is to push points away from a, either down towards 0 or up towards 1.

1.2.2 Our Approach

We are studying propagation failure of waves in the FitzHugh-Nagumo model. To do so we look for standing wave solutions of these equations. Standing wave solutions are steady state solutions of (1.4)-(1.5). They are waves that do not propagate through the media. In a steady state solution the system is not moving, so there is no time-dependence, and so the derivatives with respect to time will vanish. So we can set $\dot{u}_k(t)$ and $\dot{v}_k(t)$ in equations (1.4) and (1.5) equal to zero.

We first set $\dot{v}_k(t) = 0$ in (1.5) and solve for v_k.

$$\begin{aligned} 0 = \dot{v}_k(t) &= bu_k(t) - rv_k(t) \\ rv_k(t) &= bu_k(t) \end{aligned}$$

$$v_k(t) = \left(\frac{b}{r}\right) u_k(t) \tag{1.12}$$

We then set $\dot{u}_k(t) = 0$ in (1.4) so that

$$\dot{u}_k(t) = 0 = Lu_k(t) - v_k(t) - f(u_k(t); a), \tag{1.13}$$

and then plug (1.12) into (1.13) to get

$$0 = Lu_k(t) - \left(\frac{b}{r}\right) u_k(t) - f(u_k(t); a). \tag{1.14}$$

Now that we have substituted to eliminate the recovery variable v and get an equation with only the voltage variable u, we will no longer need to consider the recovery variable in finding steady states. It is important to note now that once we find steady state solutions for the voltage wave u_k, we can easily construct the corresponding recovery wave v_k using the *recovery relation* (1.12).

We call the ratio of parameters $\frac{b}{r}$ the *recovery ratio*, and define $\gamma = \frac{b}{r}$. Note that $\gamma \geq 0$. In the rest of our analytical work on standing waves, we only encounter the parameters b and r in terms of the ratio $\frac{b}{r}$. We will therefore use the term γ instead and treat this as one parameter. It is only when we look at traveling waves in Chapter 5 that the individual values of b and r matter.

Note: Since we are finding steady states of this system by setting time derivatives equal *to zero, the steady state solutions of this system that we will derive are also steady states of other equations such as the spatially discrete, nonlinear Klein-Gordon equation,*

$$\ddot{u}_k(t) = Lu_k(t) - f'(u_k(t))$$

and the spatially discrete, nonlinear Schrödinger equation,

$$i\dot{u}_k(t) = Lu_k(t) - f'(u_k(t))$$

with $f' = \gamma u + f$.

From (1.14) we see that finding the steady state solutions for the system of equations (1.4)-(1.5) is equvalent to solving the difference equation

$$\alpha(\varphi_{k+1} - 2\varphi_k + \varphi_{k-1}) - \gamma\varphi_k = f(\varphi_k; a). \tag{1.15}$$

We transition from the variable $u_k(t)$ to φ_k because we no longer need to use a variable that has time dependence. The new variable, φ_k, only varies on the discrete spatial lattice with index $k \in \mathbb{Z}$. Throughout the rest of the text we let f be the piecewise linear function (1.10).

We focus our study on waves that have a certain general shape, that of a single pulse. In other words, we do not concern ourselves with waves that go up and down multiple times. For waves of this single pulse shape, we identify three possible cases. The first case is that the wave goes above a, so it crosses a once going up and again once going down. The second case is that the wave peaks at a never going above it. The third case is that the wave never even touches a, it stays below it entirely. For now we only concern ourselves with waves that actually cross a, but the other two cases will be discussed for completeness after this case has been solved.

We then seek solutions that satisfy

$$\begin{aligned} \varphi_k < a \qquad &\text{for} \qquad k < \eta_0, \quad k > \eta_1 \\ \varphi_k > a \qquad &\text{for} \qquad \eta_0 < k < \eta_1. \end{aligned} \tag{1.16}$$

As in [7], we define $\eta_j \in \mathbb{R}$ conceptually as the places where the wave crosses a. Hence, η_j for $j = 0, 1$ are the points at which the Heaviside function is activated, and they must satisfy $\eta_0 < \eta_1$. Using the terminology of [7], this is called a 1-pulse solution. We also may have the case where a wave crosses a at a lattice point. In this case we would have

$$\varphi_k = a \qquad \text{for} \qquad k = \eta_j, \quad j = 0 \text{ or } 1. \tag{1.17}$$

This would only happen if $\eta_j \in \mathbb{Z}$. *Note: If a wave crosses a "in-between" lattice points k^* and $k^* + 1$, i.e. $\varphi_{k^*} < a$ and $\varphi_{k^*+1} > a$ or vice-versa, then simply $\eta_j \in (k^*, k^* + 1)$, and the particular value of η_j in this interval is not important to our setup since we are really only studying points at the integer values on the lattice.*

Now the nonlinearity (1.10) may be written as a linear inhomogeneous term

$$f(\varphi_k) = \varphi_k - h(k - \eta_0) + h(k - \eta_1),$$

which is independent of a. Thus, solving (1.15) is equivalent to solving the difference equation

$$\alpha\varphi_{k+1} - (1 + \gamma + 2\alpha)\,\varphi_k + \alpha\varphi_{k-1} = h(k - \eta_1) - h(k - \eta_0) \qquad \forall k \in \mathbb{Z}, \tag{1.18}$$

with boundary conditions

$$\lim_{k\to\pm\infty} \varphi_k = 0. \tag{1.19}$$

These boundary conditions come from the boundary conditions used in a traveling wave problem. Equation (1.18) is an infinite dimensional tridiagonal linear system and general solutions may be derived using Jacobi operator theory [5]. We choose to use Jacobi operator theory in solving the problem because this approach can be applied to the more complex cases of inhomogeneous media or more complex nonlinearities which are an extension of the work done here.

As a simplification let

$$h_k = h(k - \eta_0) - h(k - \eta_1), \tag{1.20}$$

and the equation to solve is now written

$$-\alpha\varphi_{k+1} + (1 + \gamma + 2\alpha)\,\varphi_k - \alpha\varphi_{k-1} = h_k \qquad \forall k \in \mathbb{Z}. \tag{1.21}$$

The right side of (1.21), h_k, will always either be 0, 1, or [0,1]: 0 if $k < \eta_0$ or $k > \eta_1$, 1 if $\eta_0 < k < \eta_1$, and [0,1] if $k = \eta_0$ or $k = \eta_1$.

1.2.3 Bounding Our Solutions

Now that we have formulated the difference equation (1.15), we can already put an upper bound on its solutions. We can rewrite (1.15) as:

$$\alpha(\varphi_{k+1} - \varphi_k) + \alpha(\varphi_{k-1} - \varphi_k) = (1 + \gamma)\,\varphi_k - h(\varphi_k - a). \tag{1.22}$$

Let k_M be the index of the maximum value of φ_k, so that $\varphi_{k_M} \geq \varphi_k, \forall k \in \mathbb{Z}$. Setting $k = k_M$ in (1.22), we get:

$$\alpha(\varphi_{k_M+1} - \varphi_{k_M}) + \alpha(\varphi_{k_M-1} - \varphi_{k_M}) = (1 + \gamma)\,\varphi_{k_M} - h(\varphi_{k_M} - a).$$

We assume that $\varphi_{k_M} > a$, so $h(\varphi_{k_M} - a) = 1$. Also we know that the terms on the left both cannot be positive since φ_{k_M} is the maximum value, so we now have the inequality

$$0 \geq (1 + \gamma)\, \varphi_{k_M} - 1,$$

which gives us the bound

$$\varphi_{k_M} \leq \left(\frac{1}{1+\gamma} \right). \tag{1.23}$$

This tells us that the upper bound on our steady state solutions is $\frac{1}{1+\gamma}$. We define $\beta = \frac{1}{1+\gamma}$ and call this the *compression factor*. Note that $\beta \in (0, 1]$. As we have shown before, the effect of the nonlinearity is to push the highest points on the wave up towards 1. The effect of the recovery variable though is to push points down, which keeps the standing wave below β. We will see β in our formulas for φ_k and it is important to understand where this value comes from, a balancing of the opposed forces from the nonlinearity and from the recovery wave. We see from (1.12) that the amplitude of the recovery wave in a steady state is determined by the recovery ratio of parameters $\frac{b}{r} = \gamma$. It is this value γ that determines the compression factor $\frac{1}{1+\gamma} = \beta$ for standing waves φ_k.

2 DERIVATION OF SOLUTIONS

Now that we have formulated our wave problem as a difference equation, (1.21), we will derive a general solution to this equation. As an inhomogeneous difference equation, the general solution to (1.21) can be written in terms of the general solution to the homogeneous problem

$$-\alpha\varphi_{k+1} + (1+\gamma+2\alpha)\,\varphi_k - \alpha\varphi_{k-1} = 0 \qquad \forall k \in \mathbb{Z}, \tag{2.1}$$

and a particular solution of (1.21). The fundamental solutions of (2.1) are found using standard techniques of difference equations. The particular solution is derived using Jacobi Operator theory following the results of Teschl [5]. The fundamental and particular solutions are then combined to form the general solution of (1.21).

2.1 Fundamental Solutions

Start by considering

$$\varphi_{k+1} + \varphi_{k-1} = 2\mu\varphi_k \tag{2.2}$$

which is just the homogeneous equation (2.1) for

$$\mu = \frac{1}{2\alpha}(1+\gamma+2\alpha). \tag{2.3}$$

Since we are considering a second order difference equation, the space of solutions is two-dimensional, and we can write any solution of (2.2) in the form

$$\varphi_k = \varphi_{k_0}\rho(k-k_0) + \varphi_{k_0+1}\sigma(k-k_0) \tag{2.4}$$

for any starting point k_0. Our equations, and therefore the solutions of those equations, are translationally invariant. This is because we have homogeneous diffusion and so our lattice is exactly the same everywhere. There is no difference between the point $k = 0$ on the lattice and the point $k = 100$ because diffusion is the same everywhere. Our solutions can exist anywhere on the lattice and we can freely choose any index on the lattice as our starting point k_0. We will therefore choose this point in a way to formulate the problem in the simplest way possible.

The functions $\rho(k - k_0)$ and $\sigma(k - k_0)$ are a set of linearly independent solutions of (2.2), known as the fundamental solutions, which satisfy the initial conditions

$$\rho(0) = 1, \quad \rho(1) = 0, \quad \sigma(0) = 0, \quad \sigma(1) = 1. \tag{2.5}$$

Using these simple initial conditions, if we set $k = k_0$ in (2.4) we have the equality $\varphi_{k_0} = \varphi_{k_0}$, and if we set set $k = k_0 + 1$ we similarly have $\varphi_{k_0+1} = \varphi_{k_0+1}$.

Following standard theory of difference equations, in order to find expressions for $\rho(k-k_0)$ and $\sigma(k - k_0)$, substitute $\varphi_j = \lambda^j$ into (2.2) to get

$$\lambda^2 - 2\mu\lambda + 1 = 0, \tag{2.6}$$

which implies, using the quadratic formula, that

$$\lambda_\pm = \mu \pm \sqrt{\mu^2 - 1}, \tag{2.7}$$

using the principal branch of the square root. Noting that $\lambda_+\lambda_- = 1$ implies that $\lambda_+ = 1/\lambda_-$. We set $\lambda = \lambda_+ > 1$, which yields $\lambda_- = \lambda^{-1}$. Using the initial conditions (2.5), we can derive the fundamental solutions.

The fundamental solutions ρ and σ have the form

$$\rho(k) \;\; = \;\; A\lambda^k + B\lambda^{-k} \tag{2.8}$$

$$\sigma(k) = C\lambda^k + D\lambda^{-k} \tag{2.9}$$

because λ^k and λ^{-k} are two linearly independent functions of k. This is again standard theory of difference equations. We have four unknowns here, A, B, C, and D, and four initial conditions (2.5). Combining the fundamental solutions (2.8) and (2.9) with the initial conditions (2.5), we get

$$\rho(0) = 1 = A + B \tag{2.10}$$

$$\rho(1) = 0 = A\lambda + B\lambda^{-1} \tag{2.11}$$

$$\sigma(0) = 0 = C + D \tag{2.12}$$

$$\sigma(1) = 1 = C\lambda + D\lambda^{-1} \tag{2.13}$$

We can use linear algebra to quickly solve this system.

$$\begin{bmatrix} 1 & 1 \\ \lambda & \lambda^{-1} \end{bmatrix} \begin{bmatrix} A \\ B \end{bmatrix} = \begin{bmatrix} 1 \\ 0 \end{bmatrix}$$

$$\begin{bmatrix} 1 & 1 \\ \lambda & \lambda^{-1} \end{bmatrix} \begin{bmatrix} C \\ D \end{bmatrix} = \begin{bmatrix} 0 \\ 1 \end{bmatrix}$$

$$\begin{bmatrix} 1 & 1 \\ \lambda & \lambda^{-1} \end{bmatrix}^{-1} = \frac{1}{\lambda^{-1} - \lambda} \begin{bmatrix} \lambda^{-1} & -1 \\ -\lambda & 1 \end{bmatrix}$$

$$\begin{bmatrix} A \\ B \end{bmatrix} = \frac{1}{\lambda^{-1} - \lambda} \begin{bmatrix} \lambda^{-1} & -1 \\ -\lambda & 1 \end{bmatrix} \begin{bmatrix} 1 \\ 0 \end{bmatrix}$$

$$
\begin{aligned}
&= \begin{bmatrix} -\frac{\lambda^{-1}}{\lambda-\lambda^{-1}} \\ \frac{\lambda}{\lambda-\lambda^{-1}} \end{bmatrix} \\
\begin{bmatrix} C \\ D \end{bmatrix} &= \frac{1}{\lambda^{-1}-\lambda} \begin{bmatrix} \lambda^{-1} & -1 \\ -\lambda & 1 \end{bmatrix} \begin{bmatrix} 0 \\ 1 \end{bmatrix} \\
&= \begin{bmatrix} \frac{1}{\lambda-\lambda^{-1}} \\ -\frac{1}{\lambda-\lambda^{-1}} \end{bmatrix}
\end{aligned}
$$

Now that we have A, B, C, and D we can plug them into (2.8) and (2.9) to get

$$
\begin{aligned}
\rho(k) &= \frac{-\lambda^{-1}}{\lambda-\lambda^{-1}}\lambda^{k} + \frac{\lambda}{\lambda-\lambda^{-1}}\lambda^{-k} \\
&= \frac{-\lambda^{k-1}}{\lambda-\lambda^{-1}} + \frac{\lambda^{1-k}}{\lambda-\lambda^{-1}} \\
&= \frac{\lambda^{1-k}-\lambda^{k-1}}{\lambda-\lambda^{-1}} \\
\sigma(k) &= \frac{1}{\lambda-\lambda^{-1}}\lambda^{k} - \frac{1}{\lambda-\lambda^{-1}}\lambda^{-k} \\
&= \frac{\lambda^{k}-\lambda^{-k}}{\lambda-\lambda^{-1}}
\end{aligned}
$$

So now we have two linearly independent fundamental solutions $\rho(k)$ and $\sigma(k)$.

$$
\rho(k) = \frac{\lambda^{1-k}-\lambda^{k-1}}{\lambda-\lambda^{-1}} \quad \text{and} \quad \sigma(k) = \frac{\lambda^{k}-\lambda^{-k}}{\lambda-\lambda^{-1}} \tag{2.14}
$$

2.2 General Solution

Using these fundamental solutions, we are able to formulate the general solution of (1.21), which takes the form

$$\varphi_k = \varphi_{k_0}\rho(k-k_0) + \varphi_{k_0+1}\sigma(k-k_0) + \frac{1}{\alpha}\begin{cases} -\sum_{j=k_0+1}^{k} h_j\sigma(k-j) & k > k_0 \\ 0 & k = k_0 \\ \sum_{j=k+1}^{k_0} h_j\sigma(k-j) & k < k_0 \end{cases} \tag{2.15}$$

We have formulated our particular solution

$$\varphi_k = \frac{1}{\alpha}\begin{cases} -\sum_{j=k_0+1}^{k} h_j\sigma(k-j) & k > k_0 \\ 0 & k = k_0 \\ \sum_{j=k+1}^{k_0} h_j\sigma(k-j) & k < k_0 \end{cases} \tag{2.16}$$

of (1.21) using Jacobi operator theory following the work of Teschl [5] and its use by Humphries, et al. [6]. In the Appendix we perform the calculations necessary to verify that the function (2.16) is indeed a particular solution of (1.21).

Let k_0^* be the integer satisfying $k_0^* = \lfloor \eta_0 \rfloor$. Let k_1^* be the integer satisfying $k_1^* = \lceil \eta_1 \rceil$. *This choice of floor and ceiling, respectively, as specific rounding functions is arbitrary, although some kind of integer rounding is necessary here for our methods. The choice we have made here is a natural one which produces elegant results, although we could have also switched the functions to ceiling and floor respectively and had equally nice results. We could actually choose any combination of rounding functions and still solve the problem, with only slight changes to the explicit form of our results.* It simplifies our result to notice that, because it is made up of discrete Heaviside functions, the function h_k takes the form

$$h_k = \begin{cases} 0, & k > k_1^* \\ h_{k_1^*}, & k = k_1^* \\ 1, & k_0^* < k < k_1^* \\ h_{k_0^*}, & k = k_0^* \\ 0, & k < k_0^*, \end{cases} \tag{2.17}$$

where we define

$$h_{k_0^*} = \begin{cases} [0,1], & \eta_0 \in \mathbb{Z} \\ 0, & \eta_0 \notin \mathbb{Z} \end{cases} \quad \text{and} \quad h_{k_1^*} = \begin{cases} [0,1], & \eta_1 \in \mathbb{Z} \\ 0, & \eta_1 \notin \mathbb{Z}. \end{cases} \tag{2.18}$$

To illustrate this we show in Figure 2.1 two different waves, both with $a = .4$. We also plot in dashed lines the value of h_k for each of these waves. One of these waves crosses a at lattice points and the other crosses a in-between lattice points. As in (2.17), $h_k = 0$ for all points where the wave is below a, because the wave is below a for $k < k_0^*$ and $k > k_1^*$. Conversely, $h_k = 1$ for all points where the wave is above a, because the wave is above a for $k_0^* < k < k_1^*$. The value (2.18) of h_k at the points k_0^* and k_1^* depends on our choice of ceiling and floor as rounding functions. In the plot on the left, the wave does not cross a at lattice points. Since we have chosen $k_0^* = \lfloor \eta_0 \rfloor$, that means that k_0^* is to the left of the first crossing and so $\varphi(k_0^*) < a$ which means that $h_{k_0^*} = 0$. Since we have chosen $k_1^* = \lceil \eta_1 \rceil$, that means that k_1^* is to the right of the second crossing and so $\varphi(k_1^*) < a$ which means that $h_{k_1^*} = 0$. This shows why $h_{k_j^*} = 0$ if $\eta_j \notin \mathbb{Z}$. In the plot on the right, the wave crosses a at lattice points, so h_k at these points is set valued $[0,1]$. This shows why $h_{k_j^*} = [0,1]$ if $\eta_j \in \mathbb{Z}$.

To simply the form of the solution, we sum only over the range of values of j where $h_j = 1$ and do not include in the summation the indices where $h_j = 0$. That way we can

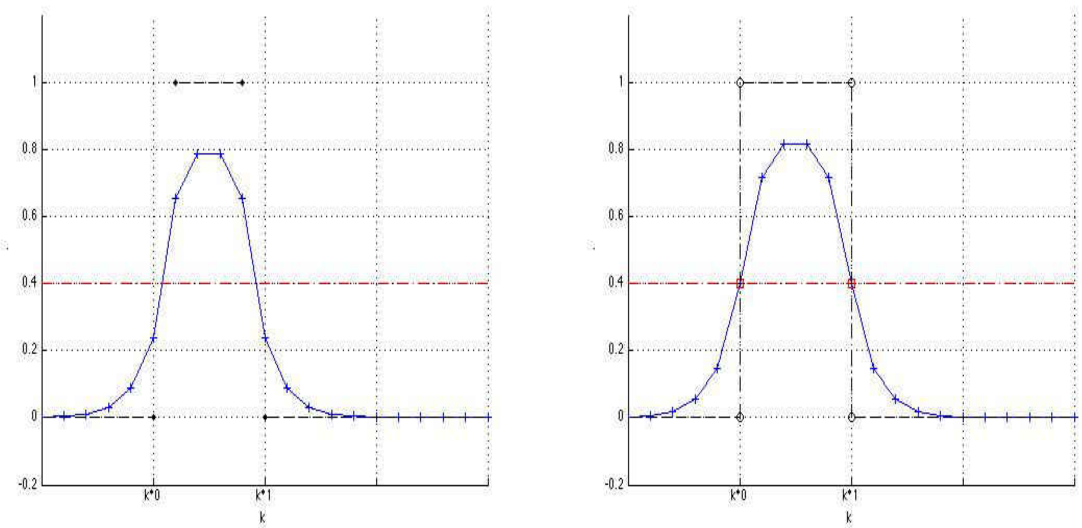

Figure 2.1: Two different waves, both with a=.4. The values of h_k are plotted as dashed lines. The wave on the left crosses a in-between lattice points. The wave on the right crosses a at lattice points.

eliminate all of the terms h_j except at the points k_0^* and k_1^*, which remain in the equation. Setting $k_0 = k_0^*$ gives us the form of the general solution:

$$\varphi_k = \varphi_{k_0^*}\rho(k-k_0^*) + \varphi_{k_0^*+1}\sigma(k-k_0^*) + \frac{1}{\alpha}\begin{cases} -[\sum_{j=k_0^*+1}^{k_1^*-1}\sigma(k-j)] - h_{k_1^*}\sigma(k-k_1^*) & k > k_1^* \\ -\sum_{j=k_0^*+1}^{k_1^*-1}\sigma(k_1^*-j) & k = k_1^* \\ -\sum_{j=k_0^*+1}^{k-1}\sigma(k-j) & k_0^* < k < k_1^* \\ 0 & k = k_0^* \\ h_{k_0^*}\sigma(k-k_0^*) & k < k_0^*. \end{cases}$$

Noting that $\sigma(0) = 0$, we can simplify this equation more to get:

$$\varphi_k = \varphi_{k_0^*}\rho(k-k_0^*)+\varphi_{k_0^*+1}\sigma(k-k_0^*)+\frac{1}{\alpha}\begin{cases} -[\sum_{j=k_0^*+1}^{k_1^*-1}\sigma(k-j)] - h_{k_1^*}\sigma(k-k_1^*) & k \geq k_1^* \\ -\sum_{j=k_0^*+1}^{k-1}\sigma(k-j) & k_0^* < k < k_1^* \\ h_{k_0^*}\sigma(k-k_0^*) & k \leq k_0^*. \end{cases} \tag{2.19}$$

This formulation of the solution becomes important in the case of inhomogeneous diffusion. We see from [6] that in the case of inhomogeneous diffusion, we would have the same form of the solution as in (2.19), except that the fundamental solutions ρ and σ would be different since the diffusion coefficients would be different.

Note: Due to translational invariance of solutions, we could choose to simply set $k_0^* = 0$ *and thus have one less term in our solutions. We choose to leave* k_0^* *in our equations in order for the solutions to be more general, and having* k_0^* *in the final solutions will help to illustrate their symmetry. Keeping the formula more general in this way will also be beneficial when moving forward to the case of inhomogeneous diffusion.*

In order to state the solution (2.19) explicitly, we must find $\varphi_{k_0^*}$ and $\varphi_{k_0^*+1}$.

2.3 Derivation of $\varphi_{k_0^*}$ and $\varphi_{k_0^*+1}$

The formula (2.19) we have for φ_k includes the two terms $\varphi_{k_0^*}$ and $\varphi_{k_0^*+1}$. These terms are not arbitrary and in order to explicitly state our solutions, we must find the values of $\varphi_{k_0^*}$ and $\varphi_{k_0^*+1}$ that give us solutions satisfying the two boundary conditions (1.19). We will use these boundary conditions to find $\varphi_{k_0^*}$ and $\varphi_{k_0^*+1}$.

For $k \leq k_0^*$:

$$\varphi_k = \varphi_{k_0^*}\rho(k-k_0^*) + \varphi_{k_0^*+1}\sigma(k-k_0^*) + \frac{1}{\alpha}(h_{k_0^*}\sigma(k-k_0^*))$$

Substituting in (2.14), we get

$$\begin{aligned}
\varphi_k &= \varphi_{k_0^*}\frac{\lambda^{1+k_0^*-k}-\lambda^{k-k_0^*-1}}{\lambda-\lambda^{-1}}+\varphi_{k_0^*+1}\frac{\lambda^{k-k_0^*}-\lambda^{k_0^*-k}}{\lambda-\lambda^{-1}}+\frac{1}{\alpha}h_{k_0^*}\frac{\lambda^{k-k_0^*}-\lambda^{k_0^*-k}}{\lambda-\lambda^{-1}}\\
&= \frac{\lambda^{k_0^*-k}}{\lambda-\lambda^{-1}}\left(\lambda\varphi_{k_0^*}-\varphi_{k_0^*+1}-\frac{h_{k_0^*}}{\alpha}\right)+\frac{\lambda^{k-k_0^*}}{\lambda-\lambda^{-1}}\left(-\lambda^{-1}\varphi_{k_0^*}+\varphi_{k_0^*+1}+\frac{h_{k_0^*}}{\alpha}\right)
\end{aligned}$$

To satisfy the boundary condition (1.19) at $k\to-\infty$, it must be that

$$\lambda\varphi_{k_0^*}-\varphi_{k_0^*+1}-\frac{h_{k_0^*}}{\alpha}=0. \tag{2.20}$$

For $k\geq k_1^*$:

$$\begin{aligned}
\varphi_k &= \varphi_{k_0^*}\rho(k-k_0^*)+\varphi_{k_0^*+1}\sigma(k-k_0^*)+\frac{1}{\alpha}\left\{-\left[\sum_{j=k_0^*+1}^{k_1^*-1}\sigma(k-j)\right]-h_{k_1^*}\sigma(k-k_1^*)\right\}\\
&= \varphi_{k_0^*}\frac{\lambda^{1+k_0^*-k}-\lambda^{k-k_0^*-1}}{\lambda-\lambda^{-1}}+\varphi_{k_0^*+1}\frac{\lambda^{k-k_0^*}-\lambda^{k_0^*-k}}{\lambda-\lambda^{-1}}\\
&\quad+\frac{1}{\alpha}\left\{-\left[\sum_{j=k_0^*+1}^{k_1^*-1}\frac{\lambda^{k-j}-\lambda^{j-k}}{\lambda-\lambda^{-1}}\right]-h_{k_1^*}\frac{\lambda^{k-k_1^*}-\lambda^{k_1^*-k}}{\lambda-\lambda^{-1}}\right\}\\
&= \frac{\lambda^{k_0^*-k}}{\lambda-\lambda^{-1}}\left\{\lambda\varphi_{k_0^*}-\varphi_{k_0^*+1}+\frac{1}{\alpha}\lambda^{-k_0^*}\left[\left(\sum_{j=k_0^*+1}^{k_1^*-1}\lambda^{j}\right)+h_{k_1^*}\lambda^{k_1^*}\right]\right\}\\
&\quad-\frac{\lambda^{k-k_0^*}}{\lambda-\lambda^{-1}}\left\{\lambda^{-1}\varphi_{k_0^*}-\varphi_{k_0^*+1}+\frac{1}{\alpha}\lambda^{k_0^*}\left[\left(\sum_{j=k_0^*+1}^{k_1^*-1}\lambda^{-j}\right)+h_{k_1^*}\lambda^{-k_1^*}\right]\right\}
\end{aligned}$$

To satisfy the boundary condition (1.19) at $k\to\infty$, it must be that

$$\lambda^{-1}\varphi_{k_0^*}-\varphi_{k_0^*+1}+\frac{1}{\alpha}\lambda^{k_0^*}\left[\left(\sum_{j=k_0^*+1}^{k_1^*-1}\lambda^{-j}\right)+h_{k_1^*}\lambda^{-k_1^*}\right]=0. \tag{2.21}$$

Consider the finite geometric series involved here:

$$\sum_{j=k_0^*+1}^{k_1^*-1} \lambda^{-j} \quad = \quad \frac{\lambda^{-k_0^*-1} - \lambda^{-k_1^*}}{1-\lambda^{-1}}$$

Substituting this into (2.21), we get

$$\lambda^{-1}\varphi_{k_0^*} - \varphi_{k_0^*+1} + \frac{1}{\alpha}\lambda^{k_0^*}\left[\frac{\lambda^{-k_0^*-1} - \lambda^{-k_1^*}}{1-\lambda^{-1}} + h_{k_1^*}\lambda^{-k_1^*}\right] = 0.$$

$$\lambda^{-1}\varphi_{k_0^*} - \varphi_{k_0^*+1} + \frac{1}{\alpha}\left[\frac{\lambda^{-1} - \lambda^{k_0^*-k_1^*}}{1-\lambda^{-1}} + h_{k_1^*}\lambda^{k_0^*-k_1^*}\right] = 0. \tag{2.22}$$

We also have the identity

$$\frac{1}{\alpha} = \frac{(\lambda-1)(1-\lambda^{-1})}{(1+\gamma)}. \tag{2.23}$$

To verify this identity, we start with (2.6).

$$\begin{aligned}
\lambda^2 - 2\mu\lambda + 1 &= 0 \\
\lambda - 2\mu + \lambda^{-1} &= 0 \\
\lambda + \lambda^{-1} &= 2\mu \\
&= \frac{1}{\alpha}(1+\gamma+2\alpha) \\
&= \frac{1}{\alpha}(1+\gamma) + 2 \\
\lambda + \lambda^{-1} - 2 &= \frac{1}{\alpha}(1+\gamma) \\
(\lambda-1)(1-\lambda^{-1}) &= \frac{1}{\alpha}(1+\gamma) \\
\frac{(\lambda-1)(1-\lambda^{-1})}{(1+\gamma)} &= \frac{1}{\alpha}
\end{aligned}$$

We can plug this identity (2.23) into (2.20) and (2.22) to take α out of the equations. We have already defined $\beta = \frac{1}{(1+\gamma)}$, so $\frac{1}{\alpha} = \beta(\lambda - 1)(1 - \lambda^{-1})$. (2.20) becomes:

$$\lambda\varphi_{k_0^*} - \varphi_{k_0^*+1} - h_{k_0^*}\beta(\lambda - 1)(1 - \lambda^{-1}) = 0.$$

This gives us:

$$\varphi_{k_0^*+1} = \lambda\varphi_{k_0^*} - h_{k_0^*}\beta(\lambda - 1)(1 - \lambda^{-1}). \tag{2.24}$$

Using (2.23), (2.22) becomes:

$$\lambda^{-1}\varphi_{k_0^*} - \varphi_{k_0^*+1} + \beta(\lambda - 1)(1 - \lambda^{-1}) \left[\frac{\lambda^{-1} - \lambda^{k_0^*-k_1^*}}{1 - \lambda^{-1}} + h_{k_1^*}\lambda^{k_0^*-k_1^*}\right] = 0. \tag{2.25}$$

Now we can substitute (2.24) into (2.25) to get

$$\begin{aligned}
\lambda^{-1}\varphi_{k_0^*} - \lambda\varphi_{k_0^*} + h_{k_0^*}\beta(\lambda - 1)(1 - \lambda^{-1}) + \beta(\lambda - 1)(1 - \lambda^{-1}) \left[\frac{\lambda^{-1} - \lambda^{k_0^*-k_1^*}}{1 - \lambda^{-1}} + h_{k_1^*}\lambda^{k_0^*-k_1^*}\right] &= 0 \\
(\lambda^{-1} - \lambda)\varphi_{k_0^*} + \beta(\lambda - 1)(1 - \lambda^{-1}) \left[h_{k_0^*} + \frac{1 - \lambda^{1+k_0^*-k_1^*}}{\lambda - 1} + h_{k_1^*}\lambda^{k_0^*-k_1^*}\right] &= 0 \\
(\lambda - \lambda^{-1})\varphi_{k_0^*} &= \beta(\lambda - 1)(1 - \lambda^{-1}) \left[h_{k_0^*} + \frac{1 - \lambda^{1+k_0^*-k_1^*}}{\lambda - 1} + h_{k_1^*}\lambda^{k_0^*-k_1^*}\right] \\
\varphi_{k_0^*} &= \beta\frac{(\lambda - 1)(1 - \lambda^{-1})}{(\lambda - \lambda^{-1})} \left[h_{k_0^*} + \frac{1 - \lambda^{1+k_0^*-k_1^*}}{\lambda - 1} + h_{k_1^*}\lambda^{k_0^*-k_1^*}\right]
\end{aligned}$$

$$\varphi_{k_0^*} = \beta\frac{(\lambda - 1)}{(\lambda + 1)} \left[h_{k_0^*} + \frac{1 - \lambda^{1+k_0^*-k_1^*}}{\lambda - 1} + h_{k_1^*}\lambda^{k_0^*-k_1^*}\right] \tag{2.26}$$

Substituting (2.26) into (2.24), we get

$$\varphi_{k_0^*+1} = \lambda\beta\frac{(\lambda - 1)}{(\lambda + 1)} \left[h_{k_0^*} + \frac{1 - \lambda^{1+k_0^*-k_1^*}}{\lambda - 1} + h_{k_1^*}\lambda^{k_0^*-k_1^*}\right] - h_{k_0^*}\beta(\lambda - 1)(1 - \lambda^{-1}). \tag{2.27}$$

We have now solved for the terms $\varphi_{k_0^*}$ and $\varphi_{k_0^*+1}$ needed give us an explicit solution for φ_k as in (2.19).

3 SIMPLIFICATION OF SOLUTIONS

Now that we have explicit solutions for φ_k, it is the purpose of this section to simplify those solutions into the most compact formulas possible. First we work on a formula that covers all possible standing waves. After that we look into the different types of wave solutions based on the different possible conditions from Section 2.2, (2.18), and create different formulas for each case.

3.1 Solution for the General Case

In this section we look to compact the formula of solutions as much as possible while still covering all of our types of solutions. This formula will still include the terms $h_{k_0^*}$ and $h_{k_1^*}$, which depend respectively on η_0 and η_1, the parameters that tell us whether a wave crosses a at lattice points or not.

For $k \leq k_0^*$, noting (2.20),

$$\begin{aligned}
\varphi_k &= \frac{\lambda^{k-k_0^*}}{\lambda-\lambda^{-1}}[-\lambda^{-1}\varphi_{k_0^*}+\varphi_{k_0^*+1}+\frac{h_{k_0^*}}{\alpha}] \\
&= \frac{\lambda^{k-k_0^*}}{\lambda-\lambda^{-1}}[-\lambda^{-1}\varphi_{k_0^*}+(\lambda\varphi_{k_0^*}-\frac{h_{k_0^*}}{\alpha})+\frac{h_{k_0^*}}{\alpha}] \\
&= \frac{\lambda^{k-k_0^*}}{\lambda-\lambda^{-1}}[(\lambda-\lambda^{-1})\varphi_{k_0^*}] \\
&= \varphi_{k_0^*}\lambda^{k-k_0^*}
\end{aligned}$$

For $k \geq k_1^*$, noting (2.21),

$$\begin{aligned}
\varphi_k &= \frac{\lambda^{k_0^*-k}}{\lambda-\lambda^{-1}}\left[\lambda\varphi_{k_0^*}-\varphi_{k_0^*+1}+\frac{1}{\alpha}\lambda^{-k_0^*}([\sum_{j=k_0^*+1}^{k_1^*-1}\lambda^j]+h_{k_1^*}\lambda^{k_1^*})\right] \\
&= \frac{\lambda^{k_0^*-k}}{\lambda-\lambda^{-1}}\left[\lambda\varphi_{k_0^*}-(\lambda\varphi_{k_0^*}-\frac{h_{k_0^*}}{\alpha})+\frac{1}{\alpha}\lambda^{-k_0^*}(\frac{\lambda^{k_0^*+1}-\lambda^{k_1^*}}{1-\lambda}+h_{k_1^*}\lambda^{k_1^*})\right]
\end{aligned}$$

$$
\begin{aligned}
&= \frac{\lambda^{k_0^*-k}}{\lambda-\lambda^{-1}}\left[\frac{1}{\alpha}(h_{k_0^*}+\frac{\lambda-\lambda^{k_1^*-k_0^*}}{1-\lambda}+h_{k_1^*}\lambda^{k_1^*-k_0^*})\right] \\
&= \frac{\lambda^{k_0^*-k}}{(\lambda+1)(1-\lambda^{-1})}\beta(\lambda-1)(1-\lambda^{-1})\left[h_{k_0^*}+\frac{\lambda^{k_1^*-k_0^*}-\lambda}{\lambda-1}+h_{k_1^*}\lambda^{k_1^*-k_0^*}\right] \\
&= \lambda^{-k}\beta\frac{(\lambda-1)}{(\lambda+1)}\left[h_{k_0^*}\lambda^{k_0^*}+\frac{\lambda^{k_1^*}-\lambda^{k_0^*+1}}{\lambda-1}+h_{k_1^*}\lambda^{k_1^*}\right] \\
&= \lambda^{k_1^*-k}\beta\frac{(\lambda-1)}{(\lambda+1)}\left[h_{k_0^*}\lambda^{k_0^*-k_1^*}+\frac{1-\lambda^{1+k_0^*-k_1^*}}{\lambda-1}+h_{k_1^*}\right]
\end{aligned}
$$

Setting $k = k_1^*$ gives us

$$
\varphi_{k_1^*} = \beta\frac{(\lambda-1)}{(\lambda+1)}\left[h_{k_0^*}\lambda^{k_0^*-k_1^*}+\frac{1-\lambda^{1+k_0^*-k_1^*}}{\lambda-1}+h_{k_1^*}\right] \tag{3.1}
$$

and so we can write, for $k \geq k_1^*$:

$$
\varphi_k = \varphi_{k_1^*}\lambda^{k_1^*-k} \tag{3.2}
$$

For $k_0^* < k < k_1^*$:

$$
\begin{aligned}
\varphi_k &= \varphi_{k_0^*}\rho(k-k_0^*)+\varphi_{k_0^*+1}\sigma(k-k_0^*)-\frac{1}{\alpha}\left[\sum_{j=k_0^*+1}^{k-1}\sigma(k-j)\right] \\
&= \varphi_{k_0^*}\frac{\lambda^{1+k_0^*-k_1^*}-\lambda^{k-k_0^*-1}}{\lambda-\lambda^{-1}}+\varphi_{k_0^*+1}\frac{\lambda^{k-k_0^*}-\lambda^{k_0^*-k}}{\lambda-\lambda^{-1}}-\frac{1}{\alpha}\left[\sum_{j=k_0^*+1}^{k-1}\frac{\lambda^{k-j}-\lambda^{j-k}}{\lambda-\lambda^{-1}}\right] \\
&= \frac{1}{\lambda-\lambda^{-1}}\left[\varphi_{k_0^*}(\lambda^{1+k_0^*-k_1^*}-\lambda^{k-k_0^*-1})+\varphi_{k_0^*+1}(\lambda^{k-k_0^*}-\lambda^{k_0^*-k})\right. \\
&\quad \left.-\frac{1}{\alpha}\lambda^k\left(\sum_{j=k_0^*+1}^{k-1}\lambda^{-j}\right)+\frac{1}{\alpha}\lambda^{-k}\left(\sum_{j=k_0^*+1}^{k-1}\lambda^{j}\right)\right] \\
&= \frac{1}{\lambda-\lambda^{-1}}\left[\varphi_{k_0^*}(\lambda^{1+k_0^*-k_1^*}-\lambda^{k-k_0^*-1})+(\lambda\varphi_{k_0^*}-\frac{h_{k_0^*}}{\alpha}(\lambda^{k-k_0^*}-\lambda^{k_0^*-k})\right. \\
&\quad \left.-\frac{1}{\alpha}\lambda^k\left(\frac{\lambda^{-k_0^*-1}-\lambda^{-k}}{1-\lambda^{-1}}\right)+\frac{1}{\alpha}\lambda^{-k}\left(\frac{\lambda^{k_0^*+1}-\lambda^{k}}{1-\lambda}\right)\right] \\
&= \frac{1}{\lambda-\lambda^{-1}}\left[\varphi_{k_0^*}(\lambda^{k-k_0^*+1}-\lambda^{k-k_0^*-1})-\frac{h_{k_0^*}}{\alpha}(\lambda^{k-k_0^*}-\lambda^{k_0^*-k})\right.
\end{aligned}
$$

$$
\begin{aligned}
& -\frac{1}{\alpha}\left(\frac{\lambda^{k-k_0^*-1}-1}{1-\lambda^{-1}}\right)+\frac{1}{\alpha}\left(\frac{\lambda^{k_0^*+1-k}-1}{1-\lambda}\right)\Bigg]\Bigg] \\
= \;& \frac{1}{\lambda-\lambda^{-1}}\left[\varphi_{k_0^*}\lambda^{k-k_0^*}(\lambda-\lambda^{-1})-\frac{h_{k_0^*}}{\alpha}(\lambda^{k-k_0^*}-\lambda^{k_0^*-k})\right. \\
& \left.-\beta(\lambda-1)(1-\lambda^{-1})\frac{(\lambda^{k-k_0^*}-\lambda)}{(\lambda-1)}+\beta(\lambda-1)(1-\lambda^{-1})\frac{(1-\lambda^{k_0^*+1-k})}{(\lambda-1)}\right] \\
= \;& \varphi_{k_0^*}\lambda^{k-k_0^*}+\frac{1}{(\lambda+1)(1-\lambda^{-1})}\left[-h_{k_0^*}\beta(\lambda-1)(1-\lambda^{-1})(\lambda^{k-k_0^*}-\lambda^{k_0^*-k})\right. \\
& \left.-\beta(1-\lambda^{-1})(\lambda^{k-k_0^*}-\lambda)+\beta(1-\lambda^{-1})(1-\lambda^{k_0^*+1-k})\right] \\
= \;& \varphi_{k_0^*}\lambda^{k-k_0^*}+\beta\frac{1}{(\lambda+1)}\left[-h_{k_0^*}(\lambda-1)(\lambda^{k-k_0^*}-\lambda^{k_0^*-k})-(\lambda^{k-k_0^*}-\lambda)+(1-\lambda^{k_0^*+1-k})\right] \\
= \;& \lambda^{k-k_0^*}\beta\frac{(\lambda-1)}{(\lambda+1)}\left[h_{k_0^*}+\frac{1-\lambda^{1+k_0^*-k_1^*}}{\lambda-1}+h_{k_1^*}\lambda^{k_0^*-k_1^*}\right] \\
& +\beta\frac{(\lambda-1)}{(\lambda+1)}\left[-h_{k_0^*}(\lambda^{k-k_0^*}-\lambda^{k_0^*-k})\right]+\beta\frac{1}{(\lambda+1)}\left[1+\lambda-\lambda^{k-k_0^*}-\lambda^{k_0^*+1-k}\right] \\
= \;& \beta\frac{(\lambda-1)}{(\lambda+1)}\left[h_{k_0^*}\lambda^{k-k_0^*}+\frac{\lambda^{k-k_0^*}-\lambda^{k+1-k_1^*}}{\lambda-1}+h_{k_1^*}\lambda^{k-k_1^*}\right] \\
& +\beta\frac{(\lambda-1)}{(\lambda+1)}\left[-h_{k_0^*}(\lambda^{k-k_0^*}-\lambda^{k_0^*-k})\right]+\beta-\beta\frac{1}{(\lambda+1)}\left[\lambda^{k-k_0^*}+\lambda^{k_0^*+1-k}\right] \\
= \;& \beta\frac{(\lambda-1)}{(\lambda+1)}\left[h_{k_0^*}\lambda^{k-k_0^*}+h_{k_1^*}\lambda^{k-k_1^*}-h_{k_0^*}(\lambda^{k-k_0^*}-\lambda^{k_0^*-k})\right]+\beta \\
& +\beta\frac{1}{(\lambda+1)}\left[\lambda^{k-k_0^*}-\lambda^{k-k_1^*}-\lambda^{k-k_0^*}-\lambda^{k_0^*+1-k}\right] \\
= \;& \beta\left[1-\frac{\lambda}{(\lambda+1)}\left[\lambda^{k_0^*-k}+\lambda^{k-k_1^*}\right]+\frac{(\lambda-1)}{(\lambda+1)}\left[h_{k_0^*}\lambda^{k_0^*-k}+h_{k_1^*}\lambda^{k-k_1^*}\right]\right]
\end{aligned}
$$

Now we have a compact set of formulas for φ_k depending explicitly on λ, β, k_0^*, k_1^*, $h_{k_0^*}$, and $h_{k_1^*}$. Note that we already have formulas (2.26) and (3.1) for $\varphi_{k_0^*}$ and $\varphi_{k_1^*}$ which depend on these same parameters.

$$
\varphi_k = \begin{cases}
\varphi_{k_1^*}\lambda^{k_1^*-k} & k \geq k_1^* \\
\beta\left[1-\frac{\lambda}{(\lambda+1)}\left[\lambda^{k_0^*-k}+\lambda^{k-k_1^*}\right]+\frac{(\lambda-1)}{(\lambda+1)}\left[h_{k_0^*}\lambda^{k_0^*-k}+h_{k_1^*}\lambda^{k-k_1^*}\right]\right] & k_0^* < k < k_1^* \\
\varphi_{k_0^*}\lambda^{k-k_0^*} & k \leq k_0^*
\end{cases} \tag{3.3}
$$

Let $L = k - k_0^*$. This is a measure of a point k in relation to the left crossing, at the point k_0^*. Terms that involve L come from interaction with the left side or front. Let $R = k - k_1^*$. This is a measure of a point k in relation to the right crossing, at the point k_1^*. Terms that involve R come from interaction with the right side or front. Let $W = k_1^* - k_0^*$. This is a measure of the width of the pulse wave, or the distance between the two opposing fronts. This is also a measure of the amount of interaction between the two opposing fronts, with a small W indicating more interaction and a large W indicating less interaction. Note that $W = L - R$. At times, after we formulate a result, we restate it in terms of L, R, and W instead of k_0^* and k_1^* in order to illustrate which terms relate to which aspects of the wave. For example the formula (3.3) above can be restated as

$$\varphi_k = \begin{cases} \varphi_{k_1^*}\lambda^{-R} & k \geq k_1^* \\ \beta\left[1 - \frac{\lambda}{(\lambda+1)}\left[\lambda^{-L} + \lambda^R\right] + \frac{(\lambda-1)}{(\lambda+1)}\left[h_{k_0^*}\lambda^{-L} + h_{k_1^*}\lambda^R\right]\right] & k_0^* < k < k_1^* \\ \varphi_{k_0^*}\lambda^L & k \leq k_0^* \end{cases} \tag{3.4}$$

For the waves that we are focusing on, waves that cross a, we must have $W \geq 2$. This is because for a wave to actually cross a, it must have at least one point above a. To illustrate this point, in Figure 3.1 we show waves that have $W = 2$. It should then be clear that for $W < 2$ there could not be a point above a, and therefore the wave could not actually be crossing a.

We now have formulas of the solutions, but they still include the terms $h_{k_0^*}$ and $h_{k_1^*}$ whose values can be different under different cases. We cannot get precise individual waveforms until we assign single values to these two terms. It is important to note that we start out with these terms possibly being set valued, i.e. $[0, 1]$, so if they are equal to a range of values, this gives us a family of waves that fit the solution. But if we specify an exact wave or an exact value of a, that corresponds to single values of $h_{k_0^*}$ and $h_{k_1^*}$ inside this interval, and

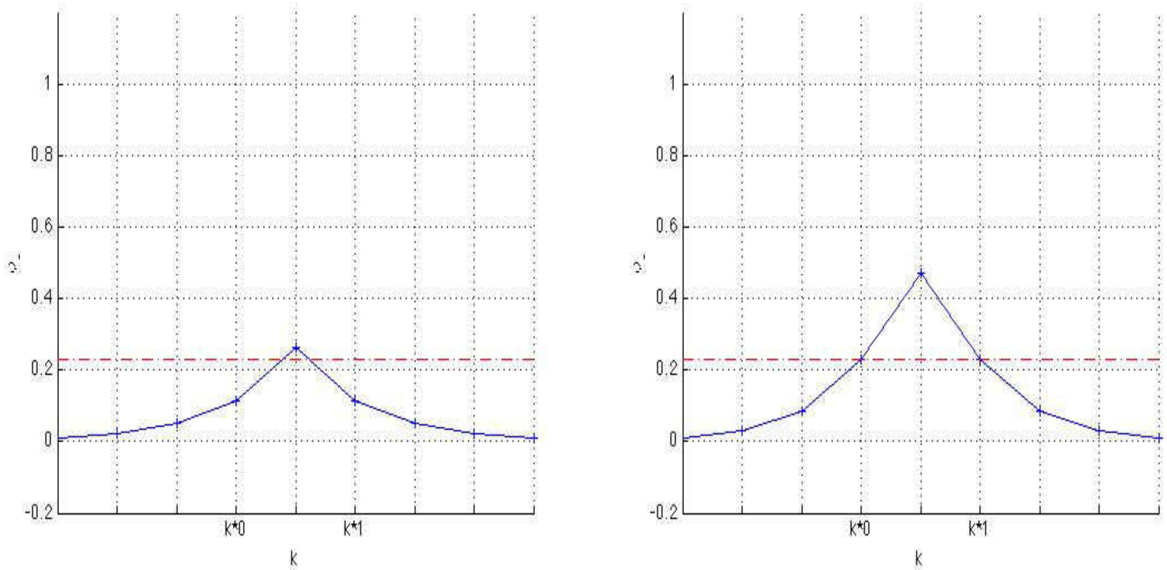

Figure 3.1: Waves with $W = 2$

vice-versa. To be able to determine the values of $h_{k_0^*}$ and $h_{k_1^*}$, we must break into cases and look at different possible types of waves depending on how the wave crosses a.

3.2 Final Solutions in the 4 Different Cases

We have four different cases depending on whether η_0 and η_1 are integers or not, or in other words depending on whether the wave crosses a at lattice points or not. The four cases will be named as follows. The *Stable* case has both crossings in-between lattice points, so $\eta_0 \notin \mathbb{Z}$ and $\eta_1 \notin \mathbb{Z}$. The *Unstable* case has both crossings at lattice points, so $\eta_0 \in \mathbb{Z}$ and $\eta_1 \in \mathbb{Z}$. The *Right-Unstable* case has the left side crossing in-between lattice points and the right side crossing at a lattice point, so $\eta_0 \notin \mathbb{Z}$ and $\eta_1 \in \mathbb{Z}$. The *Left-Unstable* case has the left side crossing at a lattice point and the right side crossing in-between lattice points, so $\eta_0 \in \mathbb{Z}$ and $\eta_1 \notin \mathbb{Z}$.

The reason for the stability related names given to each of these waves has to do with the unstable equilibrium point of the nonlinearity, $\varphi_{k_j^*} = a$, discussed in Section 1.2.1. All of the three types of standing wave solutions whose name includes "Unstable" have points, either two or one, that are at this unstable point $\varphi_{k_j^*} = a$. We show in Chapter 5 numerical results for waves of these types; the instability of this point makes the entire standing wave solution unstable. We call waves that do not have any points at the unstable equilibrium point "Stable", and we demonstrate numerically the stability of these waves in Chapter 5 as well. We do not analytically prove the stability or instability of entire wave solutions, but we use these terms as descriptive names for types of waves in the rest of the text.

We also divide these cases into another categorization. We call stable case and unstable case waves *symmetrical*, and we call right-unstable case and left-unstable case waves *asymmetrical*. For now this naming is based on the conditions of η_0 and η_1 that define the cases, but we will see that the solutions we derive for symmetrical waves really are symmetrical.

3.2.1 Stable Case

First, we consider the case where both of the crossings are not at lattice points, so $\eta_0, \eta_1 \notin \mathbb{Z}$. This means that $h_{k_0^*} = h_{k_1^*} = 0$. Substituting this into (2.26) and (3.1) we get

$$\varphi_{k_0^*} = \beta \frac{(1 - \lambda^{1+k_0^*-k_1^*})}{(\lambda + 1)}, \tag{3.5}$$

and

$$\varphi_{k_1^*} = \beta \frac{(1 - \lambda^{1+k_0^*-k_1^*})}{(\lambda + 1)}. \tag{3.6}$$

Substituting (3.5) and (3.6) into (3.3) we get

$$\varphi_k = \begin{cases} \beta \frac{(\lambda^{k_1^*-k} - \lambda^{1+k_0^*-k})}{(\lambda+1)} & k \geqslant k_1^* \\ \beta \left[1 - \frac{\lambda}{(\lambda+1)} \left[\lambda^{k-k_1^*} + \lambda^{k_0^*-k}\right]\right] & k_0^* < k < k_1^* \\ \beta \frac{(\lambda^{k-k_0^*} - \lambda^{1+k-k_1^*})}{(\lambda+1)} & k \leq k_0^*. \end{cases} \tag{3.7}$$

In terms of L and R,

$$\varphi_k = \begin{cases} \beta\frac{(\lambda^{-R}-\lambda^{1-L})}{(\lambda+1)} & k \geqslant k_1^* \\ \beta\left[1-\frac{\lambda}{(\lambda+1)}\left[\lambda^R+\lambda^{-L}\right]\right] & k_0^* < k < k_1^* \\ \beta\frac{(\lambda^{L}-\lambda^{1+R})}{(\lambda+1)} & k \leq k_0^*. \end{cases} \tag{3.8}$$

For each set of parameters α and γ, which are the parameters that determine β and λ, we have a family of candidate stable standing wave solutions. This family of solutions is countably infinite, because for each value of $W \geq 2$ we have a unique wave. Due to translational invariance, these waves are unique up to translation. In Figure 3.2 we show a family of stable waves, $\alpha = 1$, $\gamma = .1$, with each wave centered to emphasize symmetry. In Figure 3.3 we show the same family of stable waves, this time plotted with k_0^* at the same index for each wave. In Figure 3.4 we show the same family of waves, this time separated into two different plots, one of waves with even W and one of waves with odd W. In our symmetrical cases we call waves with even W *point-top* waves, and waves with odd W *flat-top* waves, for reasons that are obvious in the graphs.

For a given set of parameters α and γ, we have a family of candidate solutions. In other words, we have a candidate solution for each value of $W \geq 2$, and that solution is given by (3.7). Each of these candidate solutions is only a real solution if a falls in a certain range. We illustrate this in Figure 3.5. It is important to note that for stable waves, the wave form of the solution is independent of a, given the other parameters. In Figure 3.5 we show a wave with $W = 4$. On the left we have a at an acceptable value, so that our solution is consistent with our setup. On the right the value of a does not work with our solution. The value of a is too low in this case. Remember that we define k_0^* and k_1^* in relation to where the wave crosses a, so in this case we would have $k_0^* = -1$ and $k_1^* = 5$, giving us $W = 6$. This wave form is for $W = 4$ so that is why this is not a real solution. We have a different wave form

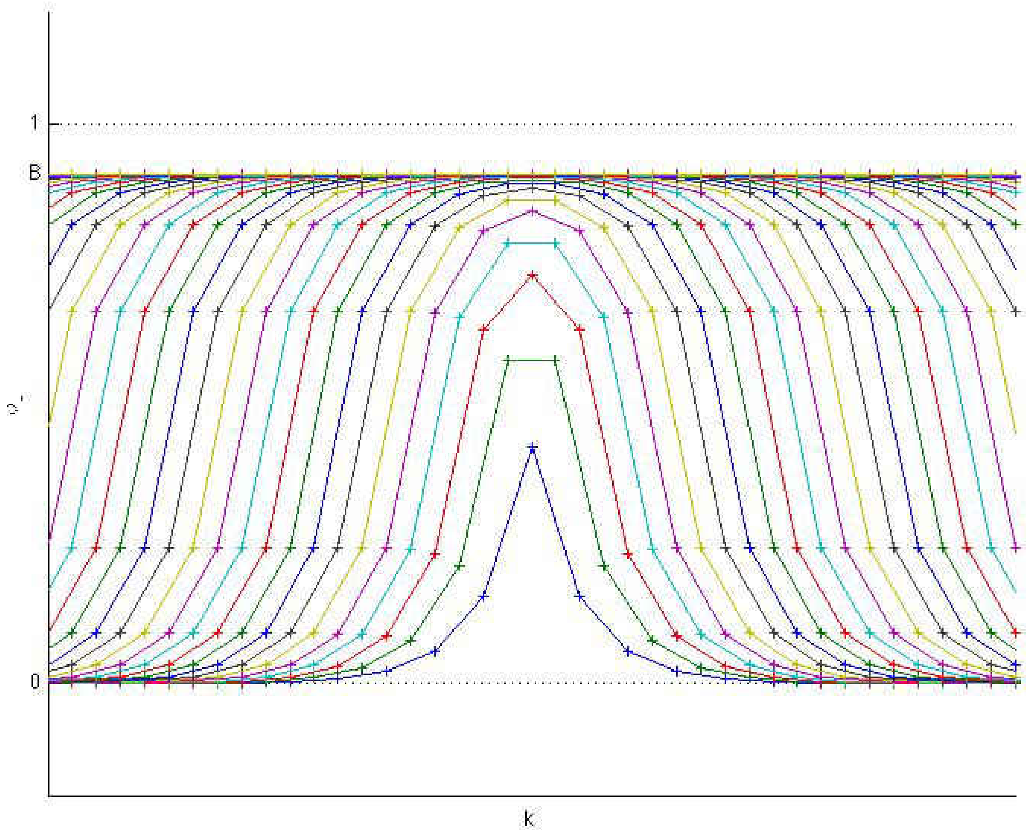

Figure 3.2: Family of stable waves, each wave centered to show symmetry. $\alpha = 1$, $\gamma = .1$. $\beta = .9091$ is labeled on the vertical axis.

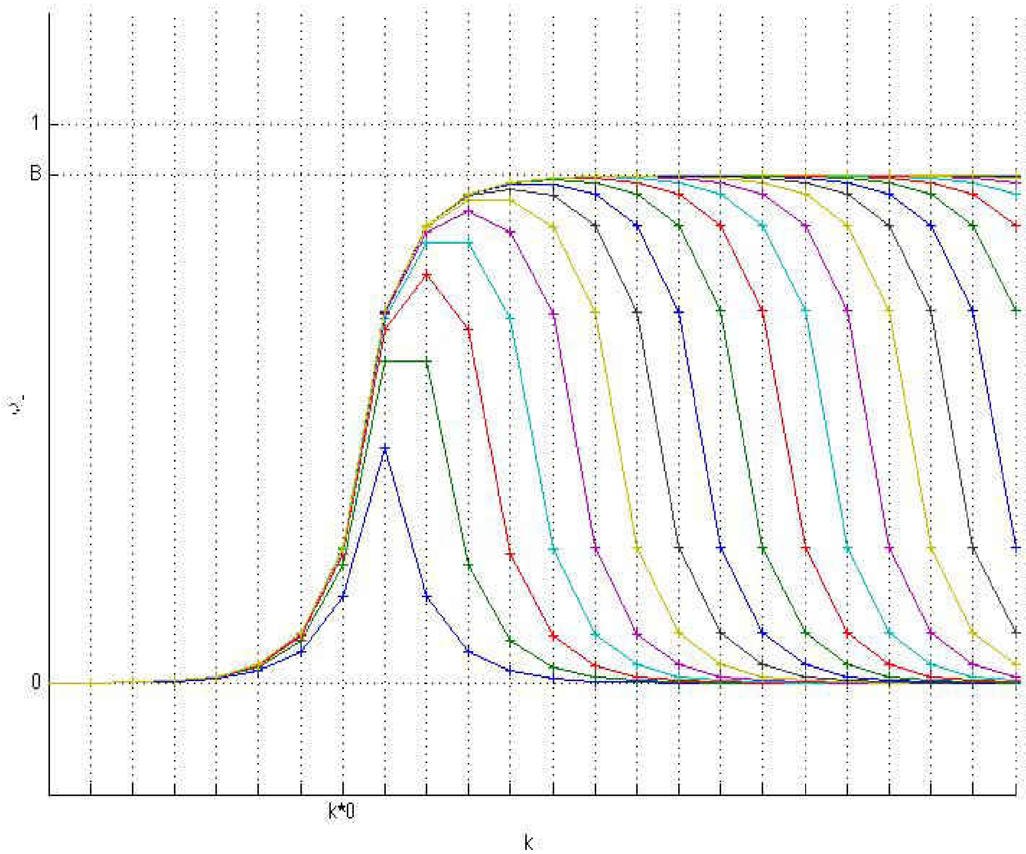

Figure 3.3: Family of stable waves, each plotted with the same k_0^*. $\alpha = 1$, $\gamma = .1$. $\beta = .9091$ is labeled on the vertical axis.

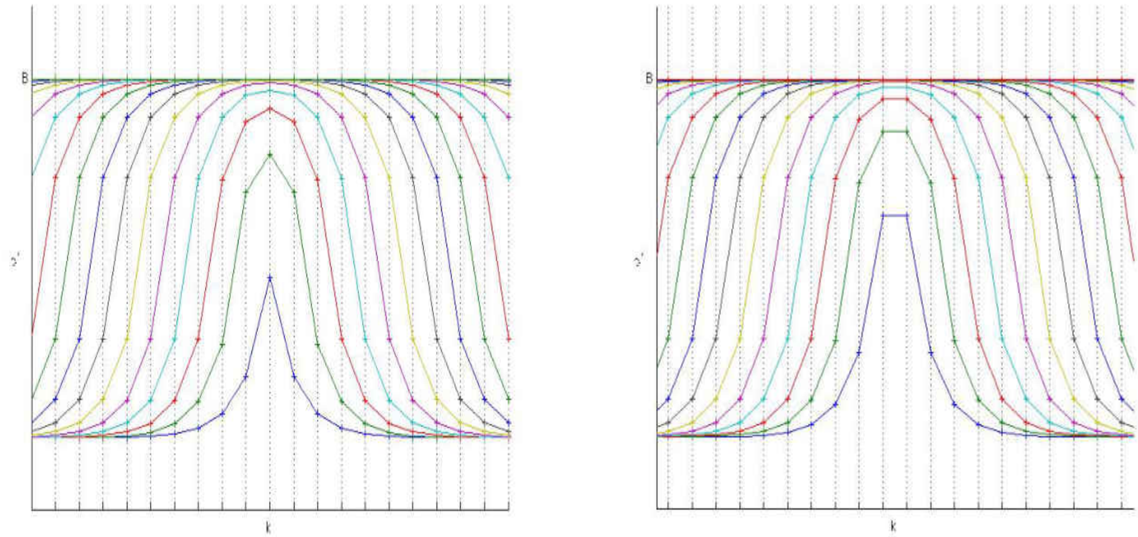

Figure 3.4: Family of stable waves. On the left, point-top waves with even W. On the right, flat-top waves with odd W. $\alpha = 1$, $\gamma = .1$

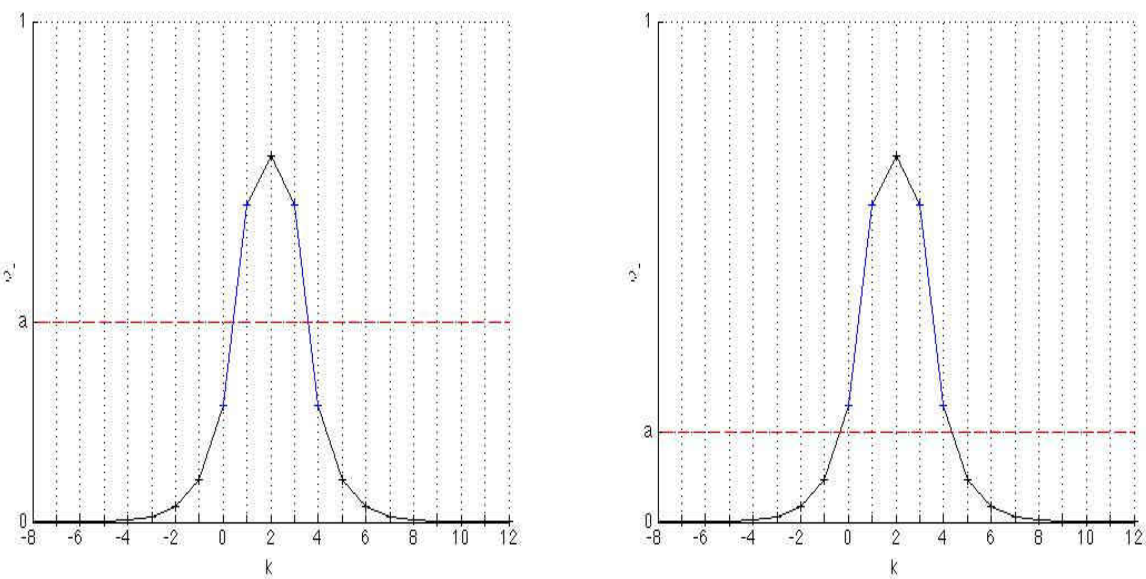

Figure 3.5: The wave form for a stable wave with $\alpha = 1$, $\gamma = .1$, and $W = 4$. On the left we have a at an acceptable value, this is a solution. On the right we have a at an unacceptable value, this is not a real solution.

for the member of this family with $W = 6$.

The range of values of a that works for each candidate solution is different, so given a family of candidate solutions, we could have values of a that work for all members of the family, for only some members of the family, or for none of the members of the family. We illustrate this in Figure 3.6 by showing a particular family of candidate solutions, and label three values of a as a1, a2, and a3. For a given family of solutions, there may be values of a, such as a1, for which all members of the family of candidate solutions are real standing wave solutions. For some values of a, such as a2, only some members of the family are real solutions. There are also values of a, such as a3, for which there exist no solutions, none of the family are real solutions. Whether or not there actually are values of a like a1 depends on the parameters α and γ. Determining the existence of these candidate solutions based on values of a is the subject of Chapter 4.

3.2.2 Unstable Case

Now we consider the case where both of the crossings are at lattice points, so $\eta_0,\ \eta_1 \in \mathbb{Z}$. This means that $h_{k_0^*} = [0, 1]$ and $h_{k_1^*} = [0, 1]$. It also means that $\varphi_{k_0^*} = \varphi_{k_1^*} = a$. So we know right away from (3.3) that for $k \leqslant k_0^*$, $\varphi_k = a\lambda^{k-k_0^*}$, and for $k \geq k_1^*$, $\varphi_k = a\lambda^{k_1^*-k}$. Also, since $\varphi_{k_0^*} = \varphi_{k_1^*}$:

$$\begin{aligned}
\varphi_{k_0^*} &= \varphi_{k_1^*} \\
\beta\frac{(\lambda-1)}{(\lambda+1)}\left[h_{k_0^*} + \frac{1-\lambda^{1+k_0^*-k_1^*}}{\lambda-1} + h_{k_1^*}\lambda^{k_0^*-k_1^*}\right] &= \beta\frac{(\lambda-1)}{(\lambda+1)}\left[h_{k_0^*}\lambda^{k_0^*-k_1^*} + \frac{1-\lambda^{1+k_0^*-k_1^*}}{\lambda-1} + h_{k_1^*}\right] \\
\left[h_{k_0^*} + \frac{1-\lambda^{1+k_0^*-k_1^*}}{\lambda-1} + h_{k_1^*}\lambda^{k_0^*-k_1^*}\right] &= \left[h_{k_0^*}\lambda^{k_0^*-k_1^*} + \frac{1-\lambda^{1+k_0^*-k_1^*}}{\lambda-1} + h_{k_1^*}\right] \\
\left[h_{k_0^*} + h_{k_1^*}\lambda^{k_0^*-k_1^*}\right] &= \left[h_{k_0^*}\lambda^{k_0^*-k_1^*} + h_{k_1^*}\right]
\end{aligned}$$

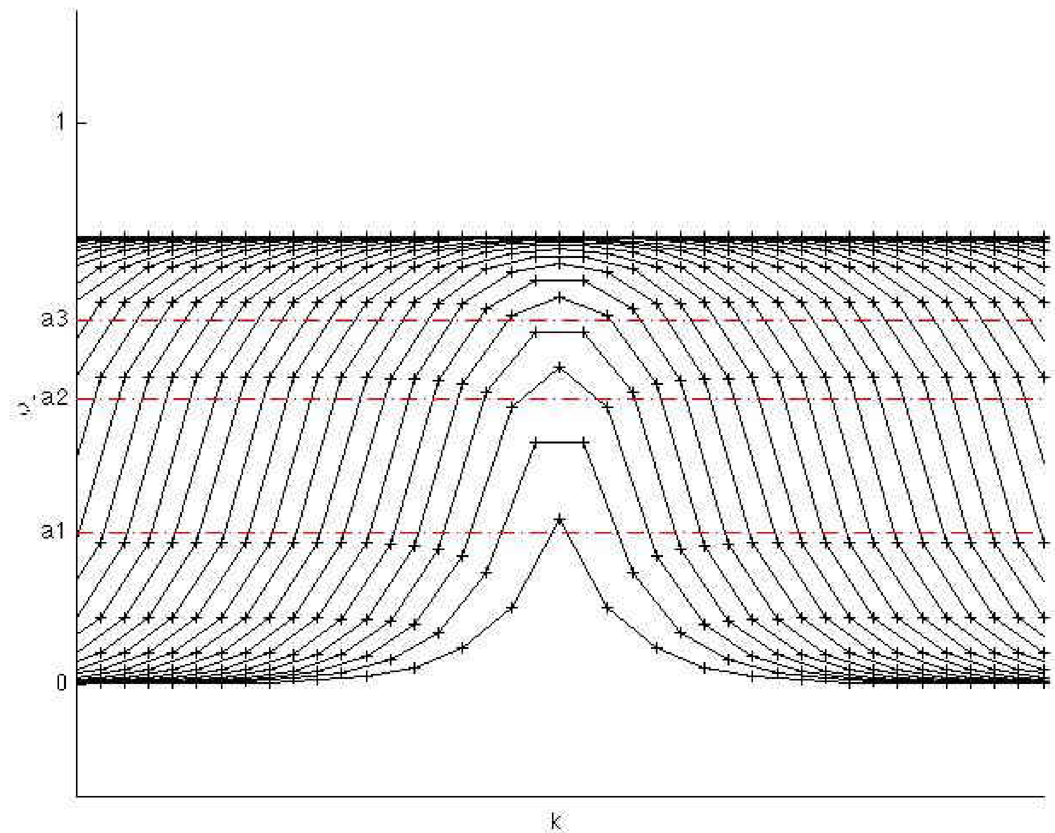

Figure 3.6: Family of stable waves. For a =a1, there exists the entire family of solutions, $W \geq 2$. For a =a2, there exist solutions for only $W \geq 5$. For a =a3, there exist no real solutions.

This implies that $h_{k_0^*} = h_{k_1^*}$. Since we have specified a single value of a, these terms $h_{k_0^*}$ and $h_{k_1^*}$ have a single value in the interval $[0, 1]$ and that value is the same for both of them. Now we need to solve for what that value is in terms of a.

$$\begin{aligned}
a &= \varphi_{k_0^*} = \beta\frac{(\lambda-1)}{(\lambda+1)}\left[h_{k_0^*} + \frac{1-\lambda^{1+k_0^*-k_1^*}}{\lambda-1} + h_{k_1^*}\lambda^{k_0^*-k_1^*}\right] \\
&= \beta\frac{(\lambda-1)}{(\lambda+1)}\left[h_{k_0^*} + \frac{1-\lambda^{1+k_0^*-k_1^*}}{\lambda-1} + h_{k_0^*}\lambda^{k_0^*-k_1^*}\right] \\
&= \beta\frac{(\lambda-1)}{(\lambda+1)}\left[h_{k_0^*}(1+\lambda^{k_0^*-k_1^*}) + \frac{1-\lambda^{1+k_0^*-k_1^*}}{\lambda-1}\right] \\
&= \beta h_{k_0^*}\frac{(\lambda-1)}{(\lambda+1)}(1+\lambda^{k_0^*-k_1^*}) + \beta\frac{(1-\lambda^{1+k_0^*-k_1^*})}{(\lambda+1)}
\end{aligned}$$

$$h_{k_0^*}\beta\frac{(\lambda-1)}{(\lambda+1)}(1+\lambda^{k_0^*-k_1^*}) = a - \beta\frac{(1-\lambda^{1+k_0^*-k_1^*})}{(\lambda+1)}$$

$$\begin{aligned}
h_{k_0^*} &= \left[a - \beta\frac{(1-\lambda^{1+k_0^*-k_1^*})}{(\lambda+1)}\right]\frac{(\lambda+1)}{\beta(\lambda-1)(1+\lambda^{k_0^*-k_1^*})} \\
&= \frac{a(\lambda+1)}{\beta(\lambda-1)(1+\lambda^{k_0^*-k_1^*})} - \frac{1-\lambda^{1+k_0^*-k_1^*}}{(\lambda-1)(1+\lambda^{k_0^*-k_1^*})}
\end{aligned}$$

$$h_{k_0^*} = \frac{\frac{a}{\beta}(\lambda+1) - 1 + \lambda^{1+k_0^*-k_1^*}}{(\lambda-1)(1+\lambda^{k_0^*-k_1^*})} = h_{k_1^*} \tag{3.9}$$

If we substitute (3.9) and $h_{k_0^*} = h_{k_1^*}$ into (3.3) we get, for $k_0^* < k < k_1^*$:

$$\begin{aligned}
\varphi_k &= \beta\left[1 - \frac{\lambda}{(\lambda+1)}\left[\lambda^{k_0^*-k} + \lambda^{k-k_1^*}\right] + \frac{(\lambda-1)}{(\lambda+1)}\left[h_{k_0^*}\lambda^{k_0^*-k} + h_{k_0^*}\lambda^{k-k_1^*}\right]\right] \\
&= \beta\left[1 - \frac{\lambda}{(\lambda+1)}\left[\lambda^{k_0^*-k} + \lambda^{k-k_1^*}\right] + \frac{(\lambda-1)}{(\lambda+1)}\left[h_{k_0^*}(\lambda^{k_0^*-k} + \lambda^{k-k_1^*})\right]\right] \\
&= \beta\left[1 - \frac{\lambda}{(\lambda+1)}\left[\lambda^{k_0^*-k} + \lambda^{k-k_1^*}\right]\right. \\
&\quad \left. + \frac{(\lambda-1)}{(\lambda+1)}\left[\left(\frac{\frac{a}{\beta}(\lambda+1) - 1 + \lambda^{1+k_0^*-k_1^*}}{(\lambda-1)(1+\lambda^{k_0^*-k_1^*})}\right)(\lambda^{k_0^*-k} + \lambda^{k-k_1^*})\right]\right]
\end{aligned}$$

$$
\begin{aligned}
&= \beta\left[1-\frac{\lambda}{(\lambda+1)}\left[\lambda^{k_0^*-k}+\lambda^{k-k_1^*}\right]+\frac{a}{\beta}\frac{(\lambda^{k_0^*-k}+\lambda^{k-k_1^*})}{(1+\lambda^{k_0^*-k_1^*})}\right.\\
&\quad\left.-\frac{(1-\lambda^{1+k_0^*-k_1^*})(\lambda^{k_0^*-k}+\lambda^{k-k_1^*})}{(\lambda+1)(1+\lambda^{k_0^*-k_1^*})}\right]\\
&= \beta\left[1+\frac{a}{\beta}\frac{(\lambda^{k_0^*-k}+\lambda^{k-k_1^*})}{(1+\lambda^{k_0^*-k_1^*})}-\frac{1}{(\lambda+1)}\left[(\lambda^{1+k_0^*-k}+\lambda^{k-k_1^*+1})\right.\right.\\
&\quad\left.\left.+\frac{(1-\lambda^{1+k_0^*-k_1^*})(\lambda^{k_0^*-k}+\lambda^{k-k_1^*})}{(1+\lambda^{k_0^*-k_1^*})}\right]\right]\\
&= \beta\left[1+\frac{a}{\beta}\frac{(\lambda^{k_0^*-k}+\lambda^{k-k_1^*})}{(1+\lambda^{k_0^*-k_1^*})}-\frac{1}{(\lambda+1)(1+\lambda^{k_0^*-k_1^*})}\left[(\lambda^{1+k_0^*-k}+\lambda^{k-k_1^*+1})(1+\lambda^{k_0^*-k_1^*})\right.\right.\\
&\quad\left.\left.+(1-\lambda^{1+k_0^*-k_1^*})(\lambda^{k_0^*-k}+\lambda^{k-k_1^*})\right]\right]\\
&= \beta\left[1+\frac{a}{\beta}\frac{(\lambda^{k_0^*-k}+\lambda^{k-k_1^*})}{(1+\lambda^{k_0^*-k_1^*})}-\frac{1}{(\lambda+1)(1+\lambda^{k_0^*-k_1^*})}\left[(\lambda^{k_0^*-k}+\lambda^{k-k_1^*})(\lambda+\lambda^{1+k_0^*-k_1^*})\right.\right.\\
&\quad\left.\left.+(1-\lambda^{1+k_0^*-k_1^*})(\lambda^{k_0^*-k}+\lambda^{k-k_1^*})\right]\right]\\
&= \beta\left[1+\frac{a}{\beta}\frac{(\lambda^{k_0^*-k}+\lambda^{k-k_1^*})}{(1+\lambda^{k_0^*-k_1^*})}-\frac{1}{(\lambda+1)(1+\lambda^{k_0^*-k_1^*})}\left[(\lambda+1)(\lambda^{k_0^*-k}+\lambda^{k-k_1^*})\right]\right]\\
&= \beta\left[1+\frac{a}{\beta}\frac{(\lambda^{k_0^*-k}+\lambda^{k-k_1^*})}{(1+\lambda^{k_0^*-k_1^*})}-\frac{(\lambda^{k_0^*-k}+\lambda^{k-k_1^*})}{(1+\lambda^{k_0^*-k_1^*})}\right]\\
&= \beta\left[1-(1-\frac{a}{\beta})\frac{(\lambda^{k_0^*-k}+\lambda^{k-k_1^*})}{(1+\lambda^{k_0^*-k_1^*})}\right]\\
&= \beta-(\beta-a)\frac{(\lambda^{k_0^*-k}+\lambda^{k-k_1^*})}{(1+\lambda^{k_0^*-k_1^*})}
\end{aligned}
$$

So for this case we have:

$$
\varphi_k=\begin{cases} a\lambda^{k_1^*-k} & k\geq k_1^* \\ \beta-(\beta-a)\frac{(\lambda^{k_0^*-k}+\lambda^{k-k_1^*})}{(1+\lambda^{k_0^*-k_1^*})} & k_0^*<k<k_1^* \\ a\lambda^{k-k_0^*} & k\leq k_0^*. \end{cases} \tag{3.10}
$$

In terms of L, R, and W,

$$\varphi_k = \begin{cases} a\lambda^{-R} & k \geq k_1^* \\ \beta - (\beta - a)\frac{(\lambda^{-L}+\lambda^{R})}{(1+\lambda^{-W})} & k_0^* < k < k_1^* \\ a\lambda^{L} & k \leq k_0^*. \end{cases} \tag{3.11}$$

Similarly to the case of stable waves, for a set of parameter values α and γ, we have a family of candidate unstable standing wave solutions whose solutions are given by 3.10. This type of family is uncountably infinite though. For each value of $W \geq 2$, we have an uncountably infinite family of waves, because for a given value of W, for each value of $h_{k_0^*} \in [0, 1]$ we have a different solution. Unlike with stable waves, the wave form of an unstable wave depends on the value of a. In Figure 3.7 we show the family of solutions for $W = 4$. In this and each subsequent picture of this type, the gradient shades illustrate the continuum of solutions. For each set of red, green, and blue gradients, as is in this picture, that shows the continuum for one value of W. In plotting entire families, we see that the continuum of solutions of point-top waves with $W = 4$ fits perfectly on top of the solutions with $W = 2$, and the solutions with $W = 6$ fit right on top of the solutions with $W = 4$, and so on. We plot the family of candidate solutions of unstable point-top waves for all even values of $W \geq 2$ in Figure 3.8. We plot the family of candidate solutions of unstable flat-top waves for all odd values of $W \geq 3$ in Figure 3.9.

As with stable waves, the existence of members of these families depends on the value of a. As we stated before, for each single value of $W \geq 2$ we have an infinite family of candidate solutions. Each solution in that family corresponds to a single value of a, so for a specific value of a, we have only one corresponding candidate solution for that value of W. For a given value of a, we have one candidate unstable solution for each value of $W \geq 2$. In Figure 3.10 we show a family of unstable waves given a particular value of a. As with the case of

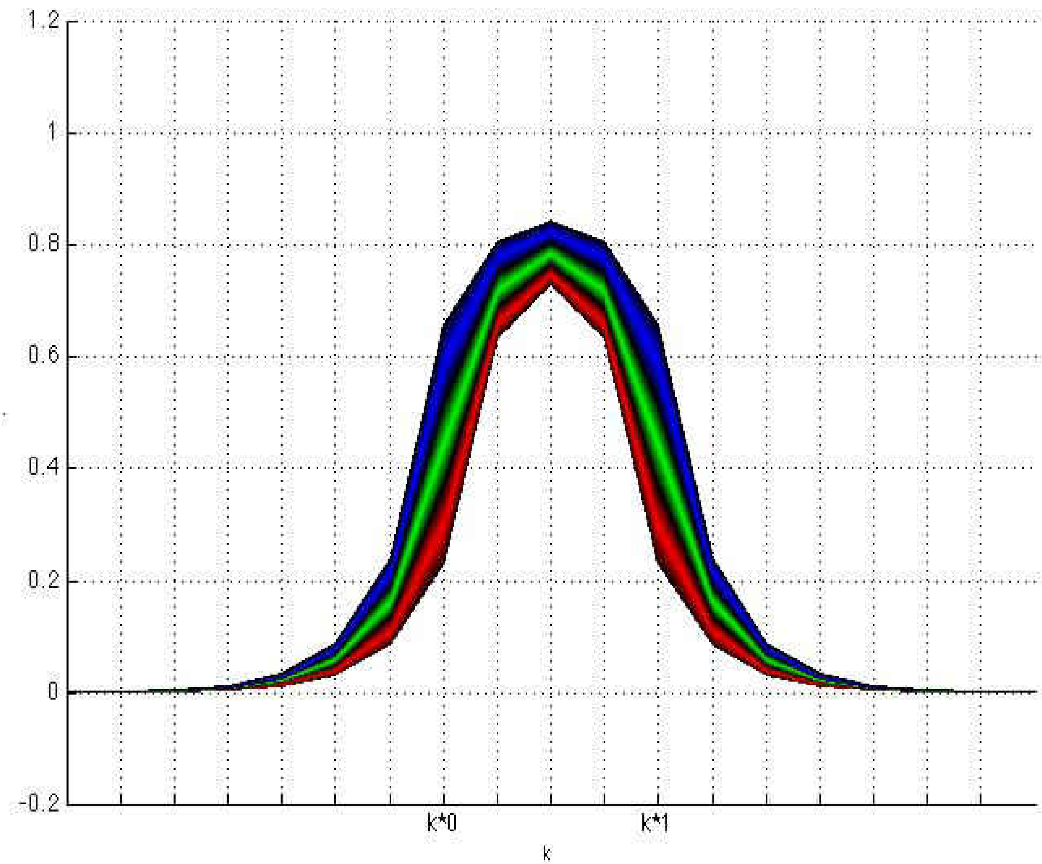

Figure 3.7: Family of Unstable Waves for W=4.

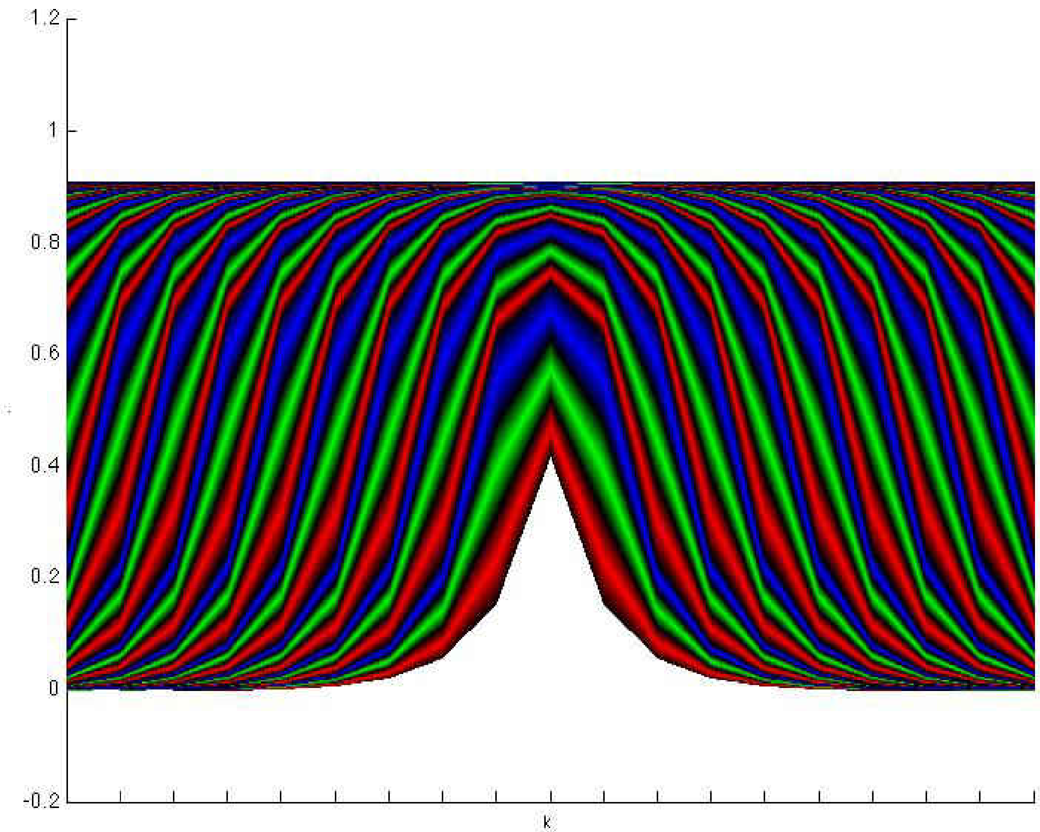

Figure 3.8: Family of Unstable point-top Waves, for all even values of $W \geq 2$.

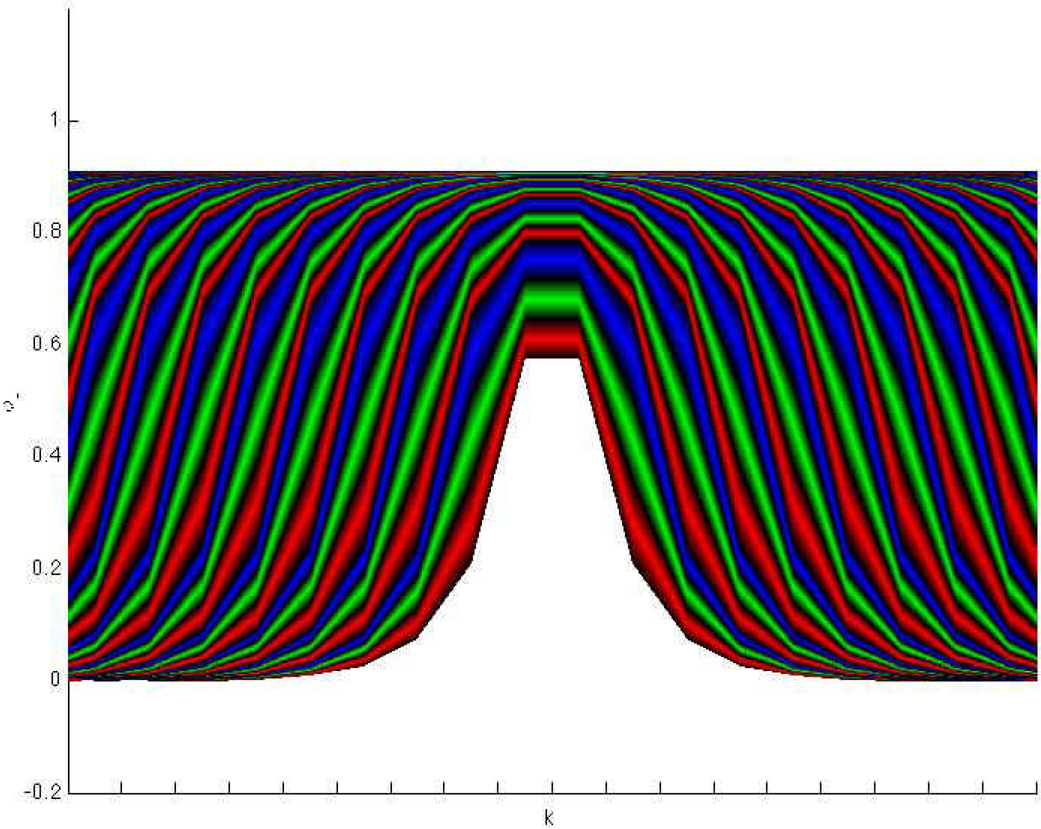

Figure 3.9: Family of Unstable flat-top Waves, for all odd values of $W \geq 3$.

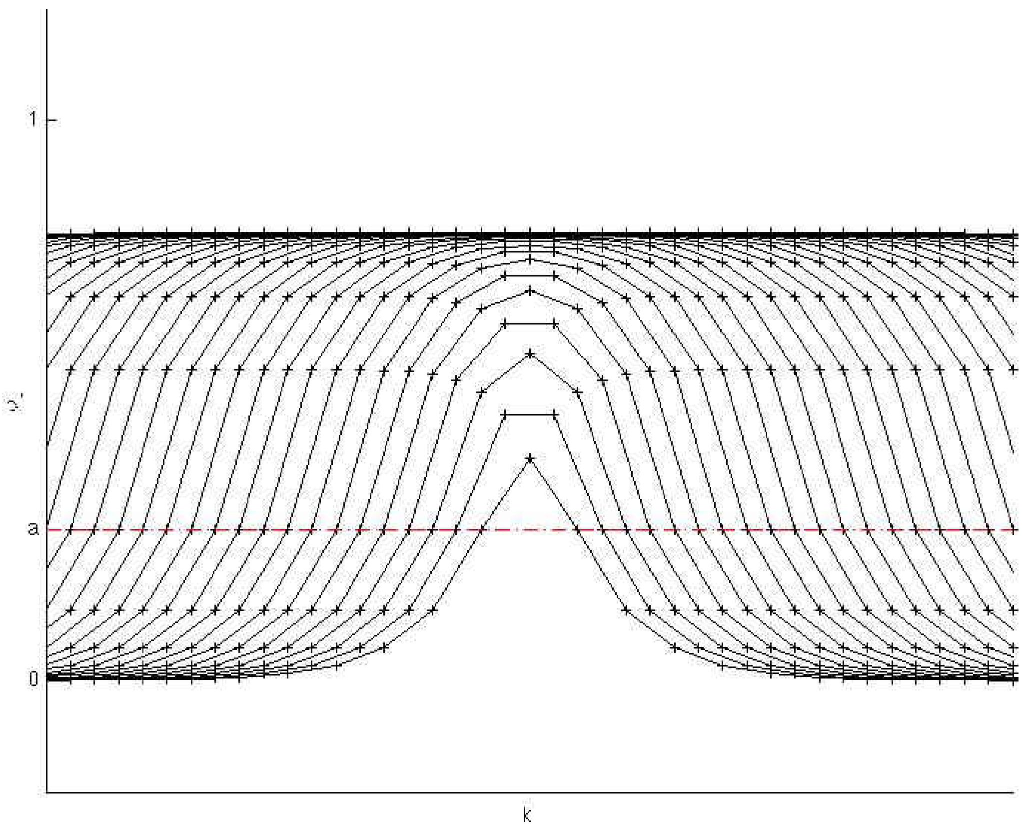

Figure 3.10: Family of unstable waves for a given a.

stable waves, whether each of these candidate solutions is an actual solution depends on the value of a, and we address this question is Chapter 4.

3.2.3 Right-Unstable Case

Now we consider the case where one crossing is at a lattice point and one crossing is not. We have two possibilities for this. We start by looking at the case where the first crossing is not at a lattice point and the second crossing is at a lattice point. In other words $\eta_0 \notin \mathbb{Z}$, $\eta_1 \in \mathbb{Z}$. So $h_{k_0^*} = 0$ and $h_{k_1^*} = (0,1)$. The reason $h_{k_1^*} = (0,1)$ instead of $[0,1]$ is simply because if $h_{k_1^*} = 0$ or 1, then the wave would actually be a member of a different case, either Stable or Unstable. Also $\varphi_{k_1^*} = a$, so that means for $k \geq k_1^*$, $\varphi_k = a\lambda^{k_1^*-k}$. Noting that $h_{k_0^*} = 0$ and $\varphi_{k_1^*} = a$, from (3.1) we have:

$$a = \beta\frac{(\lambda-1)}{(\lambda+1)}\left[\frac{1-\lambda^{1+k_0^*-k_1^*}}{\lambda-1} + h_{k_1^*}\right]$$

Solving for $h_{k_1^*}$, we get:

$$\frac{(\lambda+1)}{(\lambda-1)}\frac{a}{\beta} = \frac{1-\lambda^{1+k_0^*-k_1^*}}{\lambda-1} + h_{k_1^*}$$

$$h_{k_1^*} = \frac{(\lambda+1)}{(\lambda-1)}\frac{a}{\beta} - \frac{1-\lambda^{1+k_0^*-k_1^*}}{\lambda-1} \tag{3.12}$$

Plugging (3.12) and $h_{k_0^*} = 0$ into (2.26), we get:

$$\begin{aligned}
\varphi_{k_0^*} &= \beta\frac{(\lambda-1)}{(\lambda+1)}\left[\frac{1-\lambda^{1+k_0^*-k_1^*}}{\lambda-1} + \left(\frac{(\lambda+1)}{(\lambda-1)}\frac{a}{\beta} - \frac{1-\lambda^{1+k_0^*-k_1^*}}{\lambda-1}\right)\lambda^{k_0^*-k_1^*}\right] \\
&= \frac{\beta}{(\lambda+1)}\left[1-\lambda^{1+k_0^*-k_1^*} + (\lambda+1)\frac{a}{\beta}\lambda^{k_0^*-k_1^*} - \lambda^{k_0^*-k_1^*} + \lambda^{1+2k_0^*-2k_1^*}\right] \\
&= \frac{\beta}{(\lambda+1)}\left[(\lambda+1)(\frac{a}{\beta}\lambda^{k_0^*-k_1^*} - \lambda^{k_0^*-k_1^*}) + 1 + \lambda^{1+2k_0^*-2k_1^*}\right] \\
&= \beta\frac{1+\lambda^{1+2k_0^*-2k_1^*}}{(\lambda+1)} - (\beta-a)\lambda^{k_0^*-k_1^*}
\end{aligned}$$

So since for $k \le k_0^*$, $\varphi_k = \varphi_{k_0^*} \lambda^{k-k_0^*}$, we have for $k \le k_0^*$:

$$\varphi_k = \left[\beta \frac{1+\lambda^{1+2k_0^*-2k_1^*}}{(\lambda+1)} - (\beta - a)\lambda^{k_0^*-k_1^*}\right] \lambda^{k-k_0^*}$$

To solve for φ_k, $k_0^* < k < k_1^*$, we can plug $h_{k_0^*} = 0$ and (3.12) into (3.3) to get:

$$\begin{aligned}
\varphi_k &= \beta \left[1 - \frac{\lambda}{(\lambda+1)}[\lambda^{k-k_1^*} + \lambda^{k_0^*-k}] + \frac{(\lambda-1)}{(\lambda+1)}\left[\frac{1}{(\lambda-1)}\left[\frac{(\lambda+1)a}{\beta} - 1 + \lambda^{1+k_0^*-k_1^*}\right]\lambda^{k-k_1^*}\right]\right] \\
&= \beta \left[1 - \frac{\lambda}{(\lambda+1)}[\lambda^{k-k_1^*} + \lambda^{k_0^*-k}] + \frac{a}{\beta}\lambda^{k-k_1^*} - \frac{\lambda^{k-k_1^*} - \lambda^{k+1+k_0^*-2k_1^*}}{\lambda+1}\right] \\
&= \beta \left[1 - \lambda^{k-k_1^*} - \frac{\lambda^{1+k_0^*-k} - \lambda^{k+1+k_0^*-2k_1^*}}{\lambda+1}\right] + a\lambda^{k-k_1^*} \\
&= \beta \left[1 - \frac{\lambda^{1+k_0^*-k} - \lambda^{k+1+k_0^*-2k_1^*}}{\lambda+1}\right] - (\beta - a)\lambda^{k-k_1^*}
\end{aligned}$$

So for this case we have:

$$\varphi_k = \begin{cases} a\lambda^{k_1^*-k} & k \ge k_1^* \\ \beta\left[1 - \frac{\lambda^{1+k_0^*-k} - \lambda^{k+1+k_0^*-2k_1^*}}{\lambda+1}\right] - (\beta - a)\lambda^{k-k_1^*} & k_0^* < k < k_1^* \\ \left[\beta\frac{1+\lambda^{1+2k_0^*-2k_1^*}}{(\lambda+1)} - (\beta - a)\lambda^{k_0^*-k_1^*}\right]\lambda^{k-k_0^*} & k \le k_0^*. \end{cases} \tag{3.13}$$

In terms of L, R, and W,

$$\varphi_k = \begin{cases} a\lambda^{-R} & k \ge k_1^* \\ \beta\left[1 - \frac{\lambda^{1-L} - \lambda^{1+R-W}}{\lambda+1}\right] - (\beta - a)\lambda^{R} & k_0^* < k < k_1^* \\ \left[\beta\frac{1+\lambda^{1-2W}}{(\lambda+1)} - (\beta - a)\lambda^{-W}\right]\lambda^{L} & k \le k_0^*. \end{cases} \tag{3.14}$$

In Figure 3.11 we show a family of right-unstable waves.

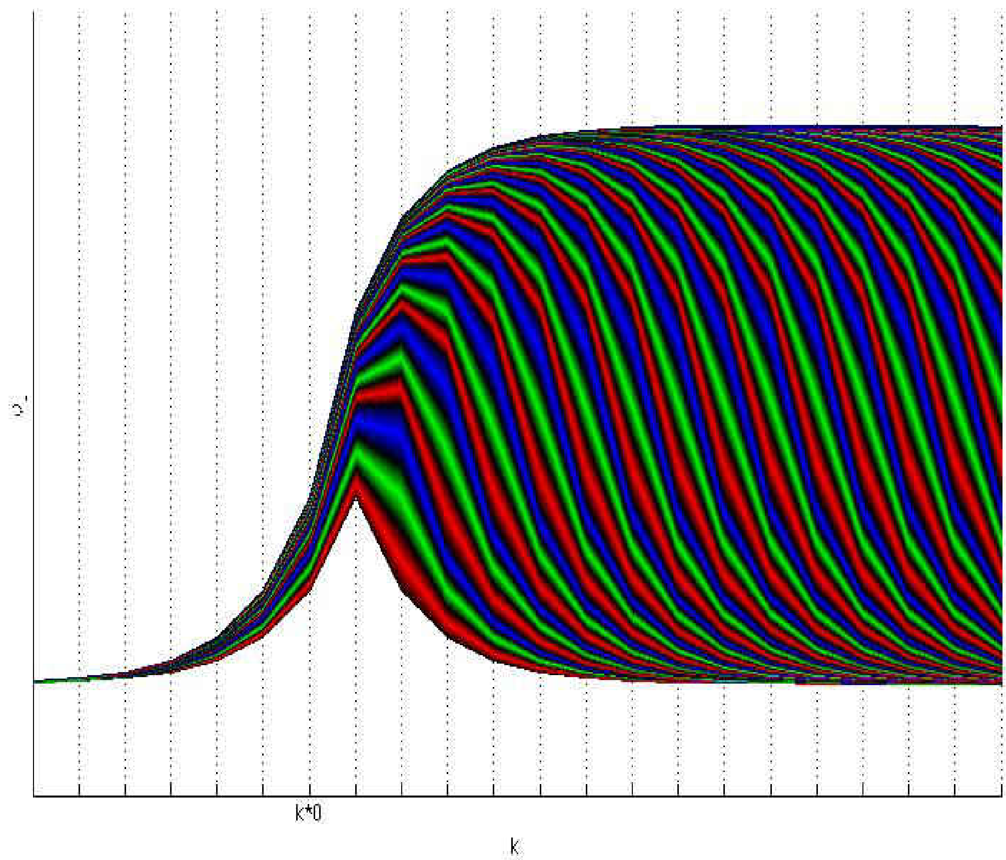

Figure 3.11: Family of Right-Unstable Waves

3.2.4 Left-Unstable Case

Now we consider the other case where one crossing is at a lattice point and one crossing is not. We now look at the case where the first crossing is at a lattice point and the second crossing is not at a lattice point. In other words $\eta_0 \in \mathbb{Z}$, $\eta_1 \notin \mathbb{Z}$. So $h_{k_0^*} = (0,1)$ and $h_{k_1^*} = 0$. Again, $h_{k_1^*} \neq 0$ or 1 because then it would simply fall into a different case of wave. Also $\varphi_{k_0^*} = a$, so that means for $k \leq k_0^*$, $\varphi_k = a\lambda^{k-k_0^*}$. Noting that $h_{k_1^*} = 0$ and $\varphi_{k_0^*} = a$, from (2.26) we have:

$$a = \beta\frac{(\lambda-1)}{(\lambda+1)}\left[h_{k_0^*} + \frac{1-\lambda^{1+k_0^*-k_1^*}}{\lambda-1}\right]$$

Solving for $h_{k_0^*}$, we get:

$$\frac{(\lambda+1)}{(\lambda-1)}\frac{a}{\beta} = h_{k_0^*} + \frac{1-\lambda^{1+k_0^*-k_1^*}}{\lambda-1}$$

$$h_{k_0^*} = \frac{(\lambda+1)}{(\lambda-1)}\frac{a}{\beta} - \frac{1-\lambda^{1+k_0^*-k_1^*}}{\lambda-1} \tag{3.15}$$

Plugging (3.15) and $h_{k_1^*} = 0$ into (3.1), we get:

$$\begin{aligned}
\varphi_{k_1^*} &= \beta\frac{(\lambda-1)}{(\lambda+1)}\left[\left(\frac{(\lambda+1)}{(\lambda-1)}\frac{a}{\beta} - \frac{1-\lambda^{1+k_0^*-k_1^*}}{\lambda-1}\right)\lambda^{k_0^*-k_1^*} + \frac{1-\lambda^{1+k_0^*-k_1^*}}{\lambda-1}\right] \\
&= \frac{\beta}{(\lambda+1)}\left[(\lambda+1)\frac{a}{\beta}\lambda^{k_0^*-k_1^*} - \lambda^{k_0^*-k_1^*} + \lambda^{1+2k_0^*-2k_1^*} + 1 - \lambda^{1+k_0^*-k_1^*}\right] \\
&= \frac{\beta}{(\lambda+1)}\left[(\lambda+1)(\frac{a}{\beta}\lambda^{k_0^*-k_1^*} - \lambda^{k_0^*-k_1^*}) + \lambda^{1+2k_0^*-2k_1^*} + 1\right] \\
&= \beta\frac{1+\lambda^{1+2k_0^*-2k_1^*}}{(\lambda+1)} - (\beta-a)\lambda^{k_0^*-k_1^*}
\end{aligned}$$

So since for $k \geq k_1^*$, $\varphi_k = \varphi_{k_1^*}\lambda^{k_1^*-k}$, we have for $k \geq k_1^*$:

$$\varphi_k = \left[\beta\frac{1+\lambda^{1+2k_0^*-2k_1^*}}{(\lambda+1)} - (\beta-a)\lambda^{k_0^*-k_1^*}\right]\lambda^{k_1^*-k}$$

To solve for φ_k, $k_0^* < k < k_1^*$, we can plug $h_{k_1^*} = 0$ and (3.15) into (3.3) to get:

$$\begin{aligned}
\varphi_k &= \beta\left[1 - \frac{\lambda}{(\lambda+1)}[\lambda^{k-k_1^*} + \lambda^{k_0^*-k}] + \frac{(\lambda-1)}{(\lambda+1)}\left[\frac{1}{(\lambda-1)}\left[\frac{(\lambda+1)a}{\beta} - 1 + \lambda^{1+k_0^*-k_1^*}\right]\lambda^{k_0^*-k}\right]\right] \\
&= \beta\left[1 - \frac{\lambda}{(\lambda+1)}[\lambda^{k-k_1^*} + \lambda^{k_0^*-k}] + \frac{a}{\beta}\lambda^{k_0^*-k} - \frac{\lambda^{k_0^*-k} - \lambda^{1+2k_0^*-k-k_1^*}}{\lambda+1}\right] \\
&= \beta\left[1 - \lambda^{k_0^*-k} - \frac{\lambda^{1+k-k_1^*} - \lambda^{1+2k_0^*-k-k_1^*}}{\lambda+1}\right] + a\lambda^{k_0^*-k} \\
&= \beta\left[1 - \frac{\lambda^{1+k_0^*-k} - \lambda^{k+1+k_0^*-2k_1^*}}{\lambda+1}\right] - (\beta-a)\lambda^{k_0^*-k}
\end{aligned}$$

So for this case we have:

$$\varphi_k = \begin{cases} \left[\beta\frac{1+\lambda^{1+2k_0^*-2k_1^*}}{(\lambda+1)} - (\beta-a)\lambda^{k_0^*-k_1^*}\right]\lambda^{k_1^*-k} & k \geq k_1^* \\ \beta\left[1 - \frac{\lambda^{1+k_0^*-k} - \lambda^{k+1+k_0^*-2k_1^*}}{\lambda+1}\right] - (\beta-a)\lambda^{k_0^*-k} & k_0^* < k < k_1^* \\ a\lambda^{k-k_0^*} & k \leq k_0^*. \end{cases} \tag{3.16}$$

In terms of L, R, and W,

$$\varphi_k = \begin{cases} \left[\beta\frac{1+\lambda^{1-2W}}{(\lambda+1)} - (\beta-a)\lambda^{-W}\right]\lambda^{-R} & k \geq k_1^* \\ \beta\left[1 - \frac{\lambda^{1-L} - \lambda^{1+R-W}}{\lambda+1}\right] - (\beta-a)\lambda^{-L} & k_0^* < k < k_1^* \\ a\lambda^{L} & k \leq k_0^*. \end{cases} \tag{3.17}$$

In Figure 3.12 we show a family of left-unstable waves.

3.3 Special Cases - Waves That Do Not Go Above a

As was mentioned in Section 1.2.2, for completeness' sake we will examine possible solutions that do not actually go above the parameter a. The two possible cases for this are waves that only touch a, but do not go above it, and waves that are entirely below a. As this section is

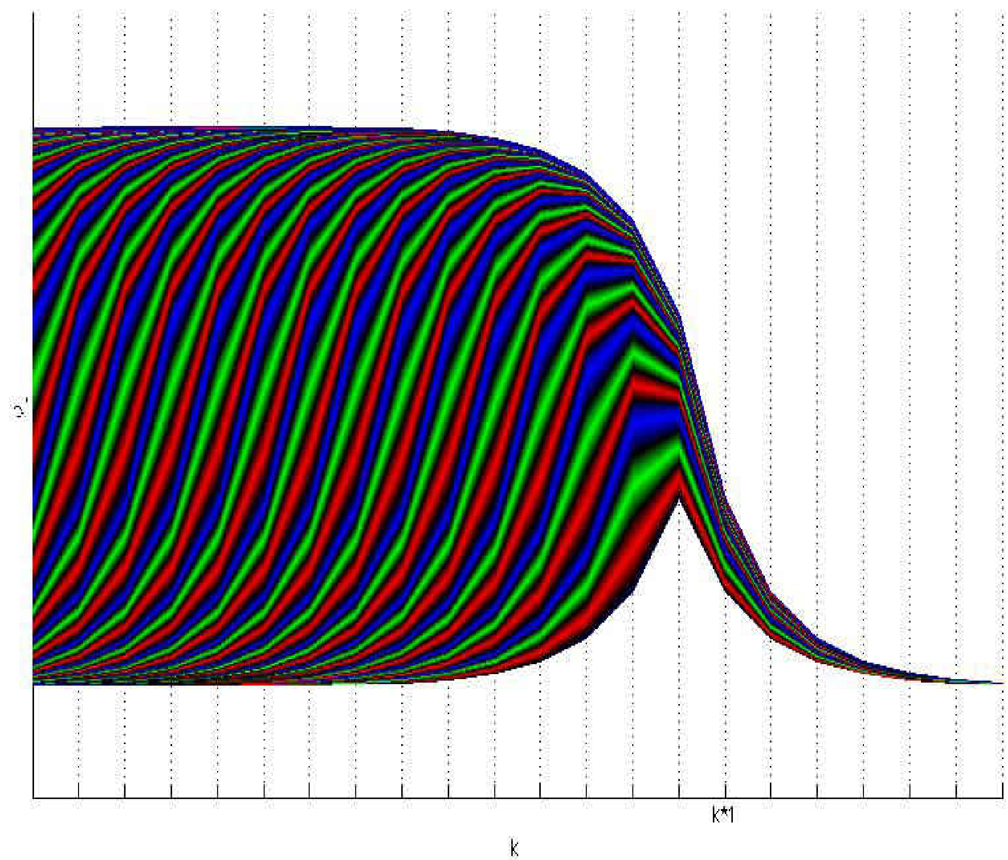

Figure 3.12: Family of Left-Unstable Waves

of minor importance to our problem, we will not go into great detail as to the derivation of solutions.

3.3.1 Waves That Peak At a

Here we look at the possibility of having a wave whose maximum value is a. We will begin by looking at the *One-Touch* case where there is only one point at a and the rest of the points below a. We need to slightly reformulate our approach because we do not have the two crossings of a that we previously had, but mostly the approach is the same. Here we say that $\eta_0 = \eta_1$. Due to translational invariance, we may let $k_0 = 0$, $\eta_0 = \eta_1 = 0$, so $k_0^* = k_1^* = 0$, and $h_{k_0^*} = h_{k_1^*} = h_0 = [0, 1]$. We also know from the setup of the problem that $\varphi_0 = a$, and that $h_k = 0, \forall k \neq 0$.

From (2.15) we get:

$$\varphi_k = \varphi_0\rho(k) + \varphi_1\sigma(k) + \frac{1}{\alpha}\begin{cases} 0 & k > 0 \\ 0 & k = 0 \\ h_0\sigma(k) & k < 0 \end{cases}$$

For $k < 0$,

$$\varphi_k = \varphi_0\rho(k) + \varphi_1\sigma(k) + \frac{1}{\alpha}h_0\sigma(k).$$

To satisfy our boundary condition (1.19) at $-\infty$ we must have

$$\lambda\varphi_0 - \varphi_1 - \frac{h_0}{\alpha} = 0,$$

$$\varphi_1 = \lambda\varphi_0 - \frac{h_0}{\alpha}. \tag{3.18}$$

For $k > 0$,

$$\varphi_k = \varphi_0\rho(k) + \varphi_1\sigma(k).$$

To satisfy our boundary condition (1.19) at ∞ we must have

$$-\lambda^{-1}\varphi_0 + \varphi_1 = 0,$$

$$\varphi_1 = \lambda^{-1}\varphi_0. \tag{3.19}$$

Combining these two conditions (3.18) and (3.19), we find that

$$\varphi_0 = h_0\beta\frac{(\lambda-1)}{(\lambda+1)} = a \tag{3.20}$$

which will be of some significance later. We find that the solution waves here are given by

$$\varphi_k = \begin{cases} a\lambda^{-k} & k \geq 0 \\ a\lambda^{k} & k \leq 0 \end{cases} \tag{3.21}$$

We also look at the *Two-Touch* case where there are two points at a and the rest of the points below a. Due to translational invariance, we may let $\varphi_0 = a$, $\varphi_1 = a$, and so $\varphi_k < a, \forall k \neq 0, 1$. Therefore $h_0 = [0,1]$, $h_1 = [0,1]$, and $h_k = 0, \forall k \neq 0, 1$. From (2.15) we get:

$$\varphi_k = a\rho(k) + a\sigma(k) + \frac{1}{\alpha}\begin{cases} -h_1\sigma(k-1) & k > 0 \\ 0 & k = 0 \\ h_0\sigma(k) & k < 0 \end{cases}$$

For $k < 0$,

$$\varphi_k = a\rho(k) + a\sigma(k) + \frac{1}{\alpha}h_0\sigma(k).$$

To satisfy our boundary condition (1.19) at $-\infty$ we must have

$$\lambda a - a - \frac{h_0}{\alpha} = 0,$$

$$h_0 = \frac{a}{\beta(1-\lambda^{-1})}. \tag{3.22}$$

For $k > 0$,

$$\varphi_k = a\rho(k) + a\sigma(k) - \frac{1}{\alpha} h_1 \sigma(k-1).$$

To satisfy our boundary condition (1.19) at ∞ we must have

$$-\lambda^{-1} a + a - \frac{h_1}{\alpha}\lambda^{-1} = 0,$$

$$h_1 = \frac{a}{\beta(1-\lambda^{-1})}. \tag{3.23}$$

The conditions (3.22) and (3.23) tell us that

$$a = h_0 \beta(1-\lambda^{-1}) = h_1 \beta(1-\lambda^{-1}) \tag{3.24}$$

which will have some significance later. The wave solution that we find in this case is:

$$\varphi_k = \begin{cases} a\lambda^{1-k} & k \geq 1 \\ a\lambda^k & k \leq 0 \end{cases} \tag{3.25}$$

In Figure 3.13 we show pictures of one-touch and two-touch waves.

It is not shown here, but turns out to be possible that we have a wide assortment of different waves of this type such as waves that have an arbitrary number of points at a between values k_0^* and k_1^* which are given by

$$\varphi_k = \begin{cases} a\lambda^{k_1^* - k} & k > k_1^* \\ a & k_0^* \leq k \geq k_1^* \\ a\lambda^{k - k_0^*} & k < k_0^* \end{cases}$$

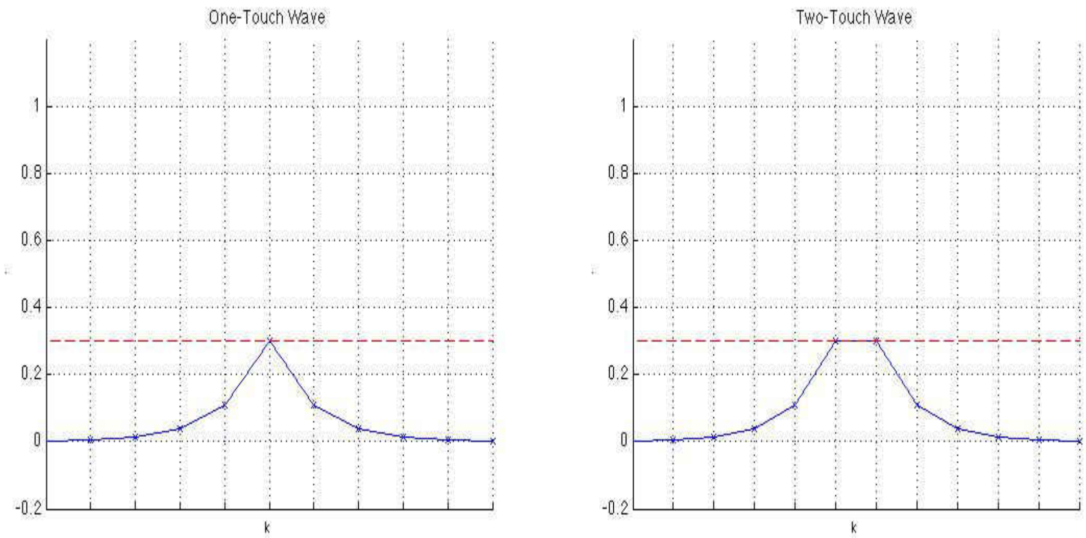

Figure 3.13: On the left a one-touch wave. On the right a two-touch wave.

These and other types of irregular waves are of little importance to our problem though because they have little physical significance or relation to propagation failure of traveling waves.

3.3.2 Waves That Are Entirely Below a

Here we look at the possibility of having a standing wave that lies completely below a. We may abandon the setup of the problem involving variables η_0, η_1, k_0^*, k_1^*, etc., because we have no crossings of a. We may simply look at the original equation (1.15) and know that since $\varphi_k < a$, $f(\varphi_k, a) = \varphi_k$, and so the difference equation we have to solve is

$$-\alpha\varphi_{k+1} + (1 + \gamma + 2\alpha)\,\varphi_k - \alpha\varphi_{k-1} = 0 \qquad \forall k \in \mathbb{Z}.$$

This equation is the same as (1.21), with $h_k = 0, \forall k \in \mathbb{Z}$. Therefore we may follow the solution to the original problem, understanding that all $h_k = 0$. We see that the solution to this problem is given by

$$\varphi_k = \varphi_{k_0}\rho(k - k_0) + \varphi_{k_0+1}\sigma(k - k_0)$$

To satisfy the boundary condition (1.19) at $-\infty$, it must be that

$$\varphi_1 = \lambda\varphi_0.$$

To satisfy the boundary condition (1.19) at ∞, it must be that

$$\varphi_1 = \lambda^{-1}\varphi_0.$$

From these two conditions it must be that $\varphi_0 = \varphi_1 = 0$ which means that the only solution is the trivial solution $\varphi_k \equiv 0$. This means there cannot exist any standing waves that lie entirely below a.

4 INTERVAL FOR STANDING WAVES

In the previous chapters we have worked to find exact solutions of standing waves. In this chapter we focus on studying the conditions of parameters that allow for the existence of standing waves. The *Interval for Standing Waves* is the set of values of a in which we can have standing waves, and we define this interval of a in terms of all of the other parameters.

We will also state our results in terms of the parameter $W = k_1^* - k_0^*$. Because of translational invariance, it does not matter to us in this chapter where any wave is on the lattice, or what the values of k_0^* or k_1^* are individually. It only matters what the width of the wave, W, is.

4.1 Existence of Standing Waves for the Different Cases

4.1.1 Stable Case

We know from our setup in (1.16) that a must be between $\varphi_{k_0^*}$ and $\varphi_{k_0^*+1}$, not including those endpoints, so $a \in (\varphi_{k_0^*}, \varphi_{k_0^*+1})$.

$$\varphi_{k_0^*} = \beta\frac{(1 - \lambda^{1+k_0^*-k_1^*})}{(\lambda + 1)}$$

By (2.24), and since $h_{k_0^*} = 0$,

$$\varphi_{k_0^*+1} = \lambda\varphi_{k_0^*} = \beta\frac{(\lambda - \lambda^{2+k_0^*-k_1^*})}{(\lambda + 1)}$$

This gives us a possible range of values of a for which we can have standing waves.

$$a \in \left(\beta\frac{(1 - \lambda^{1+k_0^*-k_1^*})}{(\lambda + 1)}, \beta\frac{(\lambda - \lambda^{2+k_0^*-k_1^*})}{(\lambda + 1)}\right) \tag{4.1}$$

$$a \in \left(\beta \frac{(1-\lambda^{1-W})}{(\lambda+1)}, \beta \frac{(\lambda-\lambda^{2-W})}{(\lambda+1)} \right) \tag{4.2}$$

In Figure 4.1 we show the ranges in which me may have standing waves for different values of W. The difference between the two graphs is that the value of β is different in each. Notice that the smaller W is, the lower the interval of standing waves will be. Both the upper and lower bounds are depressed as W is decreased.

4.1.2 Unstable Case

We know that for this case $h_{k_0^*} = h_{k_1^*} = [0,1]$. We know from our setup in (1.17) that $a = \varphi_{k_0^*}$, and from (2.26) that

$$a = \varphi_{k_0^*} = \beta \frac{(\lambda-1)}{(\lambda+1)} \left[h_{k_0^*}(1+\lambda^{k_0^*-k_1^*}) + \frac{1-\lambda^{1+k_0^*-k_1^*}}{\lambda-1} \right].$$

Since $\lambda > 1$, the lower bound of a is achieved if $h_{k_0^*} = 0$ and the upper bound is achieved if $h_{k_0^*} = 1$. If $h_{k_0^*} = 0$,

$$a = \beta \frac{(\lambda-1)}{(\lambda+1)} \left[\frac{1-\lambda^{1+k_0^*-k_1^*}}{\lambda-1} \right] = \beta \frac{(1-\lambda^{1+k_0^*-k_1^*})}{(\lambda+1)}.$$

If $h_{k_0^*} = 1$,

$$\begin{aligned}
a &= \beta \frac{(\lambda-1)}{(\lambda+1)} \left[(1+\lambda^{k_0^*-k_1^*}) + \frac{1-\lambda^{1+k_0^*-k_1^*}}{\lambda-1} \right] \\
&= \beta \frac{(\lambda-1)}{(\lambda+1)} \left[\frac{(1+\lambda^{k_0^*-k_1^*})(\lambda-1)}{(\lambda-1)} + \frac{1-\lambda^{1+k_0^*-k_1^*}}{\lambda-1} \right] \\
&= \beta \frac{1}{(\lambda+1)} \left[(1+\lambda^{k_0^*-k_1^*})(\lambda-1) + 1 - \lambda^{1+k_0^*-k_1^*} \right] \\
&= \beta \frac{1}{(\lambda+1)} \left[\lambda - 1 + \lambda^{1+k_0^*-k_1^*} - \lambda^{k_0^*-k_1^*} + 1 - \lambda^{1+k_0^*-k_1^*} \right] \\
&= \beta \frac{(\lambda-\lambda^{k_0^*-k_1^*})}{(\lambda+1)}
\end{aligned}$$

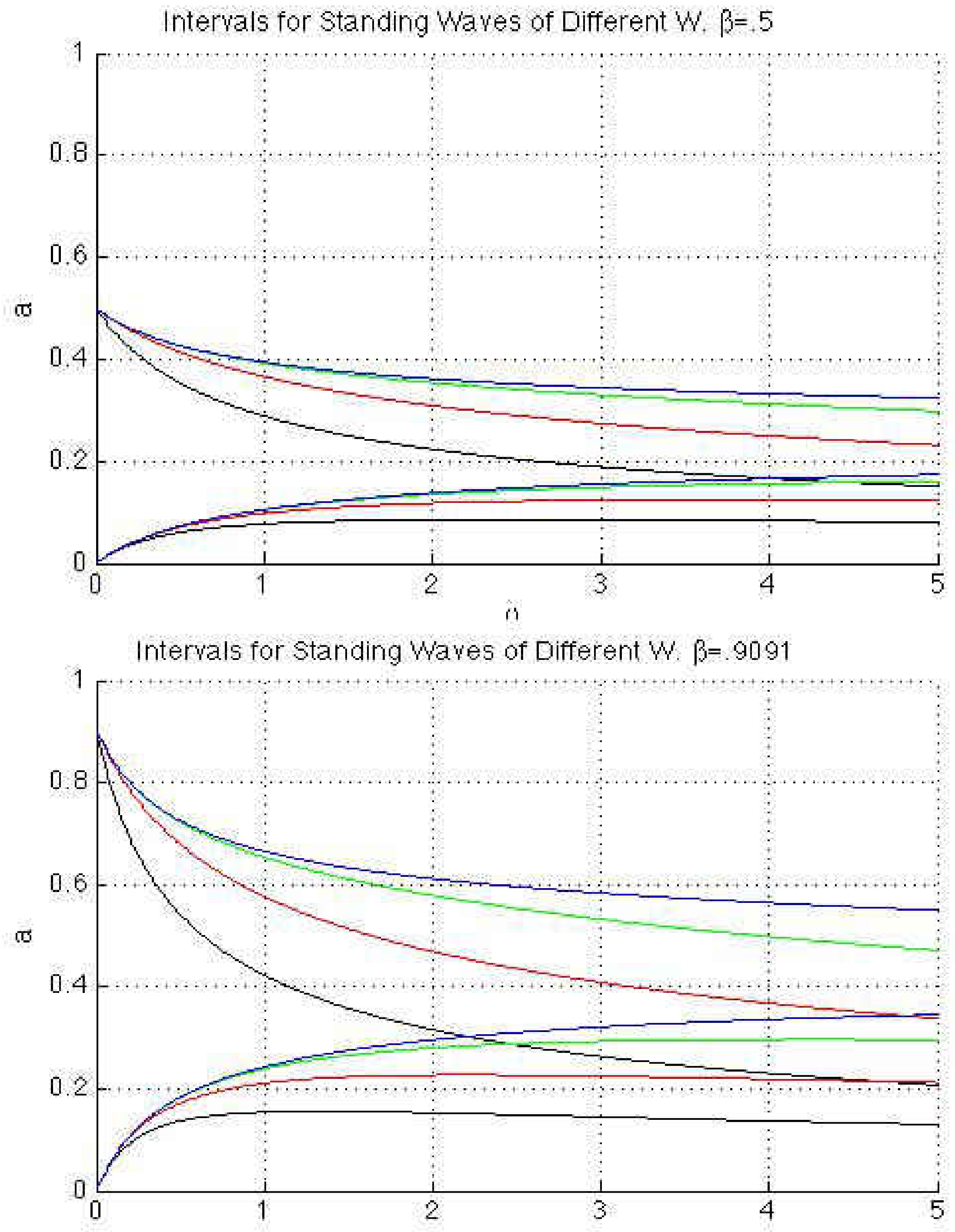

Figure 4.1: Intervals for Standing Waves for different values of W. Plotted a vs. α. In the graph on top, $\gamma = 1$; $\beta = .5$. In the graph on bottom, $\gamma = .1$; $\beta = .9091$. In each graph, from bottom to top: Black - $W = 2$. Red - $W = 3$. Green - $W = 5$. Blue - $W = 10$.

This gives us the possible range of values of a for standing waves:

$$a \in \left[\beta\frac{(1-\lambda^{1+k_0^*-k_1^*})}{(\lambda+1)}, \beta\frac{(\lambda-\lambda^{k_0^*-k_1^*})}{(\lambda+1)}\right] \tag{4.3}$$

$$a \in \left[\beta\frac{(1-\lambda^{1-W})}{(\lambda+1)}, \beta\frac{(\lambda-\lambda^{-W})}{(\lambda+1)}\right] \tag{4.4}$$

4.1.3 Right-Unstable Case

Again, we have:

$$a = \beta\frac{(\lambda-1)}{(\lambda+1)}\left[\frac{1-\lambda^{1+k_0^*-k_1^*}}{\lambda-1} + h_{k_1^*}\right]$$

$h_{k_1^*} = (0,1)$, and a is at its minimum when $h_{k_1^*} = 0$ and a is at its maximum when $h_{k_1^*} = 1$. If $h_{k_1^*} = 0$,

$$a = \beta\frac{(\lambda-1)}{(\lambda+1)}\left[\frac{1-\lambda^{1+k_0^*-k_1^*}}{\lambda-1}\right] = \beta\frac{(1-\lambda^{1+k_0^*-k_1^*})}{(\lambda+1)}$$

If $h_{k_1^*} = 1$,

$$\begin{aligned} a &= \beta\frac{(\lambda-1)}{(\lambda+1)}\left[\frac{1-\lambda^{1+k_0^*-k_1^*}}{\lambda-1} + 1\right] \\ &= \beta\frac{(\lambda-1)}{(\lambda+1)}\left[\frac{1-\lambda^{1+k_0^*-k_1^*}}{\lambda-1} + \frac{\lambda-1}{\lambda-1}\right] \\ &= \beta\frac{1}{(\lambda+1)}\left[1-\lambda^{1+k_0^*-k_1^*} + \lambda - 1\right] \\ &= \beta\frac{(\lambda-\lambda^{1+k_0^*-k_1^*})}{(\lambda+1)} \end{aligned}$$

This gives us a possible range of values for a to have a standing wave:

$$a \in \left(\beta\frac{(1-\lambda^{1+k_0^*-k_1^*})}{(\lambda+1)}, \beta\frac{(\lambda-\lambda^{1+k_0^*-k_1^*})}{(\lambda+1)}\right) \tag{4.5}$$

$$a \in \left(\beta\frac{(1-\lambda^{1-W})}{(\lambda+1)}, \beta\frac{(\lambda-\lambda^{1-W})}{(\lambda+1)}\right) \tag{4.6}$$

4.1.4 Left-Unstable Case

Again, we have:

$$a = \beta\frac{(\lambda-1)}{(\lambda+1)}\left[h_{k_0^*} + \frac{1-\lambda^{1+k_0^*-k_1^*}}{\lambda-1}\right]$$

$h_{k_0^*} = (0,1)$, and a is at its minimum when $h_{k_0^*} = 0$ and a is at its maximum when $h_{k_0^*} = 1$. If $h_{k_0^*} = 0$,

$$a = \beta\frac{(\lambda-1)}{(\lambda+1)}\left[\frac{1-\lambda^{1+k_0^*-k_1^*}}{\lambda-1}\right] = \beta\frac{(1-\lambda^{1+k_0^*-k_1^*})}{(\lambda+1)}$$

If $h_{k_0^*} = 1$,

$$\begin{aligned}
a &= \beta\frac{(\lambda-1)}{(\lambda+1)}\left[1 + \frac{1-\lambda^{1+k_0^*-k_1^*}}{\lambda-1}\right] \\
&= \beta\frac{(\lambda-1)}{(\lambda+1)}\left[\frac{\lambda-1}{\lambda-1} + \frac{1-\lambda^{1+k_0^*-k_1^*}}{\lambda-1}\right] \\
&= \beta\frac{1}{(\lambda+1)}\left[\lambda - 1 + 1 - \lambda^{1+k_0^*-k_1^*}\right] \\
&= \beta\frac{(\lambda-\lambda^{1+k_0^*-k_1^*})}{(\lambda+1)}
\end{aligned}$$

This gives us a possible range of values for a to have a standing wave:

$$a \in \left(\beta\frac{(1-\lambda^{1+k_0^*-k_1^*})}{(\lambda+1)}, \beta\frac{(\lambda-\lambda^{1+k_0^*-k_1^*})}{(\lambda+1)}\right) \tag{4.7}$$

$$a \in \left(\beta\frac{(1-\lambda^{1-W})}{(\lambda+1)}, \beta\frac{(\lambda-\lambda^{1-W})}{(\lambda+1)}\right) \tag{4.8}$$

4.1.5 Unstable One-Touch and Two-Touch Cases

Here we look at the special cases from Section 3.3.1 of waves that touch a but do no go above it.

In the one-touch case, we have $h_0 = [0, 1]$ and so from (3.20) we see that

$$a \in \left(0, \beta\frac{(\lambda - 1)}{(\lambda + 1)}\right] \tag{4.9}$$

noting that the parameter a cannot equal 0 by definition. This upper bound is the same as is given in (4.3) with $W = 0$. The lower bound given in (4.3) with $W = 0$ would be negative so having that bound be zero instead makes sense.

In the two-touch case, we have $h_0 = [0, 1]$ and $h_1 = [0, 1]$ and so from (3.24) we see that

$$a \in \left(0, \beta(1 - \lambda^{-1})\right] \tag{4.10}$$

noting that the parameter a cannot equal 0 by definition. This range is the same as is given in (4.3) with $W = 1$, except that we must have $a > 0$.

These are examples of unstable waves, since they have points at the unstable point $\varphi = a$. Combining the results from these cases with the case of unstable waves, we see that for $W \geq 0$, we can have an unstable standing wave of pulse width W if (4.4) and $a > 0$ are satisfied.

4.2 Theorems on Existence of Standing Waves

In the theorems we will describe the interval for standing waves as a range of values of a depending on the parameters α, γ, and W. The first theorem is on the existence of stable standing waves. The second theorem is on the existence of standing waves of any of the types presented.

4.2.1 Theorem on Existence of Stable Standing Waves

Theorem 1 *Given a set of parameters α and γ, we have a family of candidate stable standing wave solutions given by (3.7). There is one candidate solution in this family for each value of $W \geq 2$ that is unique up to translation. The value of a determines if each of these individual candidate solutions in the family is a real solution.*

1. *If*

$$a \in \left(\beta \frac{1}{(\lambda+1)}, \beta \frac{(\lambda-1)}{(\lambda+1)}\right). \tag{4.11}$$

then each member of the family of candidate solutions is a real solution. This condition on a in (4.11) can only be satisfied if $\alpha < \frac{2}{\beta}$. (Having $\alpha < \frac{2}{\beta}$ implies $\lambda > 2$, which ensures that the interval in (4.11) is nonempty.)

2. *For a given value of $W^* \geq 2$, the member of the family of candidate solutions with pulse width $W = W^*$ is a real solution if*

$$a \in \left(\beta \frac{(1-\lambda^{1-W^*})}{(\lambda+1)}, \beta \frac{(\lambda-\lambda^{2-W^*})}{(\lambda+1)}\right). \tag{4.12}$$

This solution is given by (3.7) for an arbitrary k_0^*, and $k_1^* = k_0^* + W^*$.

3. *Given values $W_L \geq 2$ and $W_U \geq 2$, such that $W_L \leq W_U$, if*

$$a \in \left(\beta \frac{(1-\lambda^{1-W_U})}{(\lambda+1)}, \beta \frac{(\lambda-\lambda^{2-W_L})}{(\lambda+1)}\right), \tag{4.13}$$

then the members of the family of candidate solutions with pulse width W satisfying $W_L \leq W \leq W_U$ are real solutions. If

$$a \in \left(\beta \frac{1}{(\lambda+1)}, \beta \frac{(\lambda-\lambda^{2-W_L})}{(\lambda+1)}\right), \tag{4.14}$$

then the members of the family of candidate solutions with W satisfying $W \geq W_L$ are real solutions.

4. *It is a necessary condition for the existence of a stable standing wave that*

$$a \in \left(\beta \frac{(1-\lambda^{-1})}{(\lambda+1)}, \beta \frac{\lambda}{(\lambda+1)} \right). \tag{4.15}$$

In other words, if

$$a \notin \left(\beta \frac{(1-\lambda^{-1})}{(\lambda+1)}, \beta \frac{\lambda}{(\lambda+1)} \right) \tag{4.16}$$

then there cannot exist any stable standing waves, and none of the family are real solutions.

In Figures 4.2 and 4.3 we show intervals for standing waves. The dark grey region contains the parameters that satisfy (4.11). Notice that this region only exists for values of $\alpha < \frac{2}{\beta}$. That is where the upper bound and the lower bound of this range meet. The entire shaded region includes all the parameters that satisfy (4.15). In both figures we show these intervals for different values of β. In Figure 4.2 we show the pictures larger to be able to see the ranges better, and in Figure 4.3 we show more ranges to be able to better see the effect on these intervals as β changes. We see that as β decreases, the ranges are compressed down and also stretched out to the right.

Proof. We have already determined as in (4.2) that there will be stable standing wave solutions if

$$a \in \left(\beta \frac{(1-\lambda^{1-W})}{(\lambda+1)}, \beta \frac{(\lambda-\lambda^{2-W})}{(\lambda+1)} \right).$$

Remember that for stable standing waves we must have $W \geq 2$.

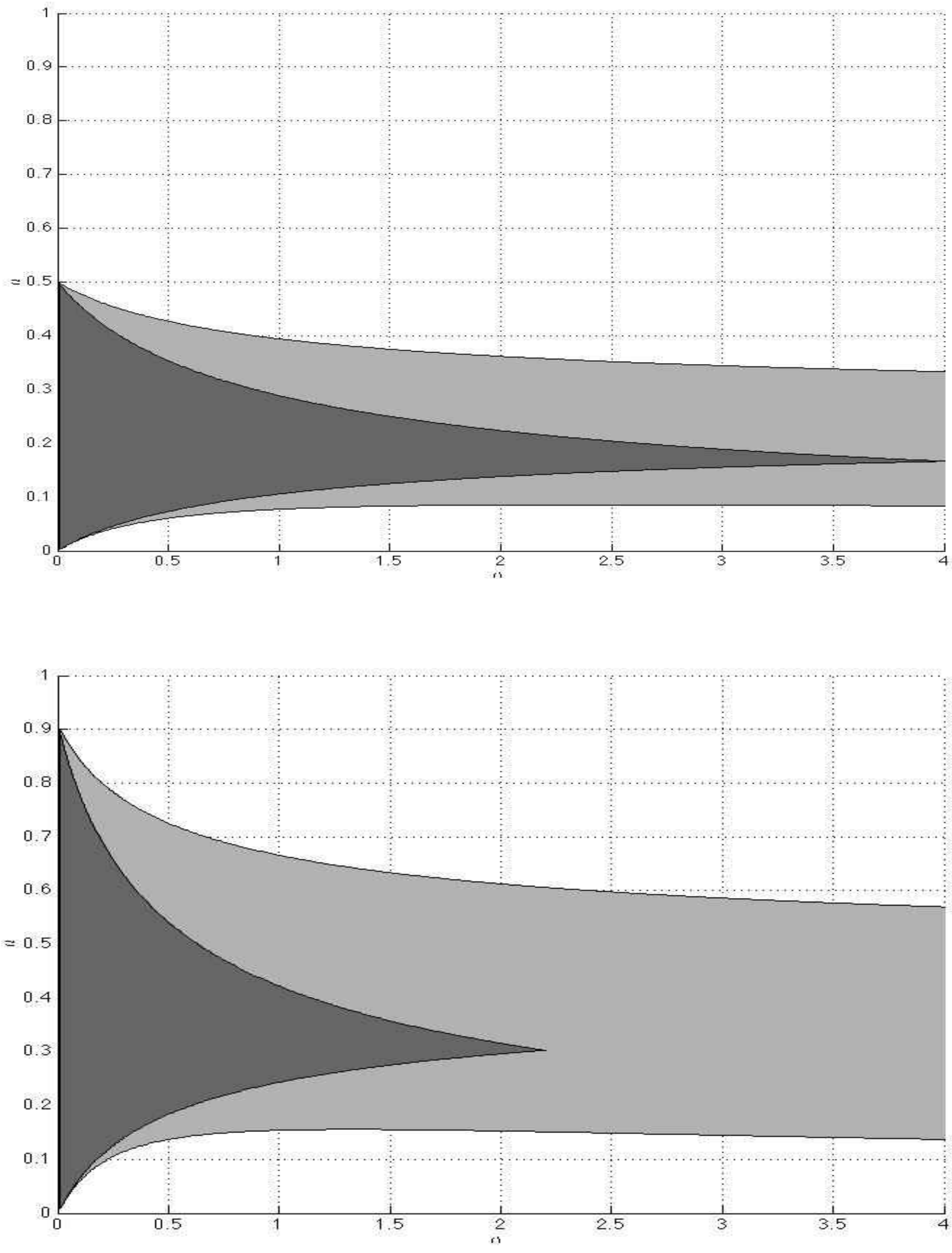

Figure 4.2: Intervals for Standing Waves, plotted a vs. α. The dark gray region are the parameters for which the entire family of candidate solutions are real solutions. The total shaded region is the region that satisfies the necessary condition for the existence of standing waves. The unshaded region is where there exist no stable standing waves. On top $\gamma = 1; \beta = .5$. On bottom $\gamma = .1; \beta = .9091$.

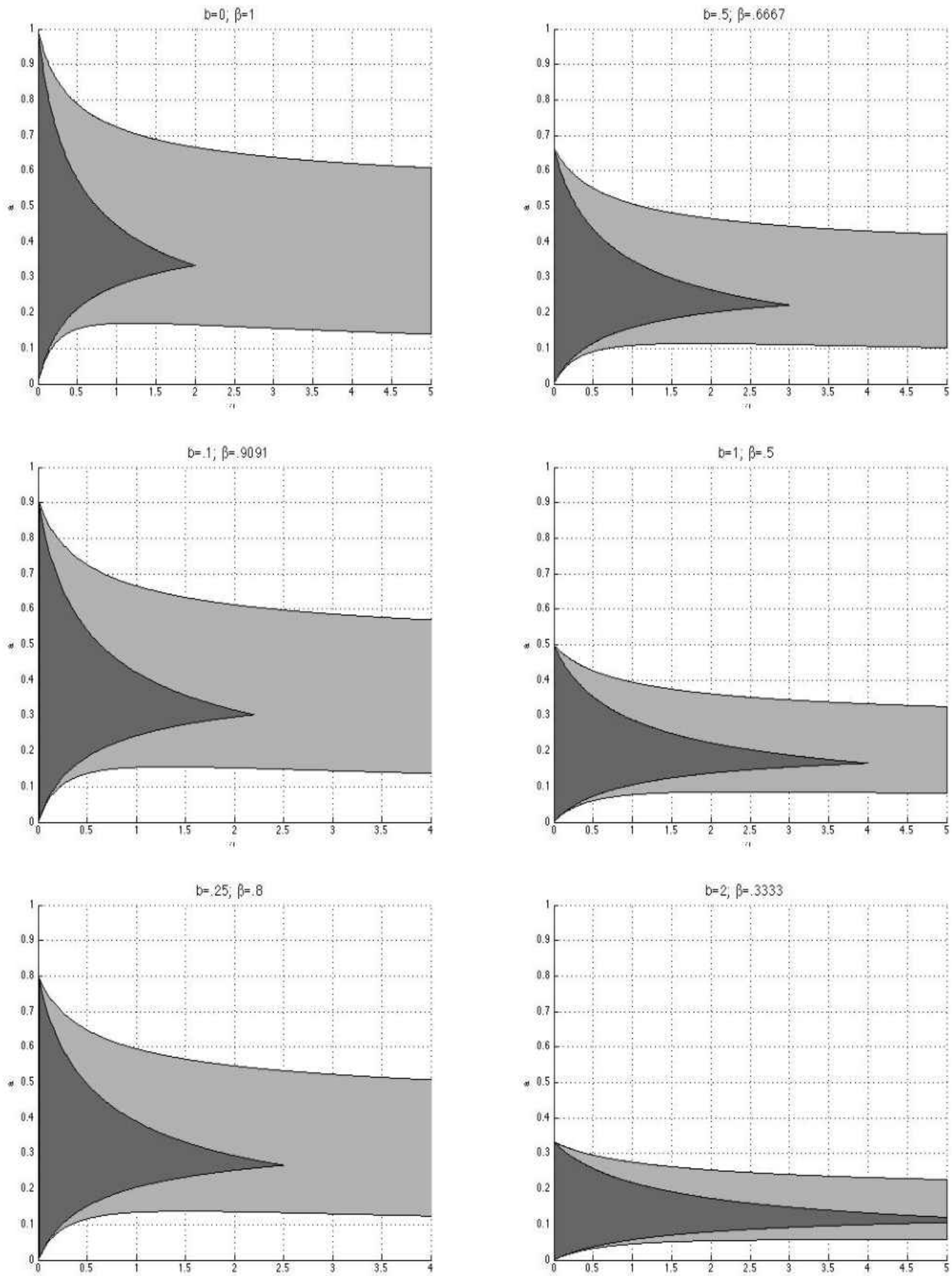

Figure 4.3: Intervals for Standing Waves for various different values of β.

1. The lower bound

$$\beta\frac{(1-\lambda^{1-W})}{(\lambda+1)}$$

will be greatest as $W \to \infty$, so since

$$\lim_{W\to\infty} \beta\frac{(1-\lambda^{1-W})}{(\lambda+1)} = \beta\frac{1}{(\lambda+1)},$$

if

$$a \;>\; \beta\frac{1}{(\lambda+1)}$$

then a will be above the lower bound for all values of W.

The upper bound

$$\beta\frac{(\lambda-\lambda^{2-W})}{(\lambda+1)}$$

will be lowest if $W = 2$, so if

$$\begin{aligned} a \;&<\; \beta\frac{(\lambda-\lambda^{2-2})}{(\lambda+1)} \\ &<\; \beta\frac{\lambda-1}{(\lambda+1)} \end{aligned}$$

then a will be below the upper bound for all values of W.

Therefore if

$$\beta\frac{1}{(\lambda+1)} < a < \beta\frac{(\lambda-1)}{(\lambda+1)},$$

then there will exist stable standing wave solutions for all values of W, and that is how we get our condition (4.11). The caveat is that this range can vanish, i.e. if $(\lambda-1) \leq 1$ so if $\lambda \leq 2$. This happens if $\alpha \geq \frac{2}{\beta}$, and so we only have this interval for standing waves if $\alpha < \frac{2}{\beta}$.

2. We have already proven this in (4.1).

3. Let W^* be such that $W_L \leq W^* \leq W_U$. Let $a \in \left(\beta\frac{(1-\lambda^{1-W_U})}{(\lambda+1)}, \beta\frac{(\lambda-\lambda^{2-W_L})}{(\lambda+1)}\right)$. Since $W_L \leq W^*$, and $a < \beta\frac{(\lambda-\lambda^{2-W_L})}{(\lambda+1)}$, then $a < \beta\frac{(\lambda-\lambda^{2-W^*})}{(\lambda+1)}$. Since $W_U \geq W^*$, and $a > \beta\frac{(1-\lambda^{1-W_U})}{(\lambda+1)}$, then $a > \beta\frac{(\lambda-\lambda^{2-W^*})}{(\lambda+1)}$. So we have that $a \in \left(\beta\frac{(1-\lambda^{1-W^*})}{(\lambda+1)}, \beta\frac{(\lambda-\lambda^{2-W^*})}{(\lambda+1)}\right)$. Therefore, from (4.2), we see that we will have a standing wave with $W = W^*$.

Now let W^* be such that $W^* \geq W_L$. Let $a \in \left(\beta\frac{1}{(\lambda+1)}, \beta\frac{(\lambda-\lambda^{2-W_L})}{(\lambda+1)}\right)$. Since $W_L \leq W^*$, and $a < \beta\frac{(\lambda-\lambda^{2-W_L})}{(\lambda+1)}$, then $a < \beta\frac{(\lambda-\lambda^{2-W^*})}{(\lambda+1)}$. Since $a > \beta\frac{1}{(\lambda+1)}$, we know $a > \beta\frac{(1-\lambda^{1-W^*})}{(\lambda+1)}$. So we have that $a \in \left(\beta\frac{(1-\lambda^{1-W^*})}{(\lambda+1)}, \beta\frac{(\lambda-\lambda^{2-W^*})}{(\lambda+1)}\right)$. Therefore, from (4.2), we see that we will have a standing wave with $W = W^*$.

4. The lower bound

$$\beta\frac{(1-\lambda^{1-W})}{(\lambda+1)} \tag{4.17}$$

will be lowest if $W = 2$, so the absolute lower bound for a to have any stable standing wave solutions is

$$\begin{aligned} a &> \beta\frac{(1-\lambda^{1-2})}{(\lambda+1)} \\ &> \beta\frac{1-\lambda^{-1}}{(\lambda+1)}. \end{aligned}$$

The upper bound

$$\beta\frac{(\lambda-\lambda^{2-W})}{(\lambda+1)}$$

will be highest as $W \to \infty$, so the absolute upper bound for a to have any stable standing wave solutions is

$$\begin{aligned} a &< \lim_{W\to\infty} \beta\frac{(\lambda-\lambda^{2-W})}{(\lambda+1)} \\ &< \beta\frac{\lambda}{(\lambda+1)}. \end{aligned}$$

Therefore we must have

$$\beta\frac{1-\lambda^{-1}}{(\lambda+1)} < a < \beta\frac{(\lambda)}{(\lambda+1)},$$

to be able to have stable standing waves. This is how we get our necessary condition (4.17).

It follows that if a does not satisfy the necessary condition, then no stable standing waves can exist. □

4.2.2 Theorem on Existence of Standing Waves of Any Type

Theorem 2 *1. If*

$$a \in \left[\beta\left(\frac{1}{\lambda+1}\right), \beta\frac{(\lambda-1)}{(\lambda+1)}\right],$$

then there exists a standing wave solution for all $W \geq 0$.

2. If

$$a \in \left(0, \beta\frac{\lambda}{(\lambda+1)}\right)$$

then there exists a standing wave solution for some particular value(s) of $W \geq 0$. Given a value of $W \geq 0$, to have a standing wave we must have that

$$a \in \left[\beta\left(\frac{1-\lambda^{1-W}}{\lambda+1}\right), \beta\frac{(\lambda-\lambda^{-W})}{(\lambda+1)}\right].$$

In the case of $W = 0, 1$, we must add a note that $a > 0$, which is a condition of the original setup which has $a \in (0, 1)$.

3. If

$$a \geq \beta\frac{(\lambda)}{(\lambda+1)}$$

then there cannot exist any standing waves whatsoever.

We illustrate these intervals in Figure 4.4.

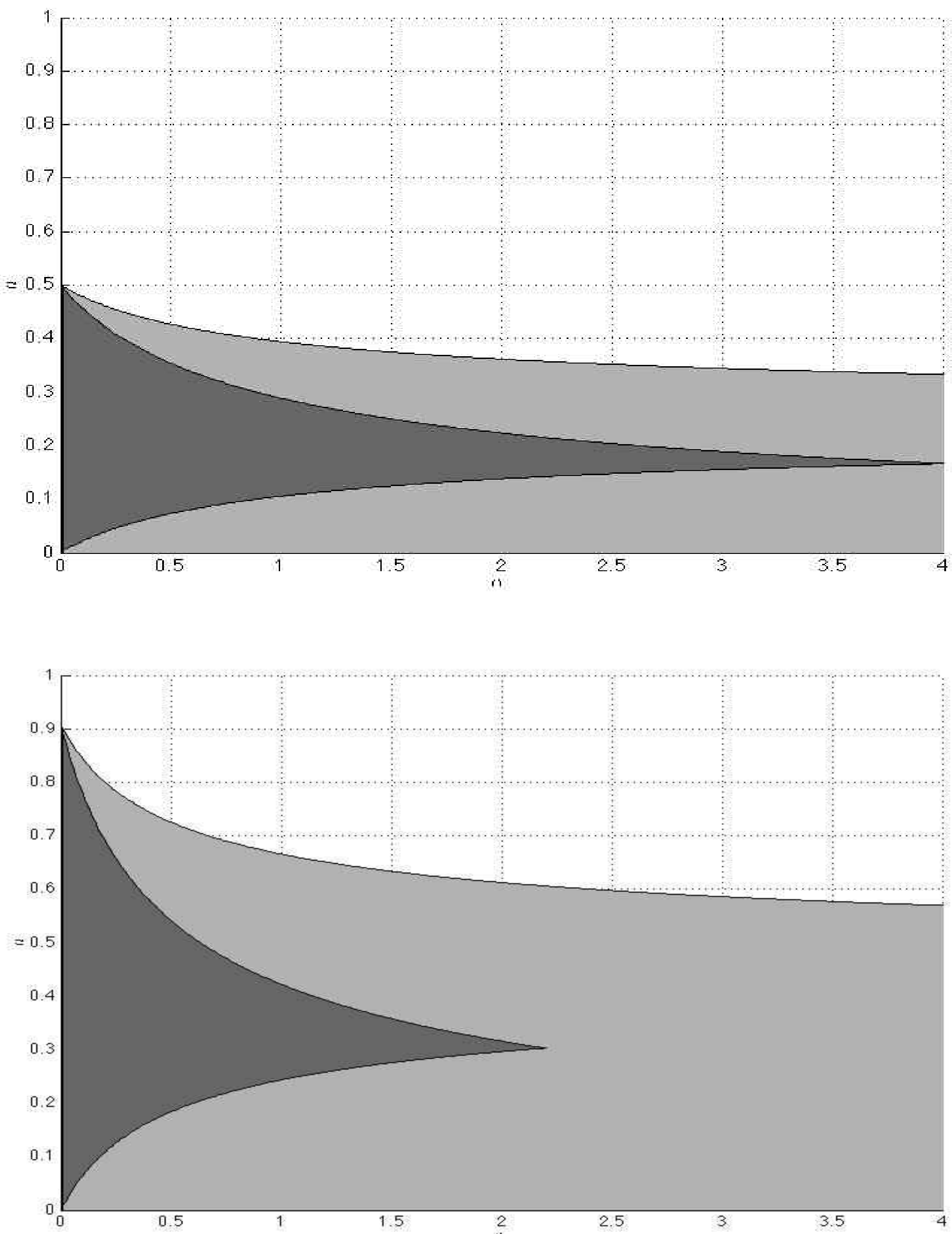

Figure 4.4: Intervals for Standing Waves of any type, plotted a vs. α. The dark gray region are the parameters for which we can have standing waves for all values of $W \geq 0$. The total shaded region is the region that satisfies the necessary condition for the existence of standing waves of any type. The unshaded region is where there exist no standing waves of any type. On top $\gamma = 1; \beta = .5$. On bottom $\gamma = .1; \beta = .9091$.

Proof.

We have shown in Section 4.1.5 that there can exist an unstable wave of $W = W^* \geq 2$ if

$$a \in \left[\beta\left(\frac{1-\lambda^{1-W^*}}{\lambda+1}\right), \beta\frac{(\lambda-\lambda^{-W^*})}{(\lambda+1)}\right]$$

and $a > 0$.

1. Let $a \in \left[\beta\left(\frac{1}{\lambda+1}\right), \beta\frac{(\lambda-1)}{(\lambda+1)}\right]$, and $W^* \geq 0$. Since $a \geq \beta\left(\frac{1}{\lambda+1}\right)$, $a \geq \beta\left(\frac{(1-\lambda^{1-W^*})}{(\lambda+1)}\right)$, and $a > 0$. Since $a \leq \beta\frac{(\lambda-1)}{(\lambda+1)}, a \leq \beta\frac{(\lambda-\lambda^{-W^*})}{(\lambda+1)}$. So we have $a \in \left[\beta\left(\frac{1-\lambda^{1-W^*}}{\lambda+1}\right), \beta\frac{(\lambda-\lambda^{-W^*})}{(\lambda+1)}\right]$ and $a > 0$. Therefore there exists a standing wave with pulse width W^*.

2. The lower bound of our interval for standing waves is least if $W = 0$ and that lower bound is zero. The upper bound of (4.4) is greatest as $W \to \infty$. As we have shown in the proof of Theorem 1, this largest upper bound will be $\beta\frac{\lambda}{(\lambda+1)}$. We cannot actually have a standing wave if $a = \beta\frac{\lambda}{(\lambda+1)}$, though, since we cannot have a wave with $W = \infty$. So the largest range of a that can possibly give us standing waves is $a \in \left(0, \beta\frac{\lambda}{(\lambda+1)}\right)$.

3. If we do not have a in the range from part 2, then we cannot have standing waves of any type for any W.

□

5 NUMERICAL RESULTS

We know from our analytical work that the solutions we have found are indeed steady states of (1.4)-(1.5). In this section we use numerics to perform experiments to test, verify, and illustrate properties of our solutions. For this section we go back to using the variables $u_k(t)$ and $v_k(t)$ because we look at how waves change as time passes. We have code that solves the evolution equation on the system (1.4)-(1.5) using a forward Euler method. We define a small value of time step, usually $\Delta t = .01$ works well, and treat that as a numerical representation of the infinitesimal calculus dt. The basic method consists of taking individual time steps of size Δt and calculating new values of $u_k(t)$ and $v_k(t)$ at each succesive increment of time. The basic calculation that is performed for each time step is as follows:

$$u_k(t + \Delta t) = u_k(t) + \Delta t * \dot{u}_k(t)$$
$$v_k(t + \Delta t) = v_k(t) + \Delta t * \dot{v}_k(t)$$

This process is repeated over many iterations to see how u_k and v_k evolve over longer periods of time. The equations (1.4)-(1.5) define for us $\dot{u}_k(t)$ and $\dot{v}_k(t)$.

Our system deals with a one-dimensional infinite lattice, so for these equations we would have $k \in \mathbb{Z}$. We obviously can't perform an infinite number of calculations so we must only look at a finite range of values on the lattice, for example $0 \leq k \leq 80$. This is acceptable for our purposes because our boundary conditions on either side say that $\lim_{k\to\infty} u_k = 0$ and our solutions tend exponentially to 0 as we go out far enough in either direction. So we use fixed endpoints, say k_L is the index of the left endpoint and k_R is the index of the right endpoint. When performing the evolution equations on u_{k_L} we use u_{k_L} in place of u_{k_L-1} and when performing the evolution equations on u_{k_R} we use u_{k_R} in place of u_{k_R+1}. The forward Euler system is sufficient for our work because our solutions do not behave wildly and we see in our results that the evolution equations behave the way we expect them to.

For steady state solutions $\dot{u}_k(t) = 0$ and $\dot{v}_k(t) = 0$ so those solutions will not change as time passes, since we would have:

$$u_k(t + \Delta t) = u_k(t)$$
$$v_k(t + \Delta t) = v_k(t)$$

In this section, we look at initial values of u_k and v_k that are not steady states and see how they evolve.

5.1 Stability of Solutions

It is simple to calculate and check numerically that our solutions from Section 3.2 satisfy (1.4)-(1.5). In this section we intend to demonstrate the stability or instability of our different types of solutions. We do so by taking an analytical solution from one of our formulas in Section 3.2 and slightly perturbing it. We then use this perturbed wave as the initial condition for our evolution equations. We run the evolution equations for a sufficient amount of time until the wave settles or stops moving significantly. We then compare the initial analytical solution we started with to the final solution we ended up with from the evolution equations. If a perturbed wave returns to its original value, then it has demonstrated stability. If a perturbed wave goes to something different, then it has demonstrated instability. We expect that our stable waves will demonstrate stability and our unstable waves will demonstrate instability.

5.1.1 Stable Waves

We begin with a stable wave that we have generated from (3.7). We use parameters $\alpha = 1$, $b = .1$, $r = 1$, $k_0^* = 0$ and $k_1^* = 6$. We perturb this wave by raising a point on the top of the pulse by a value of .01. So we add $u_3 = u_3 + .01$. We then let the evolution equations run using this perturbed wave as the initial condition. We run the equations from $0 \leq t \leq 40$ with time steps $\Delta t = .01$. Here we show in Figure 5.1 the original wave, the wave that results after running the evolution equations on the perturbed wave, and the numerical difference between the two. We see that the perturbed wave returns to the original wave, and thus we

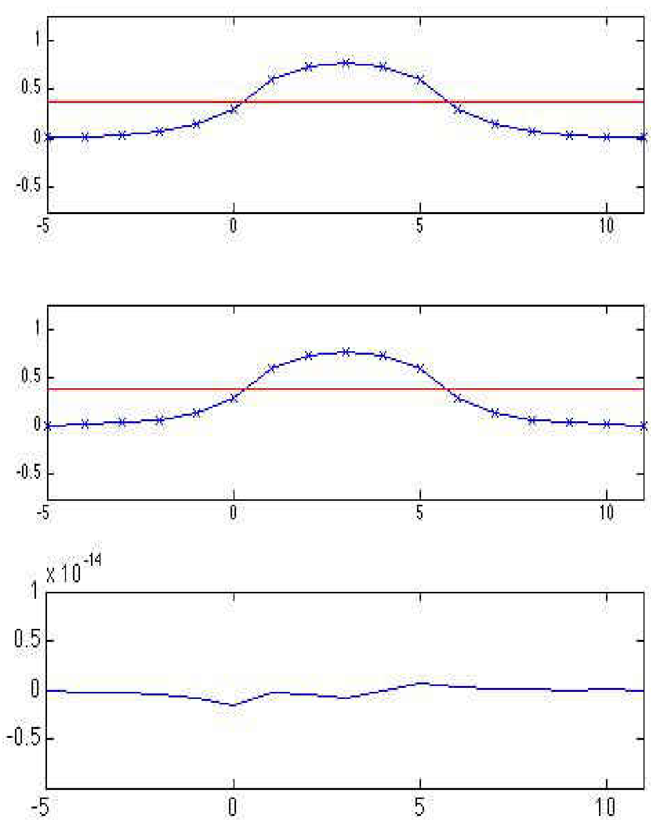

Figure 5.1: A stable wave is perturbed. On top, the original wave. In the middle, the wave that remains after the perturbed wave is put through the evolution equations and comes to a rest. On the bottom, the numerical difference between the original un-perturbed wave and the final wave. Here the difference is essentially zero. The parameter a is plotted with the waves.

have demonstrated the stability of the solution and verified our hypothesis.

5.1.2 Unstable Waves

We begin with an unstable wave that we have generated from (3.10). We use parameters $\alpha = 1$, $b = .1$, $r = 1$, $k_0^* = 0$ and $k_1^* = 5$. We perturb this wave by raising a point on the top of the pulse by a value of .001. So we add $u_2 = u_2 + .001$. We then let the evolution equations run using this perturbed wave as the initial condition. We run the equations from $0 \leq t \leq 40$ with time steps $\Delta t = .01$. Here we show in Figure 5.2 the original wave, the wave that results after running the evolution equations on the perturbed wave, and the numerical difference between the two.

For the next experiment, we begin with the same initial wave as in the last experiment We perturb this wave by lowering a point on the top of the pulse by a value of .001. So we subtract $u_2 = u_2 - .001$. We then let the evolution equations run using this perturbed wave as the initial condition. We again run the equations from $0 \leq t \leq 40$ with time steps $\Delta t = .01$. Here we show in Figure 5.3 the original wave, the wave that results after running the evolution equations on the perturbed wave, and the numerical difference between the two.

The wave we started with was an unstable case wave and had $W = 5$. We see from the first experiment that if we perturb a point up, the points on the wave will go up and settle at a stable wave with $W = 7$. We see from the second experiment that if we perturb a point down, the points on the unstable wave wave will go down and settle at a stable wave with $W = 5$. This demonstrates the instability of the unstable wave, as we expected.

We show that the perturbed unstable waves do indeed settle to one of our stable waves (3.7) by comparing the final waves from the experiments above with our solutions from (3.7). In Figure 5.4 we compare the final wave from the unstable wave that was perturbed up to the stable wave with $W = 7$. In Figure 5.5 we compare the final wave from the unstable wave that was perturbed down to the "Stable" wave with $W = 5$.

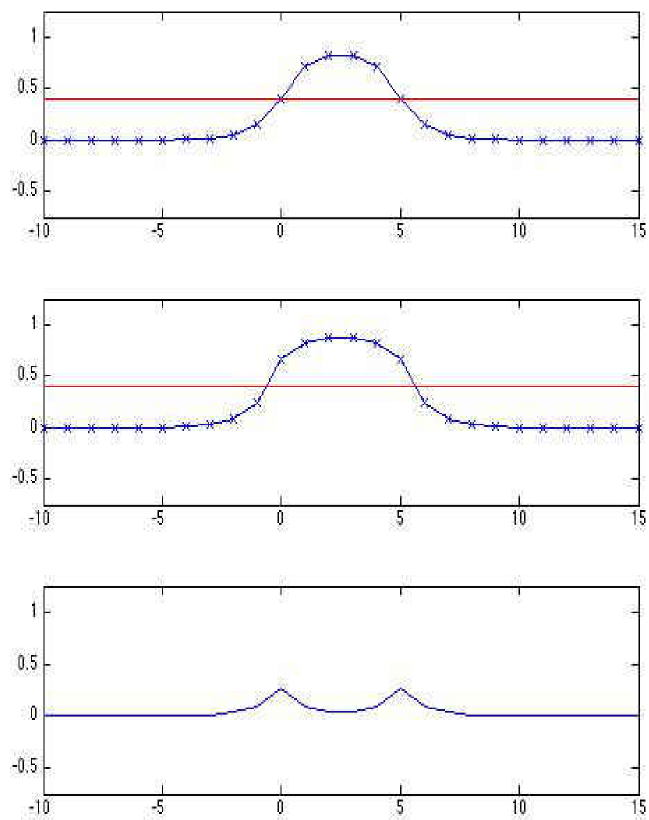

Figure 5.2: An unstable wave is perturbed up by .001 at a point at the peak ($k = 2$). On top, the original wave. In the middle, the wave that remains after the perturbed wave is put through the evolution equations and comes to a rest. On the bottom, the numerical difference of the final wave minus the original un-perturbed wave. The parameter a is plotted with the waves.

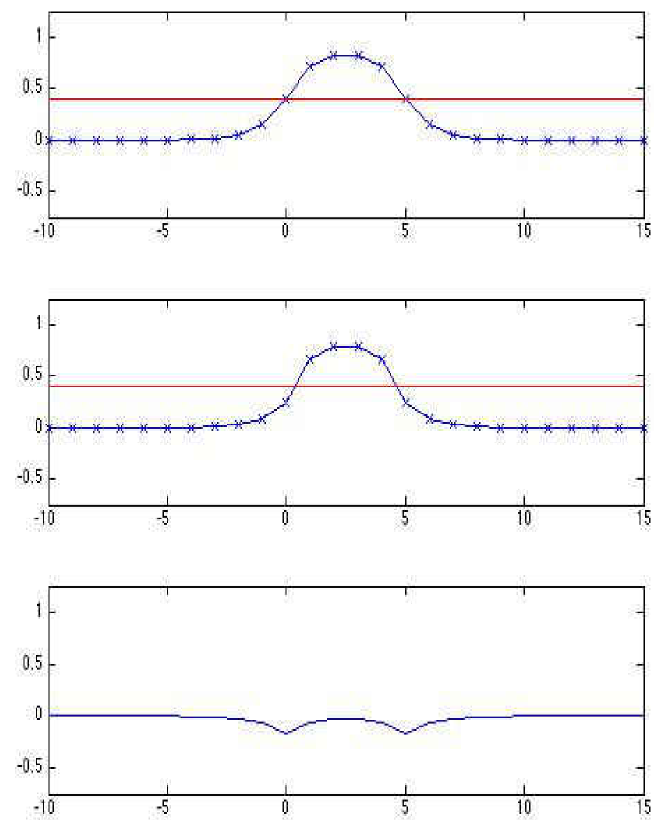

Figure 5.3: An unstable wave is perturbed down by .001 at a point at the peak ($k = 2$). On top, the original wave. In the middle, the wave that remains after the perturbed wave is put through the evolution equations and comes to a rest. On the bottom, the numerical difference of the final wave minus the original un-perturbed wave. The parameter a is plotted with the waves.

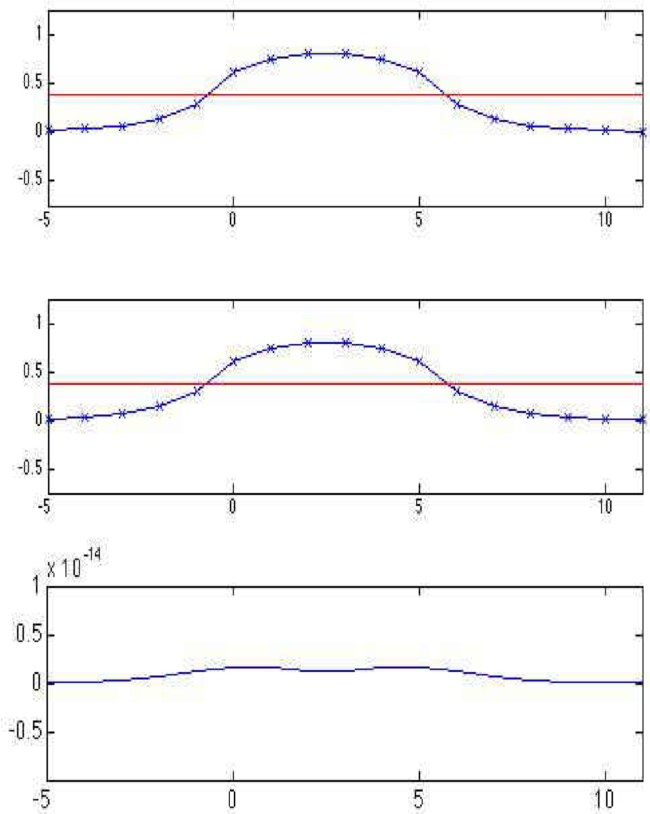

Figure 5.4: An unstable wave is perturbed up by .001 at a point at the peak ($k = 2$). On top, the wave that remains after the perturbed wave is put through the evolution equations and comes to a rest. In the middle, the stable wave, $W = 7$. On the bottom, the numerical difference between the two waves. The parameter a is plotted with the waves.

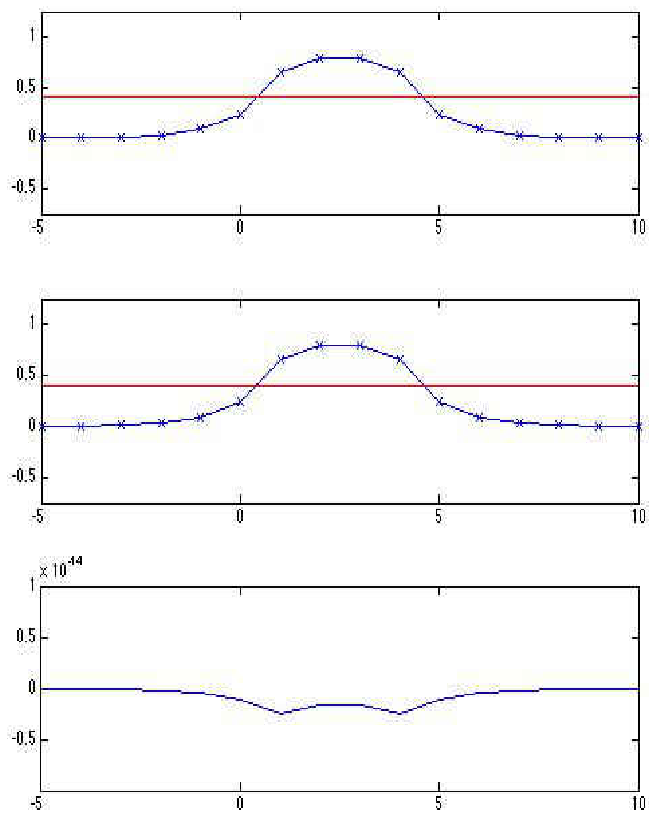

Figure 5.5: An unstable wave is perturbed down by .001 at a point at the peak ($k = 2$). On top, the wave that remains after the perturbed wave is put through the evolution equations and comes to a rest. In the middle, the stable wave, W=5. On the bottom, the numerical difference between the two waves. The parameter a is plotted with the waves.

We show that our unstable waves can also be made to settle down on one side and up on the other side. This can happen if the wave is perturbed up on one side and down on the other side, causing one of the unstable points to move up and the other unstable point to move down. We show in Figure 5.6 what happens when we perturb a point on the left side up and a point on the right side down. This causes the left unstable point to move up and the right unstable point to move down before settling at a stable wave. Here the initial unstable wave has $W = 5$ and the final stables wave has $W = 6$.

What is going on here is that if an unstable wave is perturbed in any way, it will knock the point(s) at the unstable equilibrium point $\varphi = a$ out of equilibrium, and they then will want to go away from a towards 0 or 1. Whether a point will go up or down is based on the perturbation, so whichever side of a the point is originally knocked to will be the direction that point will continue to travel until the entire wave reaches equilibrium again.

5.2 Verification of Our Ranges

We do this experiment to verify that our stable standing waves will exist within the ranges prescribed by (4.1) and that our evolution equation works in a way that agrees with the behavior that we would expect. We choose parameters $b = 1$, $r = 1$ (so $\beta = .5$), and $W = 4$ to do the experiment on. We then choose many different combinations of the parameters α and a to test. For each value of α, we have a stable wave given by (3.3). We use this wave as an initial condition and then run it through our evolution equation for several different values of a inside, above, and below the range given by (4.1). In Figure 5.7 we plot each of these points tested with a different symbol indicating a different type of behavior for that set of parameters. We show more points near the boundaries of this range to illustrate the shift in behavior precisely at these points. For values of a inside the range (4.1), the standing wave remains.

If the value of a is raised above the upper bound of (4.1), the wave will die out; we

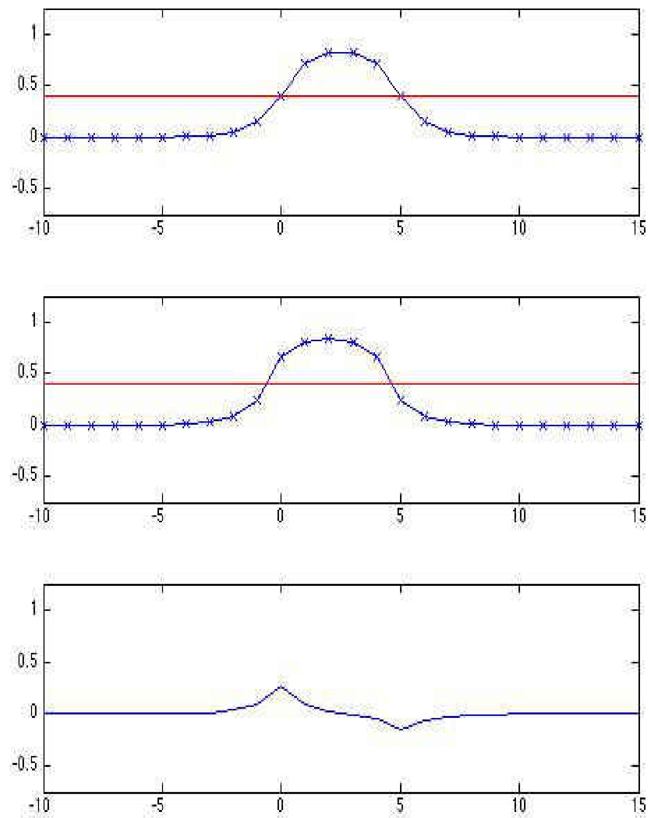

Figure 5.6: An unstable wave is perturbed up by .001 at a point on the left side of the the peak ($k = 1$) and down by .001 on the right side of the peak ($k = 4$). On top, the original wave. In the middle, the wave that remains after the perturbed wave is put through the evolution equations and comes to a rest. On the bottom, the numerical difference of the final wave minus the original un-perturbed wave. The parameter a is plotted with the waves.

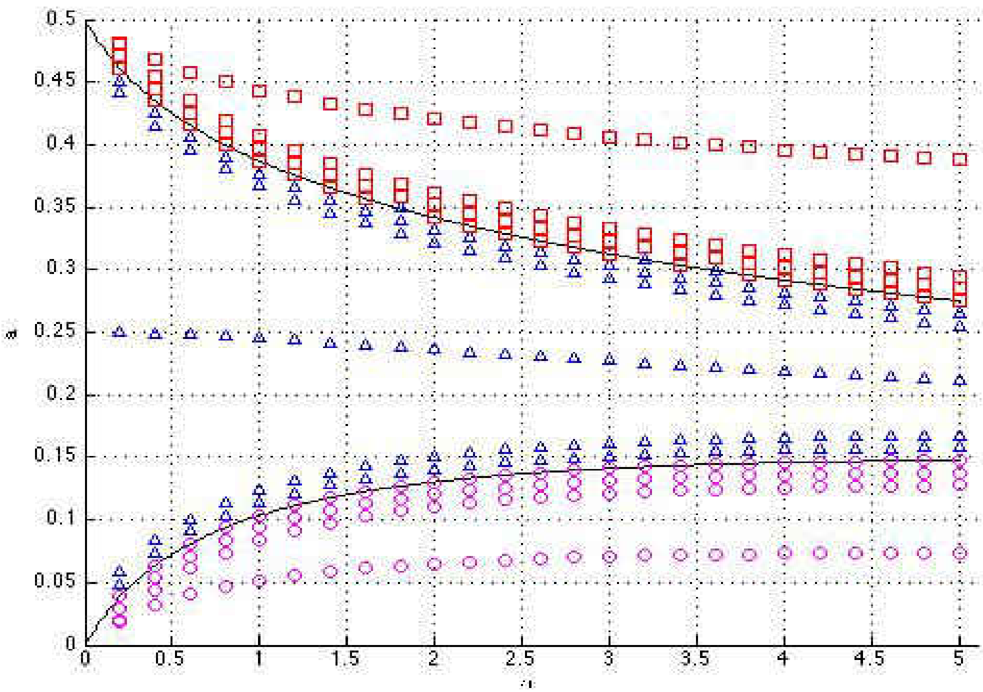

Figure 5.7: Verification of Our Ranges - Red squares are waves that died out. Blue triangles are standing waves. Magenta circles are waves that propagated outwards.

illustrate this behavior in Figure 5.8. As a standing wave dies out, the width of the wave W decreases. It is important to note that if a is above the upper bound of (4.1) for $W = W^*$, then a will be above the upper bound of (4.1) for all $W \leq W^*$, so this dying out of the wave, and shrinking of the wave's width W, will continue until the wave is completely gone and the medium is flat.

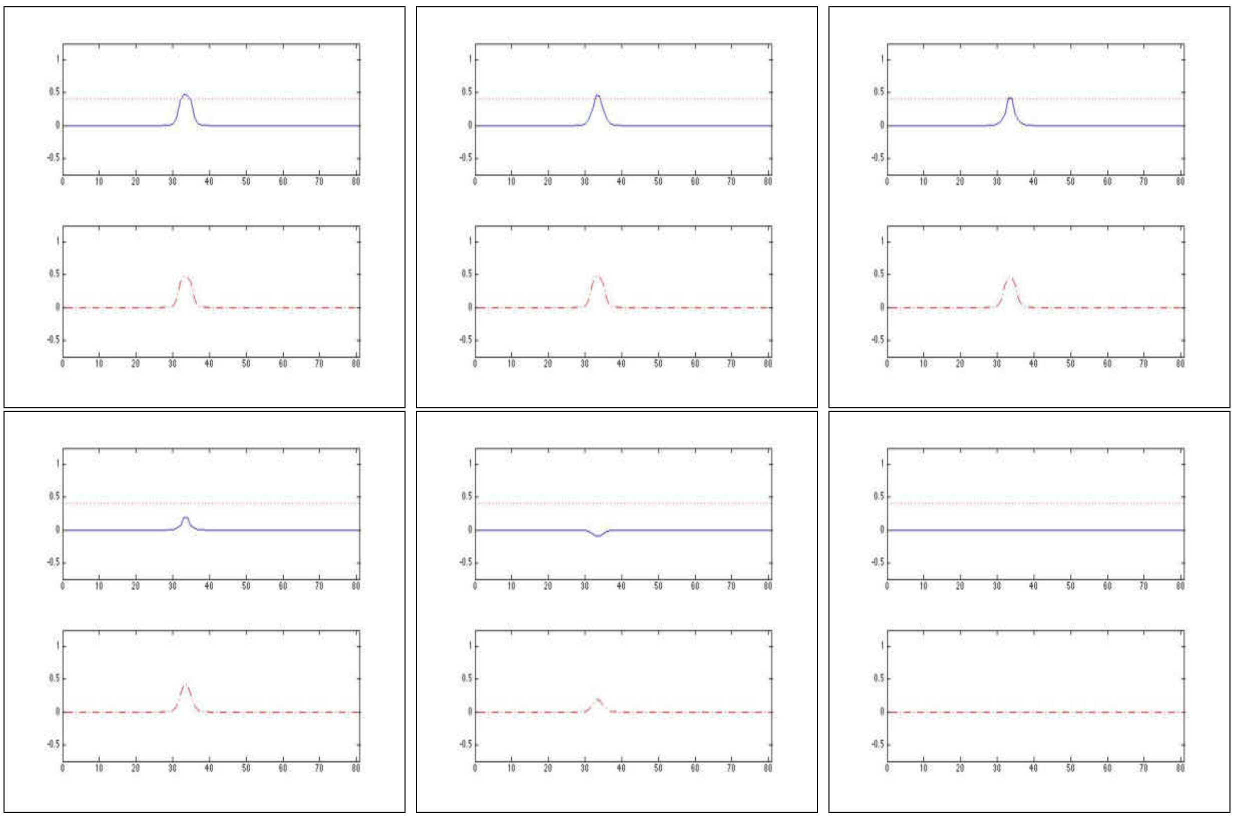

Figure 5.8: A wave dies out because the detuning parameter a is too high for it to remain a standing wave. Each box is a snapshot at a point in time. Inside each box we have the wave on top and the recovery wave on bottom. The detuning parameter a is plotted as a dotted line with the wave. Time passes from snapshot to snapshot going from left to right, and then top to bottom.

If the value of a is lowered below the lower bound of (4.1), the wave propagates outward in both directions; we illustrate this behavior in Figure 5.9. As the wave propagates outward in both directions, the value of W increases. It is important to note that if a is below the lower bound of (4.1) for $W = W^*$, then a will be below the lower bound of (4.1) for all $W \geq W^*$, so this propagation outwards, and growing of the wave's width W, will continue indefinitely.

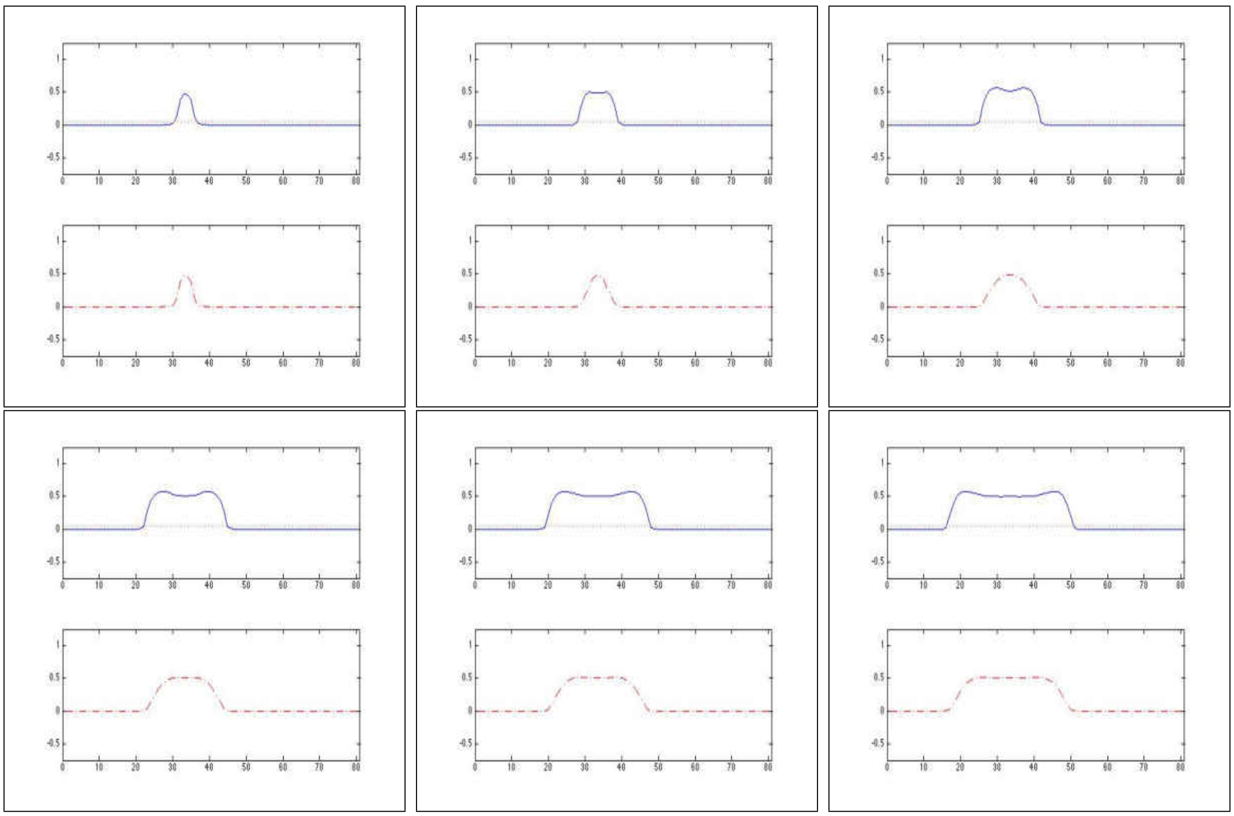

Figure 5.9: A wave propagates outward because the detuning parameter a is too low for it to remain a standing wave. Each box is a snapshot at a point in time. Inside each box we have the wave on top and the recovery wave on bottom. The detuning parameter a is plotted as a dotted line with the wave. Time passes from snapshot to snapshot going from left to right, and then top to bottom.

5.3 Comparison with Elmer-Van Vleck Paper

In their paper [7], Elmer and Van Vleck study traveling waves of a generalized version of the system (1.4)-(1.5). Our problem is a special case of their problem, and so if we match parameters up we can compare our results.

In [7] they find candidate traveling wave solutions to their generalized system. For our corresponding system they have formulas for the candidate traveling waves involving complicated integrals, with φ the voltage wave and ψ the recovery wave.

$$\varphi(\xi) = \int_0^\infty W(s)[\sin(s(\xi-\xi_0))-\sin(s(\xi-\xi_1))]ds+\int_0^\infty X(s)[\cos(s(\xi-\xi_0))-\cos(s(\xi-\xi_1))]ds \tag{5.1}$$

$$\psi(\xi) = \int_0^\infty Y(s)[\sin(s(\xi-\xi_0))-\sin(s(\xi-\xi_1))]ds+\int_0^\infty Z(s)[\cos(s(\xi-\xi_0))-\cos(s(\xi-\xi_1))]ds \tag{5.2}$$

$$W(s) = \frac{1}{\pi}\left[\frac{b^2r + C(s)A(s)}{sD(s)}\right] \tag{5.3}$$

$$X(s) = \frac{c}{\pi}\left[\frac{-b + C(s)}{D(s)}\right] \tag{5.4}$$

$$Y(s) = \frac{b}{\pi}\left[\frac{brA(s) + b - c^2s^2}{sD(s)}\right] \tag{5.5}$$

$$Z(s) = \frac{c}{\pi}\left[\frac{A(s) + br}{D(s)}\right] \tag{5.6}$$

$$A(s) = 1 + 2d(1 - cos(s)) \tag{5.7}$$

$$C(s) = b^2r^2 + c^2s^2 \tag{5.8}$$

$$D(s) = c^2s^2(A(s) + br)^2 + (brA(s) - c^2s^2 + b)^2 \tag{5.9}$$

The parameter c is the wave speed, and d is the diffusion coefficient. Their ξ_0 and ξ_1 are our η_0 and η_1. Because of translational invariance, they are able to set $\xi_0 = 0$. To satisfy the fact that they must have $\varphi(\xi_0) = \varphi(\xi_1)$, there must exist a value of ξ_1 such that

$$\int_0^\infty X(s)[1 - cos(s\xi_1)]ds = 0. \tag{5.10}$$

To be able to calculate a candidate traveling wave, we must first find a value of ξ_1 that satisfies this.

We see a lot of complex integrals in these equations. We cannot solve these equations analytically, so we try to compute approximations of them using numerics. We use the adaptive quadrature scheme of [24] in calculating these integrals. The integrals in the formulas above are from zero to infinity, but we obviously can't calculate the value of the integral all the way out to infinity. We instead only calculate the value of the integral from zero to 80. This is acceptable because the terms in the integral tend to zero as s gets bigger, so most of the area of the integral will come from the lower values of s. Since all of this approximation work that we are doing is numerical, some error will inevitably exist, but since the traveling wave solutions they find are attractors, any small error should be inconsequential.

For each combination of parameters, when we numerically compute the candidate solution and put it through our evolution equations, we get one of three results. Either we get a traveling pulse wave like we have pictured in Figure 1.1, we get a wave that dies out and we end up with a flat line, or we get a standing pulse wave which looks like one of our standing wave solutions.

We set our parameters $b = 1$, and $r = .25$. Then we perform this experiment for combinations of α and c at increments each between 0 and 5. We plot in Figure 5.10 our results for this series of experiments. Green circles represent parameter values where we got a traveling wave. Red squares are parameters where the wave died out. Blue triangles are parameters where we got standing waves.

An interesting thing we see from this is that we can have traveling waves and standing waves for the same set of parameter values. In Figure 5.11 we show just the parameter values where we got traveling waves, plotted on top of our intervals for standing waves from Theorem 1. We see that we have traveling waves for parameter values inside these regions.

We look at all of the standing waves that we got in the previous experiment, and see that they all fall within the ranges of parameter values that we would expect, from the ranges in

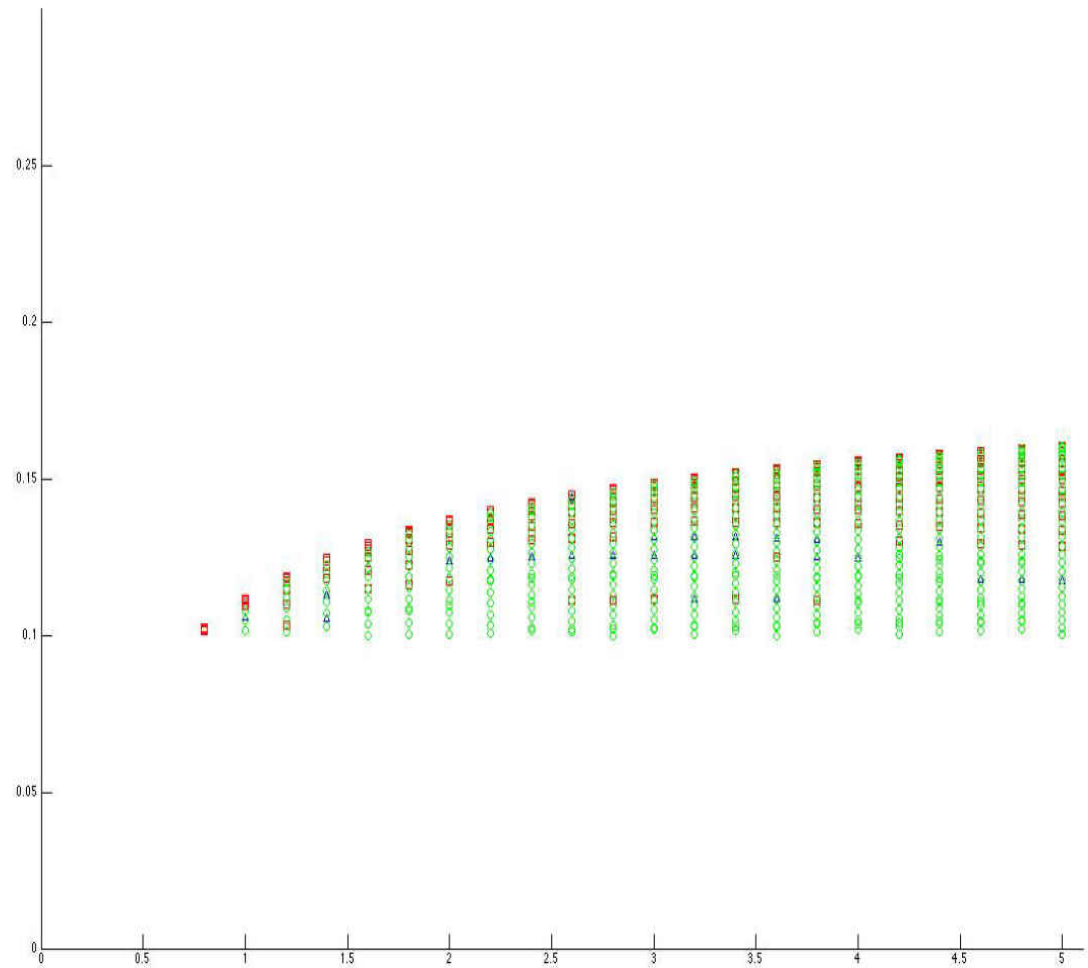

Figure 5.10: Plots of what type of waves we got for initial conditions from (5.1) and (5.2), with $r = .25$, The parameter values of α tested are between .2 and 5 at increments of .2. The values of c tested are between .1 and 5 at increments of .1. Green circles are traveling waves. Red squares are waves that died out. Blue triangles are standing waves.

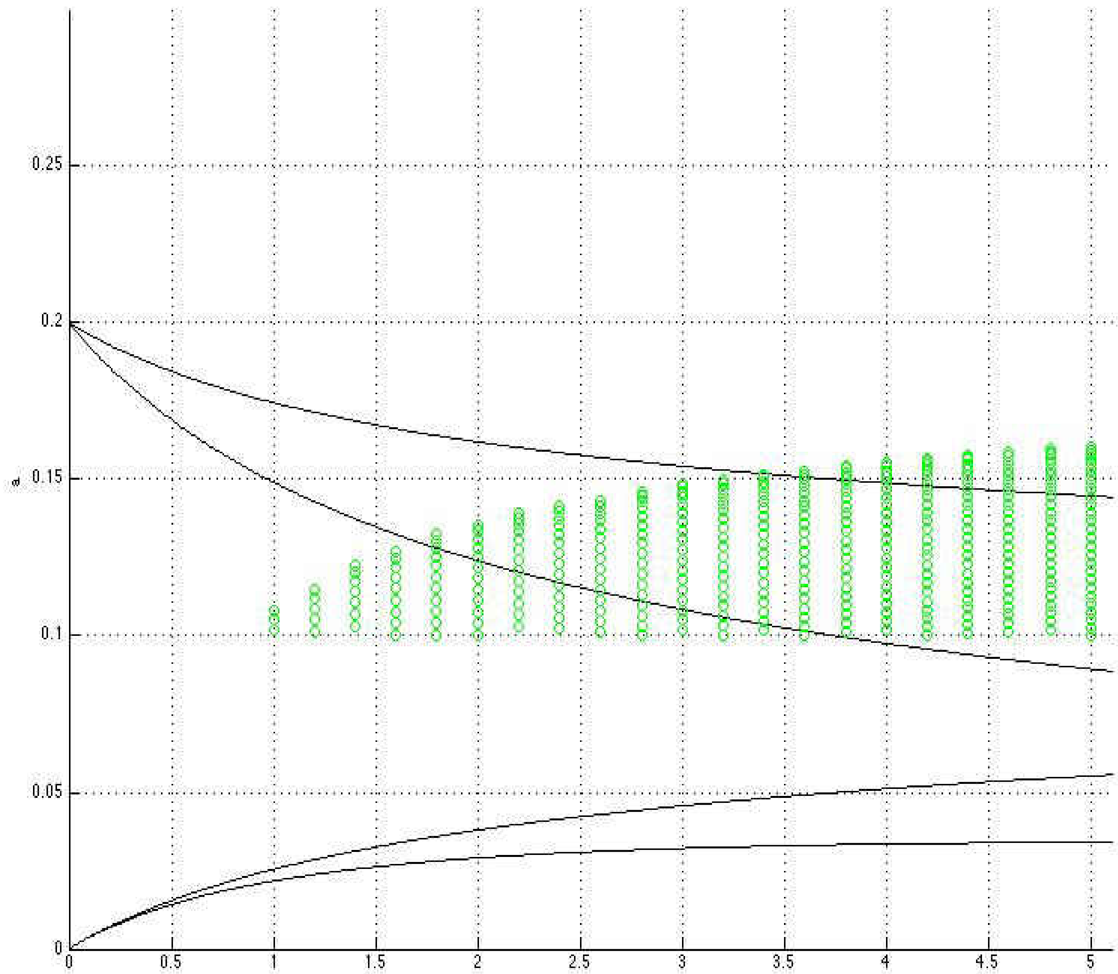

Figure 5.11: We plot with circles parameter values for which we got traveling waves. The lines denote our intervals for standing waves from Theorem 1. The graph is plotted a vs. α. $b = 1$, $r = .25$.

(4.1). We show this in Figure 5.12.

We chose one of these sets of parameter values that gave us a standing wave in the experiments above and show that it fits with one of our standing wave solutions. We choose parameters $\alpha = 2$ and wave speed $c = .9$ which gives us $a = .1238$. We show in Figure 5.13 how their initial conditions from these parameters evolved into a standing wave. We look at the standing wave that results and see that it has $W = 5$. We show in Figure 5.14 a comparison of the wave that resulted from running the evolution equations on the initial conditions from [7], as well as the wave given by (3.3), $W = 5$, that it matches up with, and the numerical difference between the two.

An important point that we have learned from these experiments is that there can exist traveling waves and standing waves for some of the same parameter values. This is different than with fronts, where if there is a standing wave there can't be a traveling wave. In the next section we look into what can happen if both a traveling wave and a standing wave exist.

5.4 Collision of Traveling Wave and Standing Wave

Here we show an experiment of a traveling wave colliding with a standing wave. For this experiment we pick parameter values for which we know that we can have both standing waves and traveling waves. We set $\alpha = d = 2$, $b = 1$, $c = 2$, $a = .1252$, and $r = .25$. We initialize a traveling wave using the adaptive quadrature method for the integrals in (5.1) and (5.2). We initialize a standing wave from our formula (3.7). We place the standing wave in the path of the traveling wave, so that they will collide. Each box in Figure 5.15 is a snapshot of the wave at a point in time. In each box, we have on top the wave, and on bottom the recovery wave. Time passes from one snapshot to another, moving from left to right, then top to bottom. The amount of time between each snapshot is not equally spaced, but the snapshots are chosen to best illustrate the behavior around the time of the collision.

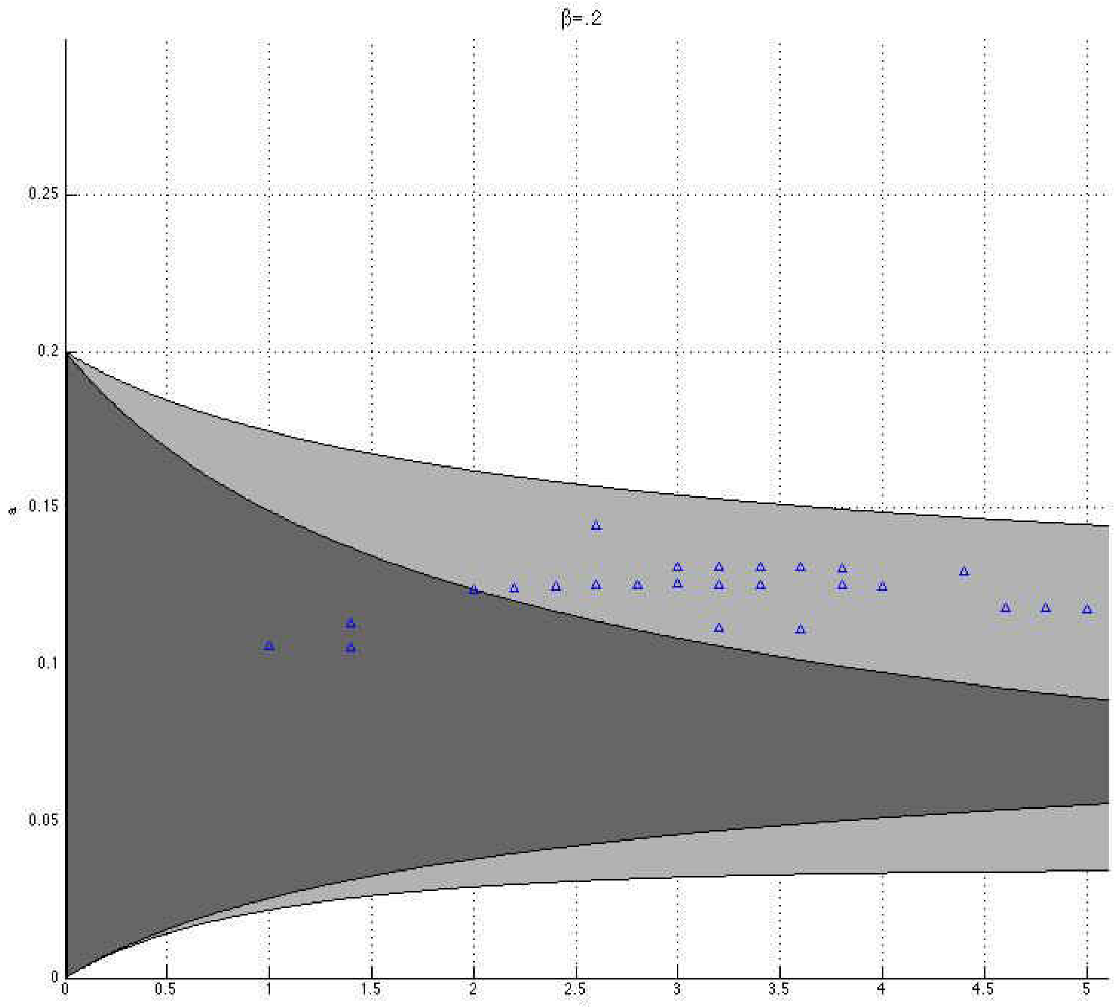

Figure 5.12: Plots of all of the standing waves the we got in the previous experiment, plotted on top of with the ranges from Theorem 4.1. We see that all of the standing waves we found fall inside the grey regions, as we would expect.

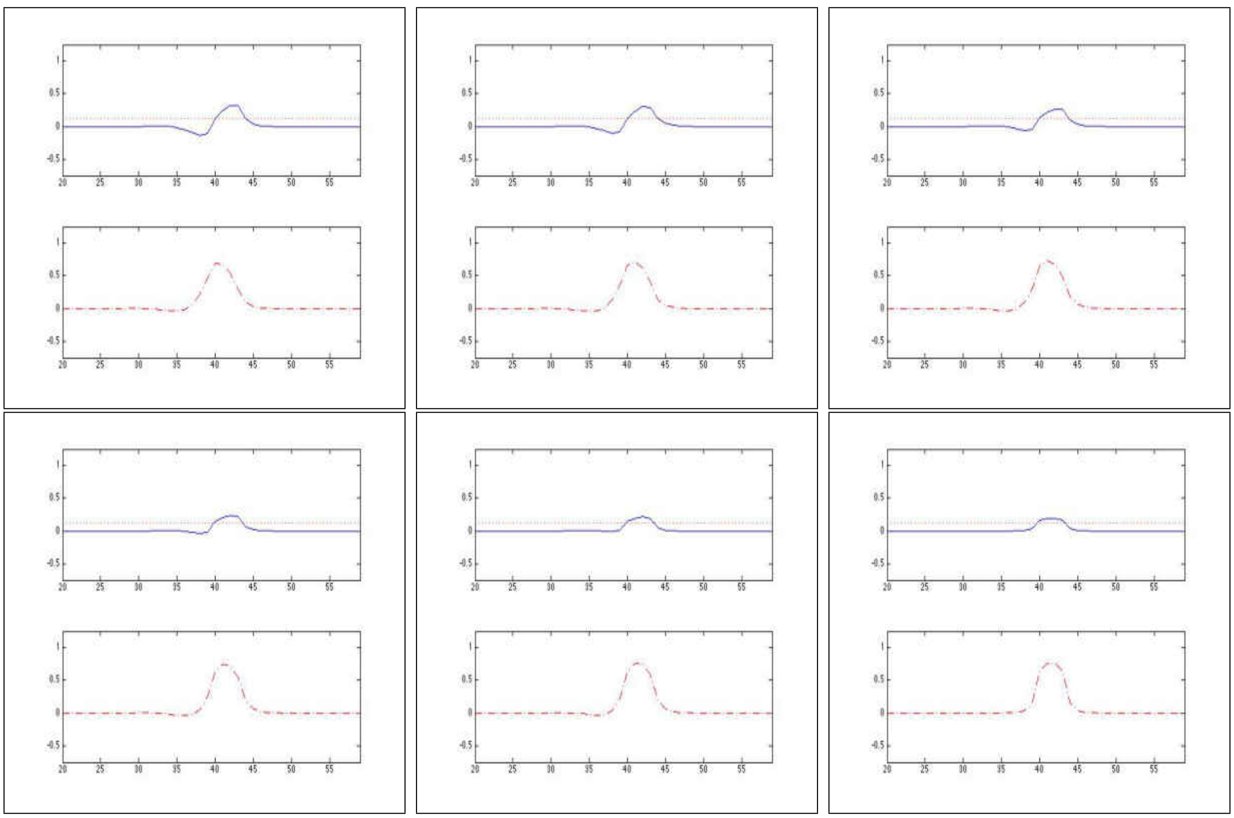

Figure 5.13: An initial condition generated from [7] turns into a standing wave. On top, the wave. On bottom, the recovery wave.

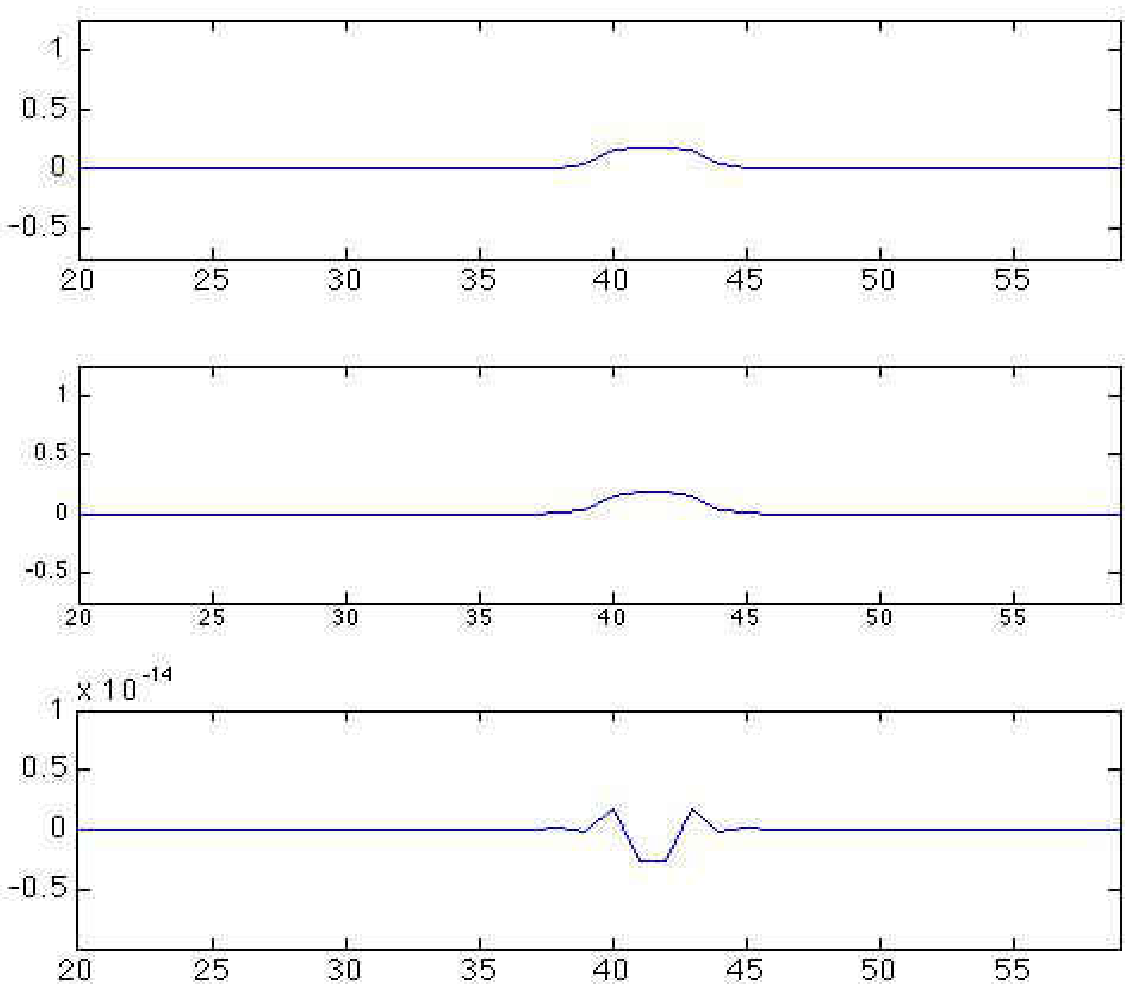

Figure 5.14: On top, the standing wave the resulted from the evolution equation. In the middle, the exact solution from our formulas. On the bottom, the numerical difference between the two waves, which is essentially zero.

We see that the traveling wave hits the standing wave and both waves are annihilated. Even though we may have the existence of a traveling wave and a standing wave for the same parameter values, if the standing wave is in the way of the traveling wave, the standing wave can block the traveling wave and cause propagation failure. It is not proved here to be true in all cases, but in all the experiments we performed for different parameter values, the traveling wave and standing wave were annihilated upon collision of the two waves.

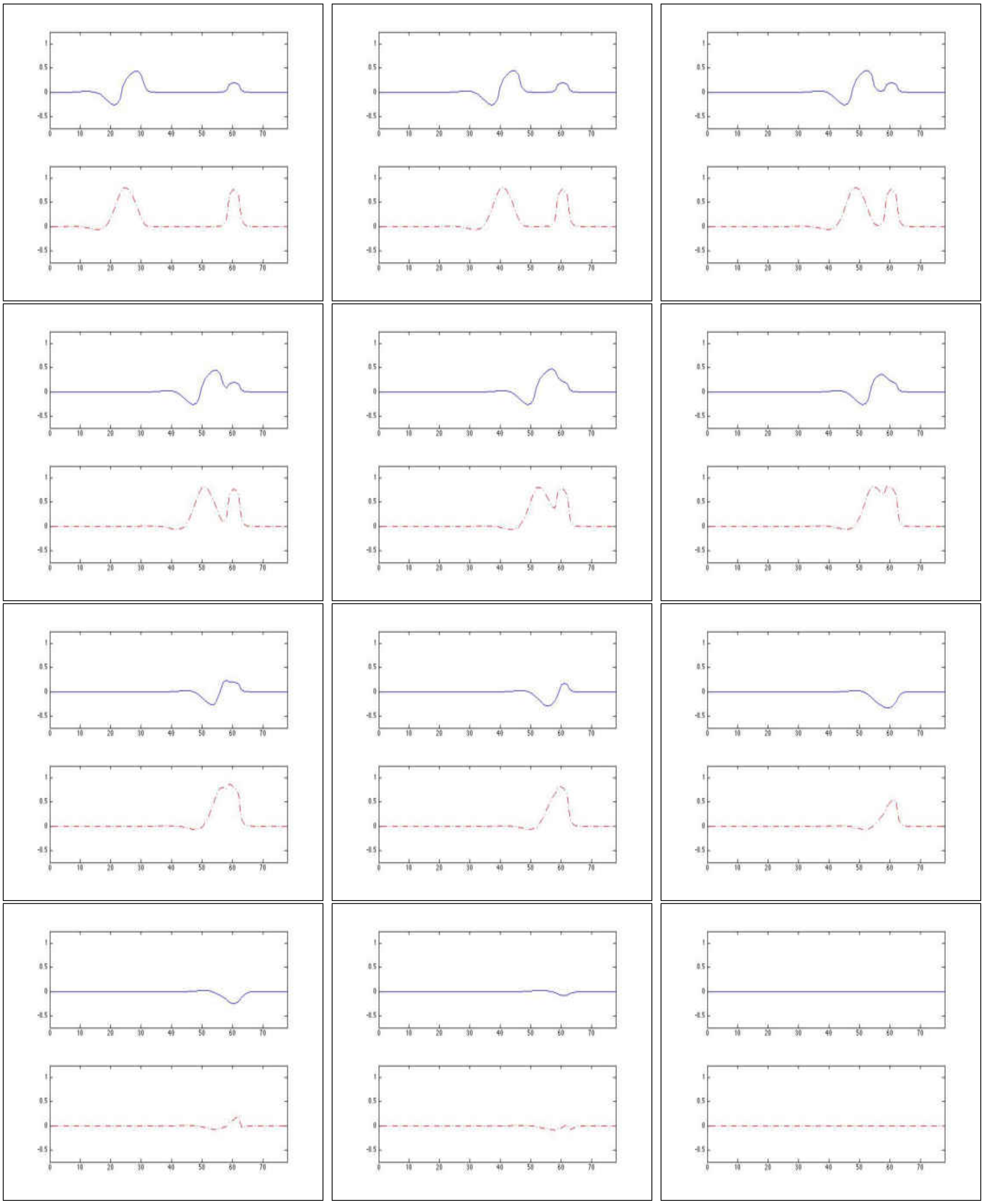

Figure 5.15: A traveling wave colliding with a standing wave. Both waves are annihilated. In each box, we have on top the wave, and on bottom the recovery wave. The snapshots are in order going left to right, then top to bottom.

6 CONCLUSIONS AND FUTURE WORK

6.1 Conclusions

A main conclusion we have come to here is that studying propagation failure pulse waves of the FitzHugh-Nagumo equations is much more complex than studying propagation failure of fronts of the Nagumo equation. We see that the direct connection between the existence of standing waves and propagation failure does not exist with the FitzHugh-Nagumo equations. We have found parameter values that allow us to have both standing waves and traveling waves, which could not exist with just the Nagumo equation. We have numerical results on when we can have traveling waves from [7], and we would like to understand where these ranges of parameter values come from. Still, we know that standing waves can block traveling waves, and so this knowledge of standing waves can be useful in studying wave blocking.

Part of this difference between fronts and pulses may come from the differences in shape of standing waves and traveling waves. With the Nagumo equation, traveling fronts and standing fronts look the same, except one is moving and the other is not. For the FitzHugh-Nagumo equations though, standing waves don't look quite like traveling waves. Our standing waves are relatively, or exactly symmetrical, while traveling waves are not. Traveling waves have an asymmetrical shape such they are oriented to travel in a specific direction, either left or right.

Standing pulse waves can be looked at as two opposing standing fronts, like the ones in Figure 6.1. We see from our results in Section 5.2 that when these symmetrical standing waves move, it is just as fronts would move, and they move in a symmetrical manner, either both inwards, or both outwards.

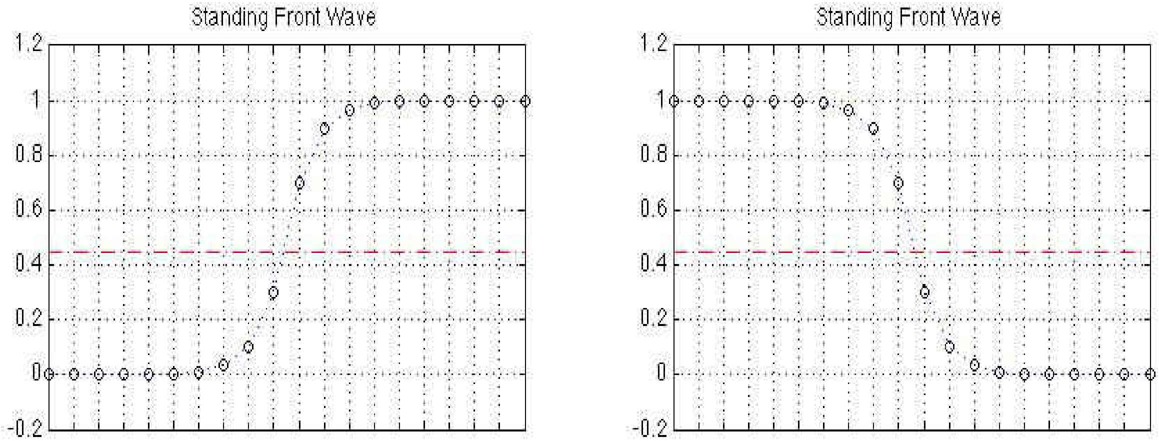

Figure 6.1: Pictures of two standing fronts oriented in opposite directions. The detuning parameter a is plotted as a dashed line.

As in [6], the formula for a standing front wave form is given by

$$\varphi_k = \begin{cases} 1 - (1-\varphi_1)\lambda^{1-k}, & k \geq 0, \\ \varphi_0 \lambda^k, & k \leq (a+1)/2. \end{cases}$$

We can see the similarities between standing fronts and pulses by comparing this formula to our formula (3.3). We can also see the similarities between our ranges for standing waves and the interval of propagation failure in [6]. For stable front waves, this range is given by

$$a \in \left(\frac{1}{\lambda+1}, \frac{\lambda}{\lambda+1} \right).$$

We see that this agrees with our range(4.2), if we let $W \to \infty$. This says that a standing pulse wave really does correspond in a way to two standing fronts, and if we let the distance W between these opposing fronts grow indefinitely, then the effect of each side of the standing pulse on each other disappears. As this happens, each side of the standing pulse converges to a front solution.

Here we plot the complete families of symmetrical waves, split onto two graphs. Figure 6.2 shows point-top waves, with even values of $W \geq 0$. Figure 6.3 shows flat-top waves, with odd values of $W \geq 1$.

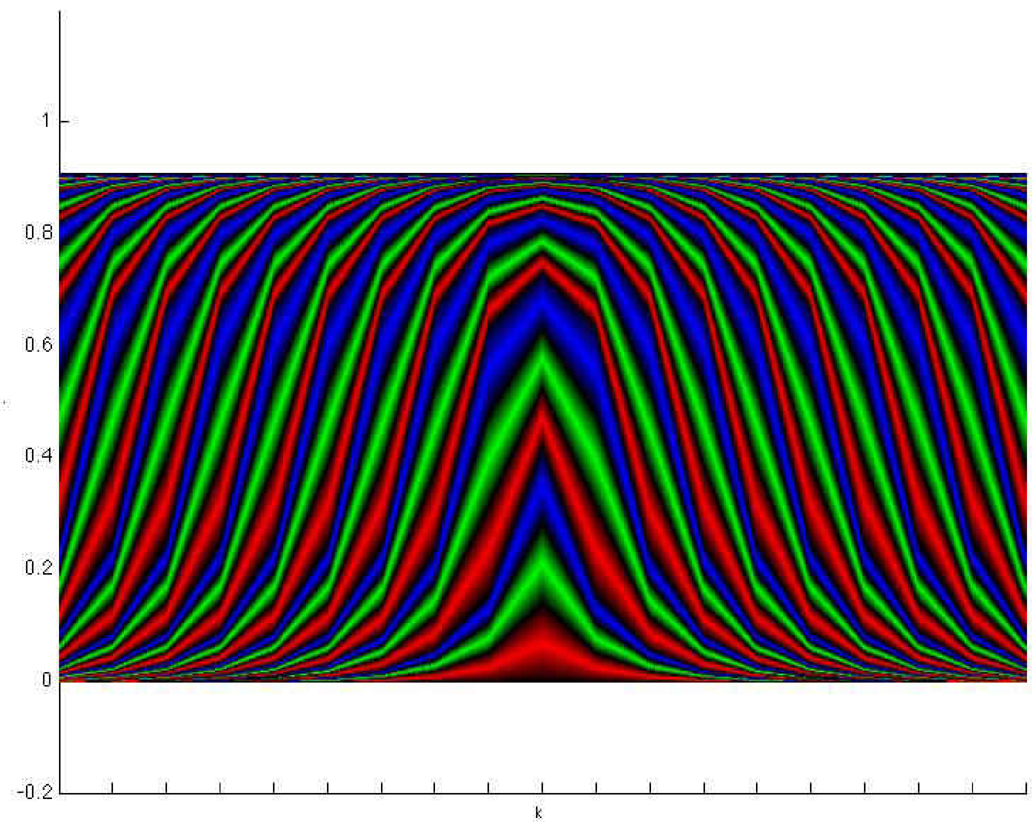

Figure 6.2: Complete Family of Symmetrical Point-Top Waves. Even $W \geq 0$, $\alpha = 1$, $\gamma = .1$.

Continuing with our symmetrical waves, we want to show that our wave forms for stable waves can also be solutions of unstable waves, with different a. For our unstable waves, given α, γ and W, we have a family of possible solutions, and we know we have $h_{k_0^*} = h_{k_1^*} \in [0, 1]$. The minimal solution in this family comes if $h_{k_0^*} = h_{k_1^*} = 0$ and the maximal solution comes if $h_{k_0^*} = h_{k_1^*} = 1$. In these cases our unstable wave form is the same as a stable wave because

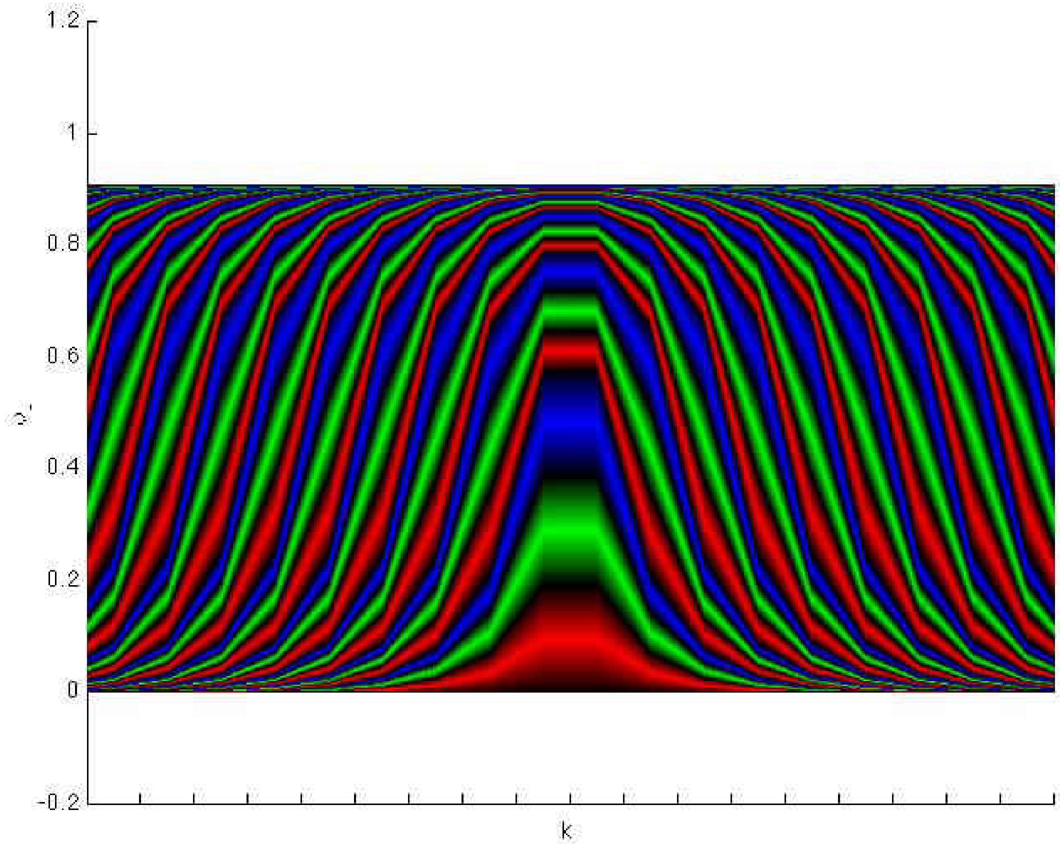

Figure 6.3: Complete Family of Symmetrical Flat-Top Waves. Odd $W \geq 1$, $\alpha = 1$, $\gamma = .1$.

when h_k equals 0 or 1 $\forall k$, then we have the same equation as we do in the case of a stable wave. The only difference is that in this unstable case, a intersects the wave at lattice points and with the stable wave it does not. In Figure 3.7 we see a family of unstable waves with $W = 4$. At the lower edge of this family is the wave form for a stable wave with $W = 4$. At the upper edge of this family is the wave form for a stable wave with $W = 6$. This is also the lower edge of the family of unstable waves with $W = 6$.

Here we show more analysis on our ranges for standing waves. We look at the case of stable waves. We look at the case where $\gamma = 0$, so $\beta = 1$. In Figure 6.4 we connect the intervals for standing waves with the family of standing waves. In blue we plot the areas

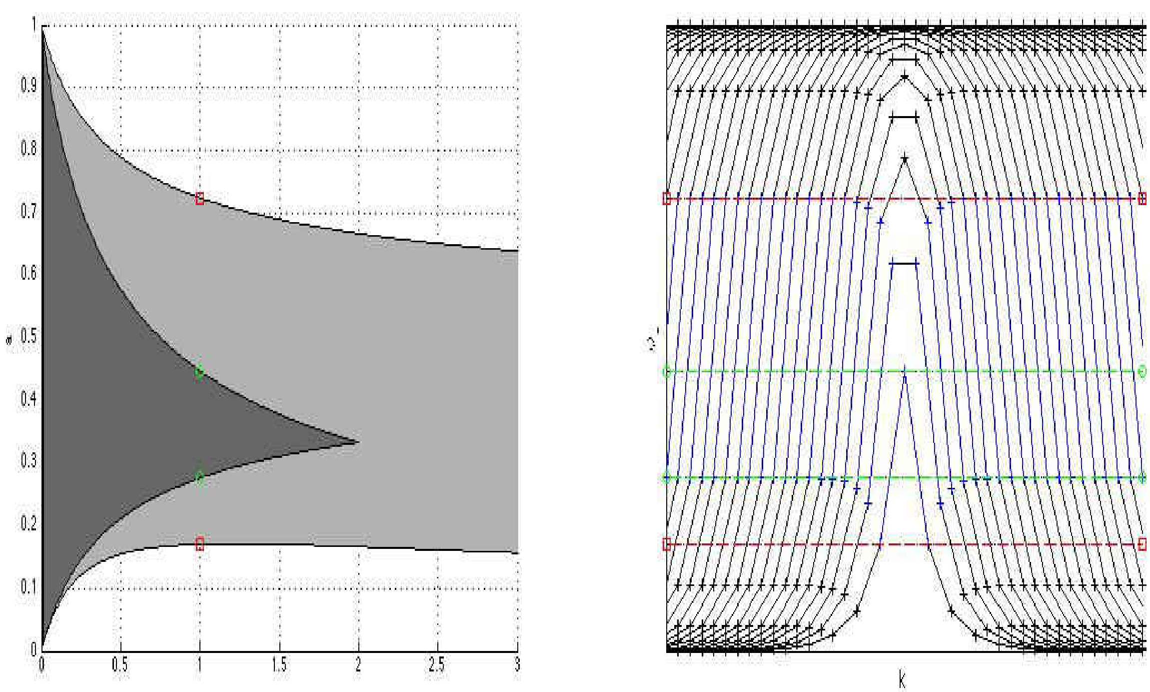

Figure 6.4: On the left we have our ranges for standing waves. We pick the value $\alpha = 1$ to look at. For $\alpha = 1$ we have four corresponding points that define our ranges. On the right we plot these four values on top of the corresponding family of standing waves with $\alpha = 1$ and $\gamma = 0$.

for each wave where the wave crosses a. Looking at where the four values from the bounds are placed on the family of standing waves, we see that the inner ranges denote the area where a can be to cross each member of the family in a blue part. The red lines denote the largest possible areas where a can be to be able to cross any of the waves in the family at an appropriate spot to allow for its existence.

6.2 Future Work

Much future work on this problem involves looking at more complex versions of the problem. One added complexity can be to look at the case of inhomogeneous media, or inhomogeneous diffusion. FH-N type and related models with in inhomogeneous media have been studied in [6, 18, 21, 17, 13]. When studying inhomogeneous media, the diffusion coefficients are allowed to vary on an integer lattice. We represent this variable diffusion over the spatially discrete domain with the operator L, a difference Laplacian operator of the form

$$Lu_k(t) = \alpha_k(u_{k+1}(t) - u_k(t)) + \alpha_{k-1}(u_{k-1}(t) - u_k(t)), \tag{6.1}$$

where

$$\alpha_k = \begin{cases} \alpha_k & -m \leq k \leq n \\ \alpha & k < -m \quad \text{or} \quad k > n \end{cases} \tag{6.2}$$

with $\alpha_k \in \mathbb{R}^+ \;\forall\; k \in \mathbb{Z}$. This means that the diffusion coefficients are allowed to vary within some finite range, but at some point they are the same for every lattice point to the right going to infinity, and at some point they are the same for every lattice point to the left going to infinity. This problem can be studied using the same approach that we used here, the theory of Jacobi operators. The difference will be that we will have more complex fundamental solutions, since the values of α_k will be different at different points.

Another complexity we can add to this problem is to examine the case of standing wave solutions with multiple pulses. Here we only looked at 1-pulse solutions, waves that went up once and then back down. A multiple pulse solution will go up and down multiple times. For this case the nonlinearity (1.10) may be written as a linear inhomogeneous term

$$f(\varphi_k) = \varphi_k + \sum_{j=0}^{n} (-1)^{j+1} h(k - \eta_j),$$

which is independent of a. For an *N-pulse* wave we will have $n = 2N - 1$, and for an *N-front* wave we will have $n = 2N - 2$. Thus, solving (1.15) is equivalent to solving the difference equation

$$\alpha_k \varphi_{k+1} - (1 + \gamma + \alpha_k + \alpha_{k-1}) \varphi_k + \alpha_{k-1} \varphi_{k-1} = \sum_{j=0}^{n} (-1)^{j+1} h(k - \eta_j) \qquad \forall k \in \mathbb{Z}, \tag{6.3}$$

The right side of (6.3) will still equal 0, 1, or $[0, 1]$ at each point. The difference here is that there will be more places where this value changes.

Another complexity we can add to this problem is to look at different nonlinearities, such as the cubic (1.9) or the zig-zag nonlinearity:

$$f(u; a) = \begin{cases} u, & u < a/2, \\ a - u, & a/2 \le u \le (a+1)/2, \\ u - 1, & u > (a+1)/2. \end{cases}$$

The zig-zag nonlinearity has been studied in [22, 23]. The zig-zag nonlinearity is useful in that it is still piecewise linear, which makes it easier for us to study. The McKean nonlinearity has an infinite slope at the point $u = a$, which the zig-zag nonlinearity has slope -1, much closer to the slope of the cubic function at that point.

We would like to further our understanding of the connection between standing waves and propagation failure of traveling waves. We have seen that we can have standing waves and traveling waves for the same parameter values. We would like to be able to understand what the parameters are that will cause propagation failure.

We would also like to explore the physical and biological significance of standing waves on their own. In what types of physical systems will we encounter standing waves, and how will they interfere with propagation of traveling waves?

APPENDIX: VERIFICATION OF PARTICULAR SOLUTION

Here I verify our particular solution

$$\varphi_k = \frac{1}{\alpha}\begin{cases} -\sum_{j=k_0^*+1}^{k} h_j\sigma(k-j) & k > k_0^* \\ 0 & k = k_0^* \\ h_{k_0^*}\sigma(k-k_0^*) & k < k_0^* \end{cases} \tag{6.4}$$

of the difference equation (1.21):

$$-\alpha\varphi_{k+1} + (1+\gamma+2\alpha)\,\varphi_k - \alpha\varphi_{k-1} = h_k \qquad \forall k \in \mathbb{Z}. \tag{6.5}$$

I will use a form of the equation (2.2) that tells me that since σ is a fundamental solution to this homogeneous equation, we have that:

$$-\sigma(k+1) + 2\mu\sigma(k) - \sigma(k-1) = 0 \qquad \forall k \in \mathbb{Z}. \tag{6.6}$$

Also keep in mind that $h_k = 0$ if $k < k_0^*$ and $h_k = 1$ if $k_0^* < k < k_1^*$.

We have three different definitions of φ_k according to (6.4) and we have three terms in our difference equation (6.5), φ_{k-1}, φ_k, and φ_{k+1}. Therefore we must look at five different cases depending on where k is so that we cover all of the possible combinations of definitions of φ in our difference equation.

Case 1: $(k < k_0^* - 1)$

$$\begin{aligned} \varphi_k &= \frac{1}{\alpha}h_{k_0^*}\sigma(k-k_0^*) \\ \varphi_{k+1} &= \frac{1}{\alpha}h_{k_0^*}\sigma(k-k_0^*+1) \\ \varphi_{k-1} &= \frac{1}{\alpha}h_{k_0^*}\sigma(k-k_0^*-1) \end{aligned}$$

(6.5) says:

$$\begin{aligned}
-\alpha\varphi_{k+1} + (1+\gamma+2\alpha)\varphi_k - \alpha\varphi_{k-1} &= h_k \\
-h_{k_0^*}\sigma(k-k_0^*+1) + 2\mu h_{k_0^*}\sigma(k-k_0^*) - h_{k_0^*}\sigma(k-k_0^*-1) &= 0 \\
h_{k_0^*}[-\sigma(k-k_0^*+1) + 2\mu\sigma(k-k_0^*) - \sigma(k-k_0^*-1)] &= 0
\end{aligned}$$

By (6.6),

$$[-\sigma(k-k_0^*+1) + 2\mu\sigma(k-k_0^*) - \sigma(k-k_0^*-1)] = 0$$

and so this case is verified.

Case 2: $(k = k_0^* - 1)$

$$\begin{aligned}
\varphi_k &= \varphi_{k_0^*-1} = \frac{1}{\alpha}h_{k_0^*}\sigma(-1) \\
\varphi_{k+1} &= \varphi_{k_0^*} = 0 \\
\varphi_{k-1} &= \varphi_{k_0^*-2} = \frac{1}{\alpha}h_{k_0^*}\sigma(-2)
\end{aligned}$$

(6.5) says:

$$\frac{(1+\gamma+2\alpha)}{\alpha}h_{k_0^*}\sigma(-1) - h_{k_0^*}\sigma(-2) = h_{k_0^*-1} = 0$$

Since $\sigma(0) = 0$, I can add in a $-h_{k_0^*}\sigma(0)$ to his equation without changing it. This gives me:

$$-h_{k_0^*}\sigma(0) + 2\mu h_{k_0^*}\sigma(-1) - h_{k_0^*}\sigma(-2) = 0$$

$$h_{k_0^*}[-\sigma(0) + 2\mu\sigma(-1) - \sigma(-2)] = 0$$

By (6.6),

$$[-\sigma(0) + 2\mu\sigma(-1) - \sigma(-2)] = 0$$

and so this case is verified.

Case 3: $(k = k_0^*)$

$$\begin{aligned}
\varphi_k &= \varphi_{k_0^*} = 0 \\
\varphi_{k+1} &= \varphi_{k_0^*+1} = -\frac{1}{\alpha}\sum_{j=k_0^*+1}^{k_0^*+1} h_j\sigma(k_0^*+1-j) = -\frac{1}{\alpha}h_{k_0^*+1}\sigma(0) = 0 \\
\varphi_{k-1} &= \varphi_{k_0^*-1} = \frac{1}{\alpha}h_{k_0^*}\sigma(-1)
\end{aligned}$$

(6.5) says:

$$-h_{k_0^*}\sigma(-1) = h_{k_0^*}$$

Since $\sigma(-1) = \frac{\lambda^{-1}-\lambda}{\lambda-\lambda^{-1}} = -1$, we are left with $h_{k_0^*} = h_{k_0^*}$ and so this case is verified.

Case 4: $(k = k_0^* + 1)$

$$\begin{aligned}
\varphi_k &= \varphi_{k_0^*+1} = 0 \\
\varphi_{k+1} &= \varphi_{k_0^*+2} = -\frac{1}{\alpha}\sum_{j=k_0^*+1}^{k_0^*+2} h_j\sigma(k_0^*+2-j) = -\frac{1}{\alpha}[h_{k_0^*+1}\sigma(1) + h_{k_0^*+2}\sigma(0)] = -\frac{1}{\alpha}h_{k_0^*+1} \\
\varphi_{k-1} &= \varphi_{k_0^*} = 0
\end{aligned}$$

(6.5) says:

$$-\alpha(-\frac{1}{\alpha}h_{k_0^*+1}) = h_{k_0^*+1}$$

$$h_{k_0^*+1} = h_{k_0^*+1}$$

So this case is verified.

Case 5: $(k > k_0^* + 1)$ (6.5) says:

$$\sum_{j=k_0^*+1}^{k+1} h_j\sigma(k+1-j) - \frac{1}{\alpha}(1+\gamma+2\alpha)\sum_{j=k_0^*+1}^{k} h_j\sigma(k-j) + \sum_{j=k_0^*+1}^{k-1} h_j\sigma(k-1-j) = h_k \quad (6.7)$$

$$\sum_{j=k_0^*+1}^{k+1} h_j\sigma(k+1-j) = h_{k+1}\sigma(0) + h_k\sigma(1) + \sum_{j=1}^{k-1} h_j\sigma(k-j+1)$$

$$\sum_{j=k_0^*+1}^{k} h_j\sigma(k-j) = h_k\sigma(0) + \sum_{j=1}^{k-1} h_j\sigma(k-j)$$

Plugging these last two equalities into (6.7), we get:

$$\left[h_{k+1}\sigma(0) + h_k\sigma(1) + \sum_{j=k_0^*+1}^{k-1} h_j\sigma(k-j+1)\right] - 2\mu\left[h_k\sigma(0) + \sum_{j=k_0^*+1}^{k-1} h_j\sigma(k-j)\right]$$

$$+ \sum_{j=k_0^*+1}^{k-1} h_j\sigma(k-1-j) = h_k$$

$$h_k + \sum_{j=k_0^*+1}^{k-1} h_j[\sigma(k-j+1) - 2\mu\sigma(k-j) + \sigma(k-j-1)] = h_k$$

By (6.6),

$$[\sigma(k-j+1) - 2\mu\sigma(k-j) + \sigma(k-j-1)] = 0$$

So we are left with $h_k = h_k$, and so this case is verified.

REFERENCES

[1] A.L. Hodgkin and A.F. Huxley, *A Quantitative Description of Membrane Current and Its Application to Conduction and Excitation in Nerve*, J. Phisiol., 117 (1952), 500–544.

[2] R. FitzHugh, *Impulses and physiological states in theoretical models of nerve membrane*, Biophys. J., 1 (1961), 445–466.

[3] J. Nagumo, S. Arimoto, and S. Yoshizawa, *An active pulse transmission line simulating nerve axon*, Proc. Inst. Radio Engrg., 50 (1964), 2061–2070.

[4] H. McKean, *Nagumo's Equation*, Adv. Math. 4 (1970), 209–223.

[5] G. Teschl, *Jacobi Operators and Completely Integrable Nonlinear Lattices* , Mathematical Surveys and Monographs v.72, American Mathematical Society, (2000), Chapter 1.

[6] A.R. Humphries, B.E. Moore and E.S. Van Vleck, *Waves for Bistable Differential-Difference Equations with Inhomogeneous Diffusion*, preprint(2009).

[7] C.E. Elmer and E.S. Van Vleck, *Spatially Discrete FitzHugh-Nagumo Equations*, SIAM J. Appld. Math. 65 (2005), 1153–1174.

[8] J. Rinzel and J. B. Keller, *Traveling Wave Solutions of a Nerve Conduction Equation*, Biophys. J. 13 (1973), 1313–1337.

[9] J. Bell, *Some threshold results for models of myelinated nerves*, Math. Biosci. 54 (1981) 181–190.

[10] J. Bell and C. Cosner, *Threshold behavior and propagation for nonlinear differential-difference systems motivated by modeling myleinated axons*, Quart. Appl. Math., 42 (1984) 1–14.

[11] J.P. Keener, *Propagation and its failure in coupled systems of discrete excitable cells*, SIAM J. Appl. Math. 47 (1987) 556–572.

[12] B. Zinner, *Stability of traveling wavefronts for the discrete Nagumo equation*, SIAM J. Math. Anal. 22 (1991) 1016–1020.

[13] J. Sneyd, J. Sherratt, *On the propagation of calcium waves in an inhomogeneous media*, SIAM J. Appld. Math. 57 (1997) 73–94.

[14] G. Fath, *Propagation failure of traveling waves in a discrete medium*, Physica D 116 (1998) 176–190.

[15] J.W. Cahn, J. Mallet-Paret, E.S. Van Vleck, *Traveling wave solutions for systems of ODEs on a two-dimensional spatial lattice*, SIAM J. Appl. Math. 59 (1999) 455–493.

[16] J.P. Keener, *Propagation of waves in an excitable medium with discrete release sites*, SIAM J. Appl. Math. 61 (2000) 317–334.

[17] T.J. Lewis, J.P. Keener, *Wave-block in excitable media due to regions of depressed excitability*, SIAM J. Appld. Math. 61 (2000) 293–316.

[18] C.E. Elmer, E.S. Van Vleck, *Traveling waves solutions for bistable differential-difference equations with periodic diffusion*, SIAM J. Appl. Math. 61 (2001) 1648–1679.

[19] A. Tonnelier, *McKean caricature of the FitzHugh-Nagumo model: Traveling pulses in a discrete diffusive medium*, Phys. Rev. E 67 (2003).

[20] E.S. Van Vleck, B. Wang, *Attractors for lattice FitzHugh-Nagumo systems*, Physica D 212 (2005) 317–336.

[21] D.G. Aronson, N.V. Mantzaris, H.G. Othmer, *Wave propagation and blocking in inhomogeneous media*, Dis. Cont. Dyn. Sys. 13 (2005) 843–876.

[22] C.E. Elmer, *Finding stationary fronts for a discrete Nagumo and wave equation; construction*, Physica D 218 (2006) 11–23.

[23] C. E. Elmer, *The stability of stationary fronts for a discrete nerve axon model*, Math. Biosci. Eng. 1 (2006).

[24] L.F. Shampine, R.C. Allen, Jr., S. Pruess. *Fundamentals of Numerical Computing*. John Wiley and Sons, New York (1998).